

# Assessing Helical Protein Interfaces for Inhibitor Design

Brooke N. Bullock, Andrea L. Jochim and Paramjit S. Arora\*

*Department of Chemistry, New York University, New York, New York 10003*

## Supporting Information

	Page
Description of methods	S2
<b>Figures S2 and S3</b>	S5
Supplementary references	S6
<b>Table S1.</b> Dataset of HIPP interactions with hotspots on one helical face	S7
<b>Table S2.</b> Dataset of HIPP interactions with hotspots on two helical faces	S38
<b>Table S3.</b> Dataset of HIPP interactions with hotspots on three helical faces	S54

## Methods used to Identify Helical Interfaces in Protein-Protein (HIPP) Interactions

Protein structures were obtained from the Protein Data Bank (<http://www.pdb.org/>). In addition to using Rosetta, we wrote computer code in Perl, C and C++ programming language to identify and analyze HIPP interactions. The key steps to identifying HIPP interactions are listed below and shown in Figure S1.

1) Using the advanced search function on the PDB website, we extract all structures with more than one protein entity.

2) Sequence alignment of all complexes was performed using the CD-HIT clustering algorithm. CD-HIT clusters similar chains according to a similarity threshold. Although this method allows for all unique chains to be clustered it does not allow for all unique protein complexes to be clustered. To overcome this problem we removed chain identifiers in the FASTA files. The popular BLAST(*I*) method was not used because the computing of “all versus all” similarities would likely not be able to identify unique complexes properly since the chain identifiers in the FASTA files were removed. Since CD-HIT uses a “short word filter” method it can cluster properly even with these FASTA file modifications.

3) **Perl script to construct individual PDB files for each interacting chain within the parent PDB file.** This script reads a PDB, identifies atoms from different chains that interact with each other, then creates a new formatted PDB file with those two chains. This process is repeated until all interacting chains have a new PDB file. If the parent PDB file contains more than one structure (*ei.* NMR structure), only the first structure is considered.

**Perl script to identify protein partner chains between separate entities.** This script reads a PDB file, identifies chains that belong to separate entities within the PDB file, and creates a list of the PDB code and partnering chains that are part of the separate entities. This enables us to find those helix interfaces that are between separate protein entities as opposed to helical interfaces between chains in a single protein.

4) **Modifications within Rosetta written in C++ programming language to identify helical interfaces between interacting protein chains.** Rosetta contains programs that identify

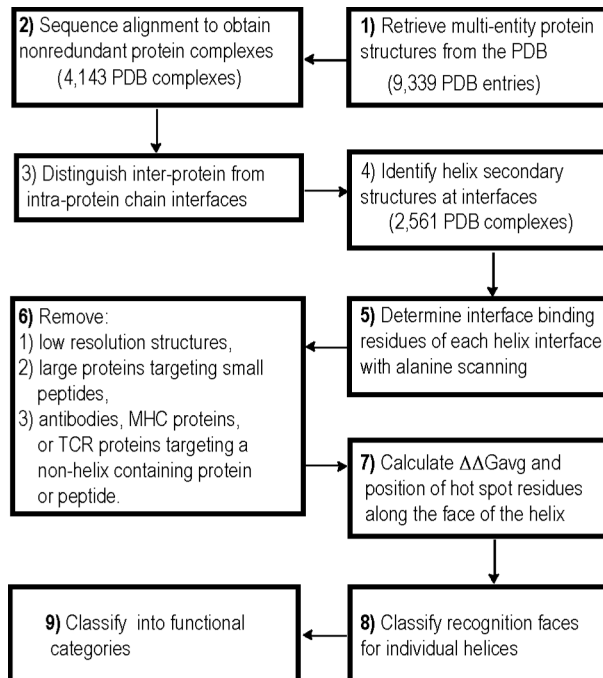


**Figure S1.** Protocol for the evaluation of structures from the Protein Data Bank to identify and assess helical interfaces in protein–protein (HIPP) interactions.

Since CD-HIT uses a “short word filter” method it can cluster properly even with these FASTA file modifications.

interface residues and assigns secondary structure to a protein backbone using  $\phi$  and  $\psi$  dihedral angle analysis. We then link the interface and secondary structure assignment subroutines to find protein chains with interface residues that lie within a helix. We define helical segment as one that contains at least four contiguous residues with  $\phi$  and  $\psi$  angles that are characteristic of the  $\alpha$ -helix ( $\phi = -47^\circ \pm 25^\circ$ ,  $\psi = -57^\circ \pm 25^\circ$ ).

The Dictionary of Secondary Structure of Proteins (DSSP)(2) and STRIDE(3) are common methods for obtaining information on protein secondary structure of proteins in the PDB. DSSP relies on hydrogen-bonding patterns in proteins to determine secondary structure and STRIDE uses a knowledge-based structure assignment. Although these methods are reliable for determining secondary structure, similar results are also obtained with  $\phi$  and  $\psi$  analysis as in Rosetta.(3) We performed random checks on secondary structures as calculated by Rosetta and defined by DSSP and STRIDE and found the that the three methods are comparable. We used Rosetta for secondary structure analysis to retain consistency across our computer codes.

Often, protein-protein interfaces are defined according to geometrically continuous patches of residues on the surface of a protein that exclude solvent by binding to another chain.(4) This definition might include some residues that are not really involved in the interaction or exclude some residues that play a key role in the interaction.(5) Therefore, we use a distance threshold between residues of different chains. When parsing PDB files, it is difficult to determine when contacting chains reflect crystal packing or a genuine biological assembly. The problem is amplified when hundreds of PDB files are automatically parsed. Two approaches are suggested for remedying this problem. One calculates the reduction of solvent accessibility due to oligomerisation(6) and while the other is based on measuring the conservation of contacting residues.(7) Instead of relying of these prediction algorithms, we visually inspected each candidate target in categories 1-3 for crystal packing multimers and eliminated those few interactions that were artifacts of crystal packing.

5) Hot spot residues were predicted by a computational alanine scan on each of the complexes in the dataset using the Rosetta 2.0 software. There are additional methods, besides Rosetta alanine scanning, for predicting hot spot residues. These methods are either based on determining hot spot residues based on amino acid sequence or a scoring function.(8-11) Glycine and proline residues were exempted from mutation to alanine as any such event may result in a conformational change in the protein backbone. In cases of multiple side chain orientations for the same residue in a PDB file, we eliminated the residue from consideration as a hot spot residue.

6) The HIPP dataset of 2,561 complexes was further analyzed to screen for potential receptors with binding clefts and extended interfaces that may be targeted by small molecules and helix mimetics, respectively. Any such undertaking inevitably involves a number of subjective decisions.(12) Our procedure involved (1) removal of all entries with resolution  $>4.00\text{ \AA}$  and all structures determined by methods other than X-ray crystallography or NMR spectroscopy. We note that hot spot analysis becomes increasingly unreliable with lower resolution structures. (2) Visually inspection of structures to eliminate complexes that we considered too large or complex to target with a small molecule or oligomer; examples include structures of nucleosomes, ribosomes, proteasomes, rubisco, and viral capsids. We also eliminated structures where

proteins containing a helix are complexed with a non-helical peptide such as T-cell receptor proteins, MHC proteins, and antibodies. Duplicate sequences and instances where a protein was identified to target a single helix or a protein with a helix targeting a non-helical peptide of length less than 12 residues were removed by automated procedures and verified by visual inspection.

7) HIPP interactions with a  $\Delta\Delta G_{avg} \geq 2$  kcal/mol were identified using a C++ program.

8) HIPPs with a  $\Delta\Delta G_{avg} \geq 2$  kcal/mol from step 7) were classified as

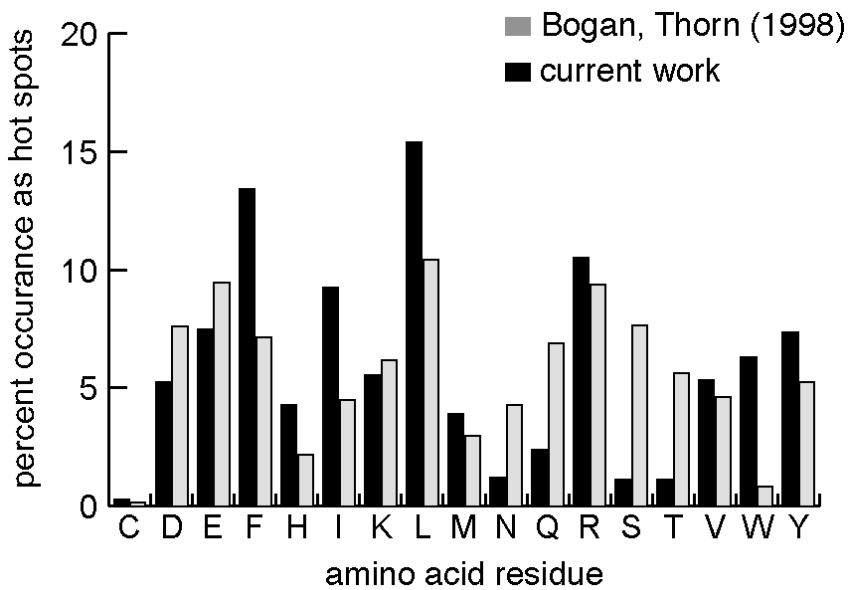
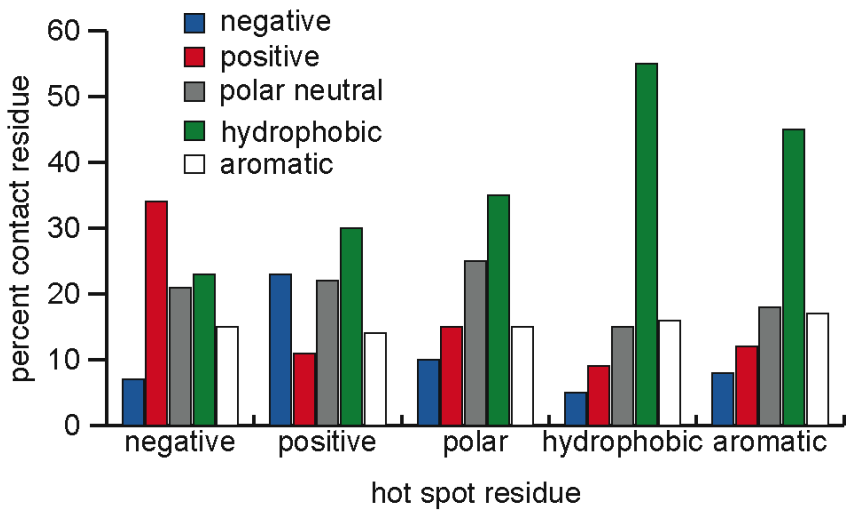


Figure S2. Comparison of amino acid preferences in hot spots from current study, and Bogan and Thorn (Bogan, A. A.; Thorn, K. S. *J. Mol. Biol.* **1998**, 280, 1.)



**Figure S3.** Classification of contact residues on partner proteins. Residues on the partner protein that are within 5 Å of the helical hotspot residue were analyzed within Rosetta.

## Supplementary References

1. Altschul, S., Gish, W., Miller, W., Myers, E., and Lipman, D. (1990) Basic local alignment search tool, *Journal of Molecular Biology* 215, 403-410.
2. Kabsch, W., and Sander, C. (1983) Dictionary of Protein Secondary Structure: Pattern Recognition of Hydrogen-Bonded and Geometrical Features, *Biopolymers* 22, 2577-2637.
3. Dmitrij, F., and Argos, P. (1995) Knowledge-Based Protein Secondary Structure Assignment, *Proteins: Structure, Function, and Genetics* 23, 566-579.
4. Jones, S., and Thornton, J. M. (1997) Analysis of protein-protein interaction sites using surface patches, *Journal of Molecular Biology* 272, 121-132.
5. Ofran, Y., and Rost, B. (2003) Analysing Six Types of Protein-Protein Interfaces, *Journal of Molecular Biology* 325, 377-387.
6. Henrick, K., and Thornton, J. M. (1998) PQS: a protein quaternary structure file server, *Trends in Biochemical Sciences* 23, 358-361.
7. Elcock, A. H., and McCammon, J. A. (2001) Identification of protein oligomerization states by analysis of interface conservation., *Proceedings of the National Academy of Sciences USA* 98, 2990-2994.
8. Guney, E., Tuncbag, N., Keskin, O., and Gursoy, A. (2008) HotSprint: database of computational hot spots in protein interfaces, *Nucleic Acids Research* 36, D662-D666.
9. Schymkowitz, J., Borg, J., Stricher, F., Nys, R., Rousseau, F., and Serrano, L. (2005) The FoldX web server: an online force field, *Nucleic Acids Research* 33, W382-W388.
10. Massova, I., and Kollman, P. A. (1999) Computational Alanine Scanning to Probe Protein-Protein Interactions: A Novel Approach to Evaluate Binding Free Energies, *J. Am. Chem. Soc.* 121, 8133-8143.
11. Ofran, Y., and Rost, B. (2007) Protein-Protein Interaction Hotspots Carved into Sequences, *PLoS Comput Biol* 3, e119.
12. Tsai, C.-J., Lin, S. L., Wolfson, H. J., and Nussinov, R. (1996) A Dataset of Protein-Protein Interfaces Generated with a Sequence-order-independent Comparison Technique, *Journal of Molecular Biology* 260, 604-620.

**Table S1.** Dataset of HIPP interactions with hotspots on one helical face

## Description of Entries:

- A. PDB code of predicted target.
- B. Chains in the complex featuring a helix at the interface.
- C. Candidate helix to be mimicked is part of the indicated chain.
- D. Title of PDB entry.
- E. Function of protein complex.
- F.  $\Delta\Delta G_{\text{avg}}$ /helix is derived from Rosetta computational alanine mutagenesis studies and indicates the average free energy penalty for mutating two or more key residues in the helix at the interface to alanine.
- G.  $\Delta\Delta G_{\text{sum}}$ /helix is derived from Rosetta computational alanine mutagenesis studies and indicates the average free energy penalty for mutating two or more key residues at the interface to alanine.
- H.  $\Delta\Delta G_{\text{sum}}$ /chain is derived from Rosetta computational alanine mutagenesis studies and indicates the sum free energy penalty for mutating two or more key residues in the helix at the interface to alanine.
- I. Helix contribution refers to the proportion of key contact residues positioned on the candidate helix as compared to the chain (see text for a detailed explanation).
- J. Number of hot spot residues in helix.
- K. Relative positioning of the hot spot residues on a helix.
- L. Hot spot residues derived from Rosetta computational alanine scanning mutagenesis.
- M. Number of residues separating end hot spot residues (see Methods for more details).
- N. Length of candidate helix to be mimicked.
- O. First residue of the candidate helix segment.
- P. Last residue of the candidate helix segment.
- Q. Sequence of candidate helix to be mimicked.
- R. Resolution of PDB structure (NOT APP indicates NMR structure).

TABLE S1

Bullock, et. al

A. PDB CODE	B. INTERFACE CHAINS	C. CHAIN	D. TITLE
1A0O	A B	A	CHEY-BINDING DOMAIN OF CHEA IN COMPLEX WITH CHEY
1A0O	C D	D	CHEY-BINDING DOMAIN OF CHEA IN COMPLEX WITH CHEY
1A4Y	D E	E	RIBONUCLEASE INHIBITOR-ANGIOGENIN COMPLEX
1A9N	A B	B	CRYSTAL STRUCTURE OF THE SPLICEOSOMAL U2B"-U2A' PROTEIN COMPLEX BOUND TO A FRAGI
1AY7	A B	B	RIBONUCLEASE SA COMPLEX WITH BARSTAR
1B0N	A B	B	SINR PROTEIN/SINI PROTEIN COMPLEX
1B27	B E	E	STRUCTURAL RESPONSE TO MUTATION AT A PROTEIN-PROTEIN INTERFACE
1B9X	A B	B	STRUCTURAL ANALYSIS OF PHOSDUCIN AND ITS PHOSPHORYLATION- REGULATED INTERACTIO
1BDJ	A B	B	COMPLEX STRUCTURE OF HPT DOMAIN AND CHEY
1BXL	A B	B	STRUCTURE OF BCL-XL/BAK PEPTIDE COMPLEX, NMR, MINIMIZED AVERAGE STRUCTURE
1D2Z	C B	C	THREE-DIMENSIONAL STRUCTURE OF A COMPLEX BETWEEN THE DEATH DOMAINS OF PELLE AN
1DE4	G I	G	HEMOCHROMATOSIS PROTEIN HFE COMPLEXED WITH TRANSFERRIN RECEPTOR
1DML	C D	D	CRYSTAL STRUCTURE OF HERPES SIMPLEX UL42 BOUND TO THE C- TERMINUS OF HSV POL
1DOA	A B	B	STRUCTURE OF THE RHO FAMILY GTP-BINDING PROTEIN CDC42 IN COMPLEX WITH THE MULTIFI
1DS6	A B	A	CRYSTAL STRUCTURE OF A RAC-RHOGDI COMPLEX
1E44	B A	B	RIBONUCLEASE DOMAIN OF COLICIN E3 IN COMPLEX WITH ITS IMMUNITY PROTEIN
1EM8	A B	B	CRYSTAL STRUCTURE OF CHI AND PSI SUBUNIT HETERODIMER FROM DNA POL III
1ES7	A D	D	COMPLEX BETWEEN BMP-2 AND TWO BMP RECEPTOR IA ECTODOMAINS
1ES7	C B	B	COMPLEX BETWEEN BMP-2 AND TWO BMP RECEPTOR IA ECTODOMAINS
1EUV	A B	A	X-RAY STRUCTURE OF THE C-TERMINAL ULP1 PROTEASE DOMAIN IN COMPLEX WITH SMT3, THE
1EUV	A B	A	X-RAY STRUCTURE OF THE C-TERMINAL ULP1 PROTEASE DOMAIN IN COMPLEX WITH SMT3, THE
1F47	B A	A	THE BACTERIAL CELL-DIVISION PROTEIN ZIPA AND ITS INTERACTION WITH AN FTSZ FRAGMENT
1FM6	U X	U	THE 2.1 ANGSTROM RESOLUTION CRYSTAL STRUCTURE OF THE HETEROGLIMERIC HUMAN J
1FOE	C D	C	CRYSTAL STRUCTURE OF RAC1 IN COMPLEX WITH THE GUANINE NUCLEOTIDE EXCHANGE REGI
1FOE	C D	C	CRYSTAL STRUCTURE OF RAC1 IN COMPLEX WITH THE GUANINE NUCLEOTIDE EXCHANGE REGI
1FOE	C D	C	CRYSTAL STRUCTURE OF RAC1 IN COMPLEX WITH THE GUANINE NUCLEOTIDE EXCHANGE REGI
1FOE	C D	D	CRYSTAL STRUCTURE OF RAC1 IN COMPLEX WITH THE GUANINE NUCLEOTIDE EXCHANGE REGI
1H2M	A S	S	FACTOR INHIBITING HIF-1 ALPHA IN COMPLEX WITH HIF-1 ALPHA FRAGMENT PEPTIDE
1H3O	A B	B	CRYSTAL STRUCTURE OF THE HUMAN TAF4-TAF12 (TAFII135-TAFII20) COMPLEX
1H59	A B	B	COMPLEX OF IGFBP-5 WITH IGF-I
1H6K	A X	X	NUCLEAR CAP BINDING COMPLEX
1HE1	A C	A	CRYSTAL STRUCTURE OF THE COMPLEX BETWEEN THE GAP DOMAIN OF THE PSEUDOMONAS AF
1HH4	A D	A	RAC1-RHOGDI COMPLEX INVOLVED IN NADPH OXIDASE ACTIVATION
1HH4	B E	B	RAC1-RHOGDI COMPLEX INVOLVED IN NADPH OXIDASE ACTIVATION
1HH4	B E	E	RAC1-RHOGDI COMPLEX INVOLVED IN NADPH OXIDASE ACTIVATION
1HV2	A B	B	SOLUTION STRUCTURE OF YEAST ELONGIN C IN COMPLEX WITH A VON HIPPEL-LINDAU PEPTIDI
1HWM	A B	A	EBULIN,ORTORHOMBIC CRYSTAL FORM MODEL
1I7W	C D	D	BETA-CATENIN/PHOSPHORYLATED E-CADHERIN COMPLEX
1IWQ	A B	A	CRYSTAL STRUCTURE OF MARCKS CALMODULIN BINDING DOMAIN PEPTIDE COMPLEXED WITH
1J1D	B C	C	CRYSTAL STRUCTURE OF THE 46kDa DOMAIN OF HUMAN CARDIAC TROPONIN IN THE CA2+ SAT
1J2J	A B	A	CRYSTAL STRUCTURE OF GGA1 GAT N-TERMINAL REGION IN COMPLEX WITH ARF1 GTP FORM
1JPW	B E	E	CRYSTAL STRUCTURE OF A HUMAN TCF-4 / BETA-CATENIN COMPLEX
1KBH	A B	A	MUTUAL SYNERGISTIC FOLDING IN THE INTERACTION BETWEEN NUCLEAR RECEPTOR COACTIV
1KI1	A B	A	GUANINE NUCLEOTIDE EXCHANGE REGION OF INTERSECTIN IN COMPLEX WITH CDC42
1L2W	A I	I	CRYSTAL STRUCTURE OF THE YERSINIA VIRULENCE EFFECTOR YOPE CHAPERONE-BINDING DO
1L8C	A B	B	STRUCTURAL BASIS FOR HIF-1ALPHA/CBP RECOGNITION IN THE CELLULAR HYPOXIC RESPONSE
1LB1	C D	D	CRYSTAL STRUCTURE OF THE DBL AND PLECKSTRIN HOMOLOGY DOMAINS OF DBS IN COMPLEX
1LB1	E F	F	CRYSTAL STRUCTURE OF THE DBL AND PLECKSTRIN HOMOLOGY DOMAINS OF DBS IN COMPLEX
1LQB	B C	B	CRYSTAL STRUCTURE OF A HYDROXYLATED HIF-1 ALPHA PEPTIDE BOUND TO THE PVHL/ELONG
1LTX	A R	A	STRUCTURE OF RAB ESCORT PROTEIN-1 IN COMPLEX WITH RAB GERANYLGERANYL TRANSFER
1LTX	A R	R	STRUCTURE OF RAB ESCORT PROTEIN-1 IN COMPLEX WITH RAB GERANYLGERANYL TRANSFER
1MZN	C D	D	CRYSTAL STRUCTURE AT 1.9 ANGSTROEMS RESOLUTION OF THE HOMODIMER OF HUMAN RXR A
1N1J	A B	B	CRYSTAL STRUCTURE OF THE NF-YB/NF-YC HISTONE PAIR
1NRL	B D	D	CRYSTAL STRUCTURE OF THE HUMAN PXR-LBD IN COMPLEX WITH AN SRC-1 COACTIVATOR PEP
1NU7	E F	E	STAPHYLOCOAGULASE-THROMBIN COMPLEX
1OLS	A B	B	STRUCTURE OF AURORA-A 122-403, PHOSPHORYLATED ON THR287, THR288 AND BOUND TO TPX2

TABLE S1

Bullock, et. al

A. PDB CODE	E. FUNCTION	F. $\Delta\Delta G_{AVG,HELIX}$ (KCAL/MOL)	G. $\Delta\Delta G_{SUM, HELIX}$ (KCAL/MOL)	H. $\Delta\Delta G_{SUM, CHAIN}$ (KCAL/MOL)
1A0O	CHEMOTAXIS	2.0	4.1	4.1
1A0O	CHEMOTAXIS	2.2	4.4	4.4
1A4Y	COMPLEX (INHIBITOR/NUCLEASE)	2.0	3.9	5.1
1A9N	RNA BINDING PROTEIN/RNA	2.0	3.9	3.9
1AY7	COMPLEX (ENZYME/INHIBITOR)	2.2	4.4	7.7
1B0N	TRANSCRIPTION REGULATOR	2.0	5.9	27.4
1B27	HYDROLASE/HYDROLASE INHIBITOR	3.2	6.3	11.2
1B9X	SIGNALING PROTEIN	2.4	7.2	18.4
1BDJ	COMPLEX (CHEMOTAXIS/TRANSFERASE)	2.1	4.1	8.0
1BXL	COMPLEX (APOPTOSIS/PEPTIDE)	2.4	4.8	7.1
1D2Z	APOPTOSIS	2.0	4.0	5.7
1DE4	METAL TRANSPORT INHIBITOR/RECEPTOR	2.0	3.9	14.5
1DML	DNA BINDING PROTEIN/TRANSFERASE	3.8	7.6	14.4
1DOA	CELL CYCLE	2.3	4.5	10.4
1DS6	SIGNALING PROTEIN	2.5	4.9	13.4
1E44	RIBONUCLEASE	4.0	8.0	11.4
1EM8	GENE REGULATION	3.5	7.0	11.5
1ES7	CYTOKINE	2.5	4.9	4.9
1ES7	CYTOKINE	2.1	4.2	4.2
1EUV	HYDROLASE	3.5	6.9	23.4
1EUV	HYDROLASE	2.6	5.1	23.4
1F47	CELL CYCLE	2.3	4.5	7.4
1FM6	TRANSCRIPTION	2.1	4.2	5.6
1FOE	SIGNALING PROTEIN, IMMUNE SYSTEM/SIGNALING	3.5	10.6	24.2
1FOE	SIGNALING PROTEIN, IMMUNE SYSTEM/SIGNALING	2.9	8.6	24.2
1FOE	SIGNALING PROTEIN, IMMUNE SYSTEM/SIGNALING	4.0	7.8	24.2
1FOE	SIGNALING PROTEIN, IMMUNE SYSTEM/SIGNALING	2.0	4.0	32.8
1H2M	TRANSCRIPTION ACTIVATOR/INHIBITOR	2.3	4.5	5.5
1H3O	TRANSCRIPTION/TBP-ASSOCIATED FACTORS	2.1	4.1	14.3
1H59	INSULIN	2.2	4.4	6.1
1H6K	NUCLEAR PROTEIN	2.2	4.3	9.4
1HE1	SIGNALING PROTEIN	2.4	4.7	9.5
1HH4	SIGNALING PROTEIN/INHIBITOR	2.6	5.1	9.1
1HH4	SIGNALING PROTEIN/INHIBITOR	2.2	4.3	13.6
1HH4	SIGNALING PROTEIN/INHIBITOR	2.2	4.3	7.1
1HV2	SIGNALING PROTEIN	2.2	4.3	4.3
1HWM	HYDROLASE	2.1	4.1	9.2
1I7W	CELL ADHESION	2.1	4.1	22.7
1IWQ	METAL BINDING PROTEIN/PROTEIN BINDING	2.5	4.9	22.1
1J1D	CONTRACTILE PROTEIN	2.0	4.0	19.6
1J2J	PROTEIN TRANSPORT	2.4	4.7	8.3
1JPW	CELL ADHESION	2.1	4.1	14.0
1KBH	TRANSCRIPTION	2.2	4.3	7.8
1KI1	SIGNALING PROTEIN	2.7	5.3	7.3
1L2W	CHAPERONE	2.1	4.1	8.3
1L8C	GENE REGULATION	2.3	4.6	16.8
1LB1	SIGNALING PROTEIN	2.1	4.1	16.3
1LB1	SIGNALING PROTEIN	2.0	3.9	10.6
1LQB	GENE REGULATION	2.3	4.5	13.8
1LTX	TRANSFERASE/PROTEIN BINDING	2.4	4.7	6.6
1LTX	TRANSFERASE/PROTEIN BINDING	3.2	6.3	9.7
1MZN	TRANSCRIPTION	2.1	6.2	7.8
1N1J	DNA BINDING PROTEIN	2.6	5.1	43.7
1NRL	TRANSCRIPTION	2.0	6.0	6.0
1NU7	HYDROLASE/PROTEIN BINDING	2.2	4.3	5.3
1OLS	TRANSFERASE/CELL CYCLE	3.0	6.0	18.6

TABLE S1

Bullock, et. al

A. PDB CODE	I. HELIX CONTRIBUTION	J. # HOTSPOT RESIDUES	K. HOTSPOT RESIDUES, RESIDUE # $\Delta\Delta G$ (kcal/mol)
1A0O	100%	2	K122, 2.0; E125, 2.0;
1A0O	100%	2	V211, 1.1; F214, 3.3;
1A4Y	76%	2	R5, 1.9; H8, 2.0;
1A9N	100%	2	R28, 1.8; Y31, 2.1;
1AY7	57%	2	D35, 1.5; D39, 2.9;
1B0N	22%	3	I32, 1.1; Y35, 2.6; L36, 2.2;
1B27	56%	2	D36, 1.5; D40, 4.8;
1B9X	39%	3	F540, 3.8; Y543, 2.4; V544, 1.0;
1BDJ	51%	2	E750, 1.3; E754, 2.8;
1BXL	68%	2	L578, 2.7; I581, 2.1;
1D2Z	70%	2	N112, 1.6; R115, 2.4;
1DE4	27%	2	E146, 1.6; H150, 2.3;
1DML	53%	2	F1231, 5.2; L1234, 2.4;
1DOA	43%	2	Y51, 2.8; L55, 1.7;
1DS6	37%	2	R66, 1.6; L67, 3.3;
1E44	70%	2	F2, 5.4; Y5, 2.6;
1EM8	61%	2	R118, 1.6; W122, 5.4;
1ES7	100%	2	F785, 3.3; K788, 1.6;
1ES7	100%	2	F285, 2.6; K288, 1.6;
1EUV	29%	2	D451, 4.6; E455, 2.3;
1EUV	22%	2	F474, 3.3; T477, 1.8;
1F47	61%	2	F11, 2.1; I8, 2.4;
1FM6	75%	2	E394, 1.2; Y397, 3.0;
1FOE	44%	3	K1195, 4.4; L1198, 5.0; L1199, 1.2;
1FOE	36%	3	I1187, 1.2; I1190, 3.6; Q1191, 3.8;
1FOE	32%	2	I1231, 3.7; N1232, 4.1;
1FOE	12%	2	R66, 2.1; L67, 1.9;
1H2M	82%	2	L818, 2.1; L819, 2.4;
1H3O	29%	2	L66, 2.6; V70, 1.5;
1H59	72%	2	L70, 3.1; L74, 1.3;
1H6K	46%	2	Y100, 2.6; R99, 1.7;
1HE1	49%	2	Q182, 2.0; Q183, 2.7;
1HH4	56%	2	H103, 3.1; H104, 2.0;
1HH4	32%	2	R66, 2.4; L67, 1.9;
1HH4	61%	2	Y351, 2.5; L355, 1.8;
1HV2	100%	2	L158, 3.2; R161, 1.1;
1HWM	45%	2	E235, 2.8; I239, 1.3;
1I7W	18%	2	K717, 1.1; L718, 3.0;
1IWQ	22%	2	L105, 1.2; M109, 3.7;
1J1D	20%	2	K72, 2.9; L76, 1.1;
1J2J	57%	2	L77, 2.7; H80, 2.0;
1JPW	29%	2	V44, 2.0; K45, 2.1;
1KBH	55%	2	I34, 3.0; V38, 1.3;
1KI1	73%	2	L67, 3.0; L70, 2.3;
1L2W	49%	2	Y39, 1.9; L43, 2.2;
1L8C	27%	2	L141, 2.4; L145, 2.2;
1LB1	25%	2	L69, 1.9; L72, 2.2;
1LB1	37%	2	H105, 2.0; F106, 1.9;
1LQB	33%	2	L101, 1.4; L104, 3.1;
1LTX	71%	2	Q216, 2.4; F220, 2.3;
1LTX	65%	2	R275, 3.5; F279, 2.8;
1MZN	79%	3	L1475, 2.2; L1478, 1.4; L1479, 2.6;
1N1J	12%	2	R47, 1.5; I51, 3.6;
1NRL	100%	3	L690, 2.6; H691, 1.0; L694, 2.4;
1NU7	81%	2	E14, 2.6; L14, 1.7;
1OLS	32%	2	W34, 2.8; F35, 3.2;

TABLE S1

Bullock, et. al

A. PDB CODE	L. HOTSPOT RESIDUE HELIX POSITIONS	M. HOTSPOT RESIDUE END TO END LENGTH	N. HELIX LENGTH	O. HELIX START RESIDUE #	P. HELIX END RESIDUE #
1A0O	i; i+3;	4	14	113	126
1A0O	i; i+3;	4	12	205	216
1A4Y	i; i+3;	4	9	5	13
1A9N	i; i+3;	4	12	23	34
1AY7	i; i+4;	5	9	34	42
1B0N	i; i+3; i+4;	5	11	29	39
1B27	i; i+4;	5	9	35	43
1B9X	i; i+3; i+4;	5	14	533	546
1BDJ	i; i+4;	5	15	744	758
1BXL	i; i+3;	4	9	576	584
1D2Z	i; i+3;	4	7	111	117
1DE4	i; i+4;	5	12	140	151
1DML	i; i+3;	4	16	1220	1235
1DOA	i; i+4;	3	12	46	57
1DS6	i; i+1;	5	5	65	69
1E44	i; i+3;	2	6	2	7
1EM8	i; i+4;	4	14	115	128
1ES7	i; i+3;	5	7	783	789
1ES7	i; i+3;	4	7	283	289
1EUV	i; i+4;	4	14	451	464
1EUV	i; i+3;	5	10	473	482
1F47	i; i+3;	4	9	8	16
1FM6	i; i+3;	4	23	386	408
1FOE	i; i+3; i+4;	4	12	1195	1206
1FOE	i; i+3; i+4;	5	8	1187	1194
1FOE	i; i+1;	5	8	1226	1233
1FOE	i; i+1;	2	5	65	69
1H2M	i; i+1;	2	7	816	822
1H3O	i; i+4;	4	12	60	71
1H59	i; i+4;	2	7	69	75
1H6K	i; i+1;	5	12	91	102
1HE1	i; i+1;	5	5	181	185
1HH4	i; i+1;	5	13	93	105
1HH4	i; i+1;	2	5	65	69
1HH4	i; i+4;	2	12	346	357
1HV2	i; i+3;	2	14	158	171
1HWM	i; i+4;	2	9	233	241
1I7W	i; i+1;	5	7	716	722
1IWQ	i; i+4;	4	11	102	112
1J1D	i; i+4;	5	18	63	80
1J2J	i; i+3;	2	7	75	81
1JPW	i; i+1;	5	6	42	47
1KBH	i; i+4;	5	8	34	41
1KI1	i; i+3;	4	7	67	73
1L2W	i; i+4;	2	8	38	45
1L8C	i; i+4;	5	11	139	149
1LB1	i; i+3;	4	7	69	75
1LB1	i; i+1;	5	19	89	107
1LQB	i; i+3;	5	11	100	110
1LTX	i; i+4;	4	18	205	222
1LTX	i; i+4;	2	7	275	281
1MZN	i; i+3; i+4;	4	9	1473	1481
1N1J	i; i+4;	4	9	45	53
1NRL	i; i+1; i+4;	5	9	688	696
1NU7	i; i+1;	5	8	14	14
1OLS	i; i+1;	4	9	33	41

TABLE S1

Bullock, et. al

A. PDB CODE	Q. HELIX SEQUENCE	R. RESOLUTION
1A0O	AATLEEKLNKIFEK	2.95
1A0O	EDDITAVLCFVI	2.95
1A4Y	RYTHFLTQH	2.00
1A9N	KEELKRSILYALF	2.38
1AY7	LDALWDCLT	1.70
1B0N	PEEIRKYLLN	1.90
1B27	LDALWDALT	2.10
1B9X	VSKCCEFRDYVEE	3.00
1BDJ	WEDNVGEWIEEMKEE	2.68
1BXL	RQLAIIGDD	NOT APP
1D2Z	HNAMRLI	2.00
1DE4	AWPTKLEWERHK	2.80
1DML	AEETRRMLHRAFDTLA	2.70
1DOA	ESLRKYKEALLG	2.60
1DS6	DRLRP	2.35
1E44	FKDYGH	2.40
1EM8	PTARAALWQQICTY	2.10
1ES7	SDFQCKD	2.90
1ES7	SDFQCKD	2.90
1EUV	DTIIEFFMKYIEKS	1.60
1EUV	SFFYTNLSER	1.60
1F47	IPAFLRKQA	1.95
1FM6	PAEVEALREKVYASLEAYCKHY	2.10
1FOE	KYPLLLRELFAL	2.80
1FOE	IKPIQRVL	2.80
1FOE	KVASHINE	2.80
1FOE	DRLRP	2.80
1H2M	EELLRAL	2.50
1H3O	KKKLQDLVREVD	2.30
1H59	PLHALLH	2.10
1H6K	RADAENAMRYIN	2.00
1HE1	LQQWG	2.00
1HH4	VRAKWYPEVRHHC	2.70
1HH4	DRLRP	2.70
1HH4	ESLRKYKEALLG	2.70
1HV2	LKERCLQVVRSVLK	NOT APP
1HWM	FEELYKITG	2.80
1I7W	KKLADMY	2.00
1IWQ	AAELRHVMNTNL	2.00
1J1D	REAEERRGEKGRALSTRA	2.61
1J2J	RPLWRHY	1.60
1JPW	ADVKSS	2.50
1KBH	IPELVNQG	NOT APP
1KI1	LRPLSYP	2.30
1L2W	QYANNLAG	2.00
1L8C	EELLRALDQVN	NOT APP
1LB1	LRPLSYP	2.81
1LB1	PDSLENIPKWTPEVKHFC	2.81
1LQB	ALELLMAANFL	2.00
1LTX	ENVLLKELELVQNAFFTD	2.70
1LTX	RADVFN	2.70
1MZM	KILHRLLQD	1.90
1N1J	LARIKKIMK	1.67
1NRL	KILHRLLQE	2.00
1NU7	ERELLESY	2.20
1OLS	SWFEEKANL	2.50

TABLE S1

Bullock, et. al

A. PDB CODE	B. INTERFACE CHAINS	C. CHAIN	D. TITLE
1OOK	A B	A	CRYSTAL STRUCTURE OF THE COMPLEX OF PLATELET RECEPTOR GPIB- ALPHA AND HUMAN ALP
1OR7	A C	A	CRYSTAL STRUCTURE OF ESCHERICHIA COLI SIGMAE WITH THE CYTOPLASMIC DOMAIN OF ITS.
1OR7	A C	A	CRYSTAL STRUCTURE OF ESCHERICHIA COLI SIGMAE WITH THE CYTOPLASMIC DOMAIN OF ITS.
1OSV	B D	D	STRUCTURAL BASIS FOR BILE ACID BINDING AND ACTIVATION OF THE NUCLEAR RECEPTOR FXF
1QLS	A D	D	S100C (S100A11),OR CALGIZZARIN, IN COMPLEX WITH ANNEXIN I N-TERMINUS
1R4A	A E	E	CRYSTAL STRUCTURE OF GTP-BOUND ADP-RIBOSYLATION FACTOR LIKE PROTEIN 1 (ARL1) AND
1R8Q	A E	A	FULL-LENGTH ARF1-GDP-MG IN COMPLEX WITH BREFELDIN A AND A SEC7 DOMAIN
1RP3	A B	B	COCRYSTAL STRUCTURE OF THE FLAGELLAR SIGMA/ANTI-SIGMA COMPLEX, SIGMA-28/FLGM
1T0F	B D	D	CRYSTAL STRUCTURE OF THE TNSA/TNSC(504-555) COMPLEX
1TTW	A B	B	CRYSTAL STRUCTURE OF THE YERSINIA PESTIS TYPE III SECRETION CHAPERONE SYCH IN COMP
1TUE	A B	B	THE X-RAY STRUCTURE OF THE PAPILLOMAVIRUS HELICASE IN COMPLEX WITH ITS MOLECULA
1TUE	H J	H	THE X-RAY STRUCTURE OF THE PAPILLOMAVIRUS HELICASE IN COMPLEX WITH ITS MOLECULA
1U0S	Y A	Y	CHEMOTAXIS KINASE CHEA P2 DOMAIN IN COMPLEX WITH RESPONSE REGULATOR CHEY FROM
1U7B	A B	B	CRYSTAL STRUCTURE OF HPCNA BOUND TO RESIDUES 331-350 OF THE FLAP ENDONUCLEASE-1 (
1U8T	B F	F	CRYSTAL STRUCTURE OF CHEY D13K Y106W ALONE AND IN COMPLEX WITH A FLIM PEPTIDE
1VCB	B C	B	THE VHL-ELONGINC-ELONGINB STRUCTURE
1X86	G H	H	CRYSTAL STRUCTURE OF THE DH/PH DOMAINS OF LEUKEMIA- ASSOCIATED RHOGEF IN COMPLE
1XCG	A B	B	CRYSTAL STRUCTURE OF HUMAN RHOA IN COMPLEX WITH DH/PH FRAGMENT OF PDZRHOGEF
1XL3	A C	A	COMPLEX STRUCTURE OF Y.PESTIS VIRULENCE FACTORS YOPN AND TYEA
1XLS	A E	A	CRYSTAL STRUCTURE OF THE MOUSE CAR/RXR LBD HETERO DIMER BOUND TO TCPOBOP AND 9C
1XV9	C G	G	CRYSTAL STRUCTURE OF CAR/RXR HETERO DIMER BOUND WITH SRC1 PEPTIDE, FATTY ACID, AN
1Y3A	A E	E	STRUCTURE OF G-ALPHA-I1 BOUND TO A GDP-SELECTIVE PEPTIDE PROVIDES INSIGHT INTO GUA
1YCR	A B	B	MDM2 BOUND TO THE TRANSACTIVATION DOMAIN OF P53
1YOK	A B	B	CRYSTAL STRUCTURE OF HUMAN LRH-1 BOUND WITH TIF-2 PEPTIDE AND PHOSPHATIDYLGLYCE
1Z2C	A B	A	CRYSTAL STRUCTURE OF MDIA1 GBD-FH3 IN COMPLEX WITH RHOC- GMPPNP
1ZNV	C D	C	HOW A HIS-METAL FINGER ENDONUCLEASE COLE7 Binds AND CLEAVES DNA WITH A TRANSITIC
1ZOQ	A C	C	IRF3-CBP COMPLEX
1ZOQ	B D	D	IRF3-CBP COMPLEX
1ZVV	B P	P	CRYSTAL STRUCTURE OF A CCPA-CRH-DNA COMPLEX
2A19	A B	B	PKR KINASE DOMAIN- EIF2ALPHA- AMP-PNP COMPLEX.
2A45	A B	A	CRYSTAL STRUCTURE OF THE COMPLEX BETWEEN THROMBIN AND THE CENTRAL "E" REGION O
2A4J	A B	B	SOLUTION STRUCTURE OF THE C-TERMINAL DOMAIN (T94-Y172) OF THE HUMAN CENTRIN 2 IN C
2AGH	B C	C	STRUCTURAL BASIS FOR COOPERATIVE TRANSCRIPTION FACTOR BINDING TO THE CBP COACTIV
2B5L	A C	C	CRYSTAL STRUCTURE OF DDB1 IN COMPLEX WITH SIMIAN VIRUS 5 V PROTEIN
2CCL	C D	D	THE S45A, T46A MUTANT OF THE TYPE I COHESIN-DOCKERIN COMPLEX FROM THE CELLULOSOM
2DWZ	A B	B	STRUCTURE OF THE ONCOPROTEIN GANKYRIN IN COMPLEX WITH S6 ATPASE OF THE 26S PROTE
2EKV	A B	A	THE CRYSTAL STRUCTURE OF RIGOR LIKE SQUID MYOSIN S1 IN THE ABSENCE OF NUCLEOTIDE
2EKV	A B	A	THE CRYSTAL STRUCTURE OF RIGOR LIKE SQUID MYOSIN S1 IN THE ABSENCE OF NUCLEOTIDE
2ERJ	F H	H	CRYSTAL STRUCTURE OF THE HETERO TRIMERIC INTERLEUKIN-2 RECEPTOR IN COMPLEX WITH
2F93	A B	B	K INTERMEDIATE STRUCTURE OF SENSORY RHODOPSIN II/TRANSDUCER COMPLEX IN COMBINA
2FM8	B C	C	CRYSTAL STRUCTURE OF THE SALMONELLA SECRETION CHAPERONE INV B IN COMPLEX WITH S
2FNJ	A C	A	CRYSTAL STRUCTURE OF A B30.2/SPRY DOMAIN-CONTAINING PROTEIN GUSTAVUS IN COMPLEX'
2FO1	D E	D	CRYSTAL STRUCTURE OF THE CSL-NOTCH-MASTERMIND TERNARY COMPLEX BOUND TO DNA
2FOI	B D	D	SYNTHESIS, BIOLOGICAL ACTIVITY, AND X-RAY CRYSTAL STRUCTURAL ANALYSIS OF DIARYL ET
2G30	A P	P	BETA APPENDAGE OF AP2 COMPLEXED WITH ARH PEPTIDE
2G4D	A B	A	CRYSTAL STRUCTURE OF HUMAN SENP1 MUTANT (C603S) IN COMPLEX WITH SUMO-1
2GPV	A G	G	ESTROGEN RELATED RECEPTOR-GAMMA LIGAND BINDING DOMAIN COMPLEXED WITH 4-HYDRO
2HRK	A B	B	STRUCTURAL BASIS OF YEAST AMINOACYL-TRNA SYNTHETASE COMPLEX FORMATION REVEAL
2HUE	A B	B	STRUCTURE OF THE H3-H4 CHAPERONE ASF1 BOUND TO HISTONES H3 AND H4
2HUE	B C	C	STRUCTURE OF THE H3-H4 CHAPERONE ASF1 BOUND TO HISTONES H3 AND H4
2HWN	A E	E	CRYSTAL STRUCTURE OF RII ALPHA DIMERIZATION/DOCKING DOMAIN OF PKA BOUND TO THE E
2I2R	A E	E	CRYSTAL STRUCTURE OF THE KCHIP1/KV4.3 T1 COMPLEX
2I2R	B F	B	CRYSTAL STRUCTURE OF THE KCHIP1/KV4.3 T1 COMPLEX
2IV8	A P	P	BETA APPENDAGE IN COMPLEX WITH B-ARRESTIN PEPTIDE
2J59	A M	M	CRYSTAL STRUCTURE OF THE ARF1:ARHGAP21-ARFB1 COMPLEX
2JTT	A C	C	SOLUTION STRUCTURE OF CALCIUM LOADED S100A6 BOUND TO C- TERMINAL SIAH-1 INTERACI

TABLE S1

Bullock, et. al

A. PDB CODE	E. FUNCTION	F. $\Delta\Delta G_{AVG,HELIX}$ (KCAL/MOL)	G. $\Delta\Delta G_{SUM, HELIX}$ (KCAL/MOL)	H. $\Delta\Delta G_{SUM, CHAIN}$ (KCAL/MOL)
1OOK	HYDROLASE	2.1	6.2	15.3
1OR7	TRANSCRIPTION	2.2	4.4	31.9
1OR7	TRANSCRIPTION	2.0	4.0	31.9
1OSV	DNA BINDING PROTEIN	2.3	4.6	4.6
1QLS	METAL-BINDING PROTEIN/INHIBITOR	7.8	15.5	15.5
1R4A	PROTEIN TRANSPORT	2.1	4.2	10.5
1R8Q	PROTEIN TRANSPORT/EXCHANGE FACTOR	2.5	4.9	14.3
1RP3	TRANSCRIPTION	2.2	4.4	31.0
1T0F	DNA BINDING PROTEIN	2.2	4.4	18.9
1TTW	CHAPERONE	2.2	4.3	11.4
1TUE	REPLICATION	2.7	8.1	13.8
1TUE	REPLICATION	2.5	5.0	16.6
1U0S	SIGNALING PROTEIN	2.1	4.1	13.7
1U7B	REPLICATION	3.0	6.0	6.0
1U8T	SIGNALING PROTEIN	2.0	5.9	7.6
1VCB	TRANSCRIPTION	2.1	4.1	10.1
1X86	SIGNALING PROTEIN/MEMBRANE PROTEIN	3.1	6.1	14.8
1XCG	SIGNALING PROTEIN ACTIVATOR/SIGNALING PR	2.9	5.8	18.5
1XL3	CELL INVASION	4.0	12.0	16.6
1XLS	TRANSCRIPTION	3.3	6.6	9.5
1XV9	DNA BINDING PROTEIN	2.7	5.4	6.4
1Y3A	SIGNALING PROTEIN	3.1	9.3	9.3
1YCR	COMPLEX (ONCOGENE PROTEIN/PEPTIDE)	3.7	11.1	12.9
1YOK	TRANSCRIPTION	2.8	8.3	8.3
1Z2C	SIGNALING PROTEIN	2.6	5.1	15.1
1ZNV	HYDROLASE/PROTEIN BINDING	2.5	4.9	9.5
1ZOQ	TRANSCRIPTION/TRANSFERASE	2.1	4.2	7.6
1ZOQ	TRANSCRIPTION/TRANSFERASE	2.0	4.0	8.2
1ZVV	TRANSCRIPTION/DNA	2.2	4.4	4.4
2A19	PROTEIN SYNTHESIS/TRANSFERASE	3.4	6.7	6.7
2A45	BLOOD CLOTTING	2.1	4.1	4.1
2A4J	STRUCTURAL PROTEIN	3.1	6.2	14.7
2AGH	TRANSCRIPTION	2.3	6.9	8.2
2B5L	PROTEIN BINDING/VIRAL PROTEIN	2.4	4.7	8.4
2CCL	CELL ADHESION	2.8	5.6	8.3
2DWZ	ONCOPROTEIN	2.4	7.2	12.5
2EKV	CONTRACTILE PROTEIN	2.9	8.6	16.3
2EKV	CONTRACTILE PROTEIN	3.0	5.9	16.3
2ERJ	IMMUNE SYSTEM/CYTOKINE	2.0	3.9	9.7
2F93	MEMBRANE PROTEIN	2.2	4.3	7.2
2FM8	CHAPERONE/CELL INVASION	2.2	4.3	4.3
2FNJ	PROTEIN TRANSPORT/SIGNALING PROTEIN	3.1	6.1	6.1
2FO1	GENE REGULATION/SIGNALLING PROTEIN/DNA	2.2	4.3	5.3
2FOI	OXIDOREDUCTASE	2.9	5.7	8.9
2G30	ENDOCYTOSIS/EXOCYTOSIS	3.3	6.6	11.1
2G4D	HYDROLASE/PROTEIN BINDING	3.6	10.8	17.9
2GPV	TRANSCRIPTION	2.1	4.2	4.2
2HRK	LIGASE/RNA BINDING PROTEIN	2.7	5.3	8.9
2HUE	DNA BINDING PROTEIN	2.1	4.2	7.2
2HUE	DNA BINDING PROTEIN	2.3	4.5	22.5
2HWN	TRANSFERASE	2.1	4.1	4.1
2I2R	TRANSPORT PROTEIN	2.0	3.9	8.3
2I2R	TRANSPORT PROTEIN	3.4	6.7	19.2
2IV8	ENDOCYTOSIS/REGULATOR	2.7	5.4	9.1
2J59	HYDROLASE	2.1	4.2	4.2
2JTT	CALCIUM BINDING PROTEIN/ANTITUMOR PROTEI	2.5	5.0	5.0

TABLE S1

Bullock, et. al

A. PDB CODE	I. HELIX CONTRIBUTION	J. # HOTSPOT RESIDUES	K. HOTSPOT RESIDUES, RESIDUE # ΔΔG (KCAL/MOL)
1OOK	41%	3	E14, 1.9; E14, 2.3; L14, 2.0;
1OR7	14%	2	R171, 1.3; F175, 3.1;
1OR7	13%	2	F22, 1.3; L24, 2.7;
1OSV	100%	2	L5, 3.3; R6, 1.3;
1QLS	100%	2	F6, 1.0; L7, 14.5;
1R4A	40%	2	E2174, 1.3; Y2177, 2.9;
1R8Q	34%	2	L77, 3.0; Y81, 1.9;
1RP3	14%	2	V60, 1.6; K64, 2.8;
1T0F	23%	2	L521, 1.5; R522, 2.9;
1TTW	38%	2	F45, 1.9; V49, 2.4;
1TUE	59%	3	I20, 1.7; Y23, 4.9; E24, 1.5;
1TUE	30%	2	F460, 2.8; I461, 2.2;
1U0S	30%	2	I91, 2.2; I94, 1.9;
1U7B	100%	2	L340, 2.8; F343, 3.2;
1U8T	78%	3	I11, 2.0; D12, 1.5; Q8, 2.4;
1VCB	41%	2	L101, 1.5; L104, 2.6;
1X86	41%	2	D67, 3.5; L69, 2.6;
1XCG	31%	2	L69, 3.7; L72, 2.1;
1XL3	72%	3	F278, 4.7; W279, 4.4; F282, 2.9;
1XLS	69%	2	R426, 2.0; S427, 4.6;
1XV9	84%	2	I632, 4.3; L633, 1.1;
1Y3A	100%	3	W5, 4.2; F8, 3.3; L9, 1.8;
1YCR	86%	3	F19, 2.5; L22, 2.5; W23, 6.1;
1YOK	100%	3	L745, 2.9; L748, 2.7; L749, 2.7;
1Z2C	34%	2	R68, 4.0; L69, 1.1;
1ZNV	52%	2	D52, 1.3; Y55, 3.6;
1ZOQ	55%	2	Q2085, 2.2; I2089, 2.0;
1ZOQ	49%	2	L2096, 1.6; F2100, 2.4;
1ZVV	100%	2	I47, 2.4; M51, 2.0;
2A19	100%	2	F489, 5.3; E490, 1.4;
2A45	100%	2	E14, 1.6; L14, 2.5;
2A4J	42%	2	2, 4.2; 5, 2.0;
2AGH	84%	3	I849, 2.0; F852, 3.8; V853, 1.1;
2B5L	56%	2	V24, 2.1; F27, 2.6;
2CCL	67%	2	K18, 1.9; R19, 3.7;
2DWZ	58%	3	R338, 2.1; R339, 1.4; R342, 3.7;
2EKV	53%	3	W828, 6.2; W829, 1.1; L831, 1.3;
2EKV	36%	2	K819, 2.5; L821, 3.4;
2ERJ	40%	2	H16, 2.9; L19, 1.0;
2F93	60%	2	I69, 2.1; I73, 2.2;
2FM8	100%	2	F54, 3.0; I58, 1.3;
2FNJ	100%	2	L241, 4.7; C245, 1.4;
2FO1	81%	2	L69, 3.1; H70, 1.2;
2FOI	64%	2	F368, 3.9; I369, 1.8;
2G30	59%	2	L11, 1.5; F8, 5.1;
2G4D	60%	3	D468, 3.2; E469, 1.2; N472, 6.4;
2GPV	100%	2	I1324, 2.0; L1328, 2.2;
2HRK	60%	2	R102, 2.2; Y106, 3.1;
2HUE	58%	2	L126, 2.5; I130, 1.7;
2HUE	20%	2	R36, 1.8; L37, 2.7;
2HWN	100%	2	V13, 2.8; M17, 1.3;
2I2R	47%	2	I77, 1.5; Y78, 2.4;
2I2R	35%	2	F11, 1.7; W8, 5.0;
2IV8	59%	2	D3, 1.5; F6, 3.9;
2J59	100%	2	I1053, 2.0; I1057, 2.2;
2JTT	100%	2	I211, 1.8; W215, 3.2;

TABLE S1

Bullock, et. al

A. PDB CODE	L. HOTSPOT RESIDUE HELIX POSITIONS	M. HOTSPOT RESIDUE END TO END LENGTH	N. HELIX LENGTH	O. HELIX START RESIDUE #	P. HELIX END RESIDUE #
1OOK	i; i; 1;	5	7	14	14
1OR7	i; i+4;	5	20	167	186
1OR7	i; i+2;	5	11	19	29
1OSV	i; i+1;	5	8	3	10
1QLS	i; i+1;	2	9	2	10
1R4A	i; i+3;	2	15	2173	2187
1R8Q	i; i+4;	4	8	75	82
1RP3	i; i+4;	5	14	56	69
1T0F	i; i+1;	3	7	521	527
1TTW	i; i+4;	2	7	44	50
1TUE	i; i+3; i+4;	2	23	4	26
1TUE	i; i+1;	4	14	460	473
1U0S	i; i+3;	5	10	87	96
1U7B	i; i+3;	5	5	340	344
1U8T	i; i+3; i+4;	2	7	8	14
1VCB	i; i+3;	5	15	97	111
1X86	i; i+2;	5	5	67	71
1XCG	i; i+3;	2	7	69	75
1XL3	i; i+1; i+4;	4	6	278	283
1XLS	i; i+1;	4	29	414	442
1XV9	i; i+1;	4	7	631	637
1Y3A	i; i+3; i+4;	4	6	5	10
1YCR	i; i+3; i+4;	5	6	19	24
1YOK	i; i+3; i+4;	4	9	743	751
1Z2C	i; i+1;	3	5	67	71
1ZNV	i; i+3;	4	6	51	56
1ZOQ	i; i+4;	5	13	2080	2092
1ZOQ	i; i+4;	5	12	2094	2105
1ZVV	i; i+4;	2	8	47	54
2A19	i; i+1;	2	12	488	499
2A45	i; 1;	5	8	14	14
2A4J	i; i+3;	5	8	2	9
2AGH	i; i+3; i+4;	5	12	847	858
2B5L	i; i+3;	2	11	23	33
2CCL	i; i+1;	3	12	11	22
2DWZ	i; i+1; i+4;	4	14	338	351
2EKV	i; i+1; i+3;	5	5	828	832
2EKV	i; i+3;	5	11	815	825
2ERJ	i; i+3;	5	26	4	29
2F93	i; i+4;	2	27	53	79
2FM8	i; i+4;	2	17	54	70
2FNJ	i; i+4;	4	10	241	250
2FO1	i; i+1;	5	17	68	84
2FOI	i; i+1;	4	12	368	379
2G30	i; i+3;	4	11	5	15
2G4D	i; i+1; i+4;	2	17	468	484
2GPV	i; i+4;	5	10	1321	1330
2HRK	i; i+4;	4	14	98	111
2HUE	i; i+4;	4	11	121	131
2HUE	i; i+1;	3	11	31	41
2HWN	i; i+4;	4	17	4	20
2I2R	i; i+1;	5	12	71	82
2I2R	i; i+3;	5	8	8	15
2IV8	i; i+3;	5	12	2	13
2J59	i; i+4;	2	22	1042	1063
2JTT	i; i+4;	2	14	205	218

TABLE S1

Bullock, et. al

A. PDB CODE	Q. HELIX SEQUENCE	R. RESOLUTION
1OOK	ERELLES	2.30
1OR7	VGTVRSRIFRAREAIDNKVQ	2.00
1OR7	QKAFNLLVVRY	2.00
1OSV	ALLRYLLD	2.50
1QLS	MVSAFLKQA	2.30
1R4A	TEFEYLRKVLFYMM	2.30
1R8Q	RPLWRHYF	1.86
1RP3	LEKKVKEKIEK	2.30
1T0F	LRYIYSQ	1.85
1TTW	RFAYAVL	2.38
1TUE	PKETLSERLSALQDKIIDHYEND	2.10
1TUE	FITFLGALKSFLKG	2.10
1U0S	QAMVIEAIKA	1.90
1U7B	LDDFF	1.88
1U8T	QAEIDAL	1.50
1VCB	PEIALELLMAANFLD	2.70
1X86	DRLRP	3.22
1XCG	LRPLSY	2.50
1XL3	FWQFFS	2.20
1XLS	RFAKLLLRLPALSIGLKCLEHLFFFKLI	2.96
1XV9	KILHRLL	2.70
1Y3A	WYDFLM	2.50
1YCR	FSDLWK	2.60
1YOK	ALLRYLLDK	2.50
1Z2C	DRLRP	3.00
1ZNV	TDLIYY	2.00
1ZOQ	PQQQQQVNLNILKS	2.37
1ZOQ	PQLMAAFIKQRT	2.37
1ZVV	IMGLMSLA	2.98
2A19	AFETSKFFTDLR	2.50
2A45	ERELLESY	3.65
2A4J	WKLLAKGL	NOT APP
2AGH	SDIMDFVLPNT	
2B5L	TVEYFTSQVT	2.85
2CCL	STDLTMLKRSVL	2.03
2DWZ	RRQKRLIFSTITSK	2.40
2EKV	WWRLF	3.40
2EKV	RNVRKWLVLRN	3.40
2ERJ	SSSTKKTQLQLEHLLLQMLNGIN	3.00
2F93	AAAVQEAAVSAILGLIILLGINGLVA	2.00
2FM8	FPALIKQASLDALFKCG	2.20
2FNJ	LMDLCRRTIR	1.80
2FO1	ELHRQRSELARANYEKA	3.12
2FOI	FIDYIAEYSEKY	2.50
2G30	DEAFSRLAQSR	1.60
2G4D	DEINFYMNMLMERSKE	2.80
2GPV	EAIIRKALMG	2.85
2HRK	RHILRWIDYMQNLL	2.05
2HUE	PKDIQLARRIR	1.70
2HUE	KPAIRRLARRG	1.70
2HWN	LAWKIAKMIVSDVMQQC	1.60
2I2R	EDTFKQIYAQFF	3.35
2I2R	WLFPARAA	3.35
2IV8	DDIVFEDFARQR	2.80
2J59	EEDTGVTNRDLISRRKEYNNL	2.10
2JTT	DDMKRTINKAWVES	NOT APP

TABLE S1

Bullock, et. al

A. PDB CODE	B. INTERFACE CHAINS	C. CHAIN	D. TITLE
2K8B	A B	B	SOLUTION STRUCTURE OF PLAA FAMILY UBIQUITIN BINDING DOMAIN (PFUC) CIS ISOMER IN COMPLEX WITH HUMAN UBIQUITIN
2OCF	A D	D	HUMAN ESTROGEN RECEPTOR ALPHA LIGAND-BINDING DOMAIN IN COMPLEX WITH ESTRADIOOL
2OF5	C J	J	OLIGOMERIC DEATH DOMAIN COMPLEX
2OZN	A B	B	THE COHESIN-DOCKERIN COMPLEX OF NAGJ AND NAGH FROM CLOSTRIDIUM PERFRINGENS
2P5T	E F	E	MOLECULAR AND STRUCTURAL CHARACTERIZATION OF THE PEZAT CHROMOSOMAL TOXIN-ANALOGUE BOUND TO THE PEZ-MT1 PROTEIN
2PHE	A C	C	MODEL FOR VP16 BINDING TO PC4
2PMS	A C	C	CRYSTAL STRUCTURE OF THE COMPLEX OF HUMAN LACTOFERRIN N- LOBE AND LACTOFERRIN-ANALOGUE BOUND TO THE PEZ-MT1 PROTEIN
2POP	C D	C	THE CRYSTAL STRUCTURE OF TAB1 AND BIR1 COMPLEX
2PQR	B D	D	CRYSTAL STRUCTURE OF YEAST FIS1 COMPLEXED WITH A FRAGMENT OF YEAST CAF4
2PV9	A B	A	CRYSTAL STRUCTURE OF MURINE THROMBIN IN COMPLEX WITH THE EXTRACELLULAR FRAGMENT OF THE PROTHROMBIN ACTIVATION PROTEIN
2QB0	A D	D	STRUCTURE OF THE 2TEL CRYSTALLIZATION MODULE FUSED TO T4 LYSOZYME WITH AN ALA-GI
2RHK	A C	C	CRYSTAL STRUCTURE OF INFLUENZA A NS1A PROTEIN IN COMPLEX WITH F2F3 FRAGMENT OF HA
2UZ6	E O	O	ACHBP-TARGETED A-CONOTOXIN CORRELATES DISTINCT BINDING ORIENTATIONS WITH NACHR1
2V1S	E L	L	CRYSTAL STRUCTURE OF RAT TOM20-ALDH PRESEQUENCE COMPLEX
2V52	B M	M	STRUCTURE OF MAL-RPEL2 COMPLEXED TO G-ACTIN
2VGO	A D	D	CRYSTAL STRUCTURE OF AURORA B KINASE IN COMPLEX WITH REVERSINE INHIBITOR
2VZD	B D	D	CRYSTAL STRUCTURE OF THE C-TERMINAL CALPONIN HOMOLOGY DOMAIN OF ALPHA PARVIN I
2W2X	B C	B	COMPLEX OF RAC2 AND PLCG2 SPPH DOMAIN
2W2X	B C	C	COMPLEX OF RAC2 AND PLCG2 SPPH DOMAIN
2W84	A B	B	STRUCTURE OF PEX14 IN COMPLEX WITH PEX5
2WAX	A B	B	STRUCTURE OF THE HUMAN DDX6 C-TERMINAL DOMAIN IN COMPLEX WITH AN EDC3-FDF PEPTIDE
2Z2S	G H	H	CRYSTAL STRUCTURE OF RHODOBACTER SPAEROIDES SIGE IN COMPLEX WITH THE ANTI-SIGNAL PEPTIDE
2ZNV	A B	A	CRYSTAL STRUCTURE OF HUMAN AMSH-LP DUB DOMAIN IN COMPLEX WITH LYS63-LINKED UBIQUITIN
2ZSH	A B	B	STRUCTURAL BASIS OF GIBBERELLIN(GA3)-INDUCED DELLA RECOGNITION BY THE GIBBERELLI
3A1G	A B	B	HIGH-RESOLUTION CRYSTAL STRUCTURE OF RNA POLYMERASE PB1-PB2 SUBUNITS FROM INFLUENZA VIRUS
3BLH	A B	B	CRYSTAL STRUCTURE OF HUMAN CDK9/CYCLINT1
3BS5	A B	A	CRYSTAL STRUCTURE OF HCNK2-SAM/DHYP-SAM COMPLEX
3CJT	A B	A	RIBOSOMAL PROTEIN L11 METHYLTRANSFERASE (PRMA) IN COMPLEX WITH DIMETHYLATED RIBOSOMAL PROTEIN L11
3CPH	G A	G	CRYSTAL STRUCTURE OF SEC4 IN COMPLEX WITH RAB-GDI
3CQX	B C	C	CHAPERONE COMPLEX
3D24	A B	B	CRYSTAL STRUCTURE OF LIGAND-BINDING DOMAIN OF ESTROGEN- RELATED RECEPTOR ALPHA
3D48	P R	P	CRYSTAL STRUCTURE OF A PROLACTIN RECEPTOR ANTAGONIST BOUND TO THE EXTRACELLULAR DOMAIN OF THE PROLACTIN RECEPTOR
3DA7	A D	D	A CONFORMATIONALLY STRAINED, CIRCULAR PERMUTANT OF BARNASE
3DAB	E F	F	STRUCTURE OF THE HUMAN MDMX PROTEIN BOUND TO THE P53 TUMOR SUPPRESSOR TRANSMER
3EBA	A B	B	CABHUL6 FGLW MUTANT (HUMANIZED) IN COMPLEX WITH HUMAN LYSOZYME
3ECH	A C	C	THE MARR-FAMILY REPRESSOR MXR IN COMPLEX WITH ITS ANTIREPRESSOR ARMRE
3EG5	A B	A	CRYSTAL STRUCTURE OF MDIA1-TSH GBD-FH3 IN COMPLEX WITH CDC42-GMPPNP
3F75	A P	P	ACTIVATED TOXOPLASMA GONDII CATHEPSIN L (TGCPL) IN COMPLEX WITH ITS PROPEPTIDE
3F9K	B C	B	TWO DOMAIN FRAGMENT OF HIV-2 INTEGRASE IN COMPLEX WITH LEDGF IBD
3FMP	A B	B	CRYSTAL STRUCTURE OF THE NUCLEOPORIN NUP214 IN COMPLEX WITH THE DEAD-BOX HELICASE
3FUB	C D	C	CRYSTAL STRUCTURE OF GDNF-GFRALPHA1 COMPLEX
3GCG	A B	B	CRYSTAL STRUCTURE OF MAP AND CDC42 COMPLEX
3H2U	A B	A	HUMAN RAVER1 RRM1, RRM2, AND RRM3 DOMAINS IN COMPLEX WITH HUMAN VINCULIN TAIL I
3H9R	A B	A	CRYSTAL STRUCTURE OF THE KINASE DOMAIN OF TYPE I ACTIVIN RECEPTOR (ACVR1) IN COMPLEX WITH HUMAN VINCULIN TAIL I
1A93	A B	B	NMR SOLUTION STRUCTURE OF THE C-MYC-MAX HETERODIMERIC LEUCINE ZIPPER, NMR, MINI
1AVO	C D	D	PROTEASOME ACTIVATOR REG(ALPHA)
1BCC	D H	H	CYTOCHROME BC1 COMPLEX FROM CHICKEN
1BIQ	A B	A	RIBONUCLEOSIDE-DIPHOSPHATE REDUCTASE 1 BETA CHAIN MUTANT E238A
1BIQ	A B	B	RIBONUCLEOSIDE-DIPHOSPHATE REDUCTASE 1 BETA CHAIN MUTANT E238A
1BP3	A B	A	THE XRAY STRUCTURE OF A GROWTH HORMONE-PROLACTIN RECEPTOR COMPLEX
1CKK	A B	B	CALMODULIN/RAT CA2+/CALMODULIN DEPENDENT PROTEIN KINASE FRAGMENT
1CP9	A B	A	CRYSTAL STRUCTURE OF PENICILLIN G ACYLASE FROM THE BRO1 MUTANT STRAIN OF PROVIDER
1CUL	A B	A	COMPLEX OF GS-ALPHA WITH THE CATALYTIC DOMAINS OF MAMMALIAN ADENYLYL CYCLASE
1DE4	G I	G	HEMOCHROMATOSIS PROTEIN HFE COMPLEXED WITH TRANSFERRIN RECEPTOR
1DKF	A B	A	CRYSTAL STRUCTURE OF A HETERO DIMERIC COMPLEX OF RAR AND RXR LIGAND-BINDING DOMAINS
1DML	A B	B	CRYSTAL STRUCTURE OF HERPES SIMPLEX UL42 BOUND TO THE C- TERMINUS OF HSV POL

TABLE S1

Bullock, et. al

A. PDB CODE	E. FUNCTION	F. $\Delta\Delta G_{AVG,HELIX}$ (KCAL/MOL)	G. $\Delta\Delta G_{SUM, HELIX}$ (KCAL/MOL)	H. $\Delta\Delta G_{SUM, CHAIN}$ (KCAL/MOL)
2K8B	PROTEIN BINDING	2.1	6.4	6.4
2OCF	HORMONE/GROWTH FACTOR	2.2	4.4	4.4
2OF5	APOPTOSIS	3.5	7.0	7.0
2OZN	TOXIN	2.3	4.5	7.0
2P5T	TRANSCRIPTION REGULATOR	2.1	4.2	17.9
2PHE	TRANSCRIPTION	2.5	7.6	7.6
2PMS	METAL TRANSPORT, HYDROLASE	2.0	4.0	8.1
2POP	SIGNALING PROTEIN/APOPTOSIS	2.3	7.0	7.0
2PQR	APOPTOSIS	2.9	5.7	22.6
2PV9	HYDROLASE	2.2	4.4	8.5
2QB0	HYDROLASE REGULATOR	2.1	4.2	10.6
2RHK	VIRAL PROTEIN/NUCLEAR PROTEIN	2.0	4.0	13.8
2UZ6	RECEPTOR	4.2	8.4	10.6
2V1S	OXIDOREDUCTASE	2.8	5.5	5.5
2V52	STRUCTURAL PROTEIN/CONTRACTILE PROTEIN	2.0	6.0	13.8
2VGO	TRANSFERASE	2.0	3.9	20.1
2VZD	CELL ADHESION	2.6	5.1	7.6
2W2X	SIGNALING PROTEIN/HYDROLASE	2.1	4.1	4.1
2W2X	SIGNALING PROTEIN/HYDROLASE	2.9	5.8	5.8
2W84	PROTEIN TRANSPORT	4.1	8.1	8.1
2WAX	HYDROLASE	2.0	3.9	18.7
2Z2S	TRANSCRIPTION	2.0	3.9	9.5
2ZNV	HYDROLASE/SIGNALING PROTEIN	2.2	4.4	9.0
2ZSH	HORMONE RECEPTOR	2.4	4.8	12.3
3A1G	TRANSFERASE	2.1	6.4	9.1
3BLH	TRANSCRIPTION	2.7	5.3	11.8
3BS5	SIGNALING PROTEIN/MEMBRANE PROTEIN	2.2	4.4	8.3
3CJT	TRANSFERASE/RIBOSOMAL PROTEIN	4.0	8.0	24.6
3CPH	PROTEIN TRANSPORT	2.4	4.8	8.8
3CQX	CHAPERONE	2.2	4.4	7.4
3D24	TRANSCRIPTION	2.1	6.4	7.5
3D48	HORMONE/HORMONE RECEPTOR	2.4	7.2	16.3
3DA7	PROTEIN BINDING	3.6	7.1	14.6
3DAB	CELL CYCLE	3.5	6.9	8.2
3EBA	IMMUNE SYSTEM/HYDROLASE	3.6	7.2	11.4
3ECH	TRANSCRIPTION, TRANSCRIPTION REGULATION	5.7	11.3	12.4
3EG5	SIGNALING PROTEIN	2.6	7.8	17.2
3F75	HYDROLASE	2.6	5.1	19.6
3F9K	VIRAL PROTEIN, RECOMBINATION	2.0	3.9	5.4
3FMP	ONCOPROTEIN/HYDROLASE	2.1	6.2	8.7
3FUB	HORMONE	2.1	4.2	5.3
3GCG	SIGNALING PROTEIN/TRANSCRIPTION	2.2	4.4	13.7
3H2U	CELL ADHESION	2.6	5.1	7.2
3H9R	ISOMERASE/PROTEIN KINASE	2.0	3.9	6.6
1A93	LEUCINE ZIPPER	2.0	7.9	7.9
1AVO	PROTEASOME ACTIVATOR	2.0	7.8	18.5
1bcc	OXIDOREDUCTASE	5.5	11.0	15.5
1BIQ	OXIDOREDUCTASE	2.4	7.2	37.3
1BIQ	OXIDOREDUCTASE	2.2	6.7	33.2
1BP3	HORMONE/GROWTH FACTOR	2.0	3.9	14.4
1CKK	CALMODULIN-PEPTIDE COMPLEX	2.6	5.1	11.6
1CP9	HYDROLASE	2.9	11.5	68.9
1CUL	LYASE/LYASE/SIGNALING PROTEIN	2.3	4.5	9.3
1DE4	METAL TRANSPORT INHIBITOR/RECEPTOR	2.7	10.6	14.5
1DKF	HORMONE/GROWTH FACTOR RECEPTOR	2.6	5.2	8.1
1DML	DNA BINDING PROTEIN/TRANSFERASE	3.1	9.2	12.1

TABLE S1

Bullock, et. al

A. PDB CODE	I. HELIX CONTRIBUTION	J. # HOTSPOT RESIDUES	K. HOTSPOT RESIDUES, RESIDUE # ΔΔG (KCAL/MOL)
2K8B	100%	3	M105, 1.4; F106, 2.3; Q109, 2.7;
2OCF	100%	2	L78, 2.3; L82, 2.1;
2OF5	100%	2	D864, 5.2; E867, 1.8;
2OZN	64%	2	I1588, 3.1; L1591, 1.4;
2P5T	23%	2	H123, 2.1; Y127, 2.1;
2PHE	100%	3	F475, 3.0; E476, 1.1; F479, 3.5;
2PMS	49%	2	E182, 2.8; N183, 1.2;
2POP	100%	3	E2212, 2.4; D2213, 1.4; F2216, 3.2;
2PQR	25%	2	F101, 3.8; R102, 1.9;
2PV9	52%	2	E14(E), 2.5; L14(F), 1.9;
2QB0	40%	2	D79, 2.4; V80, 1.8;
2RHK	29%	2	Y97, 1.7; F98, 2.3;
2UZ6	79%	2	C8, 7.0; N11, 1.4;
2V1S	100%	2	R17, 2.0; Y21, 3.5;
2V52	43%	3	L118, 2.7; K119, 1.6; I122, 1.7;
2VGO	19%	2	L833, 1.4; L836, 2.5;
2VZD	67%	2	L7, 3.1; L8, 2.0;
2W2X	100%	2	L67, 2.5; L70, 1.6;
2W2X	100%	2	F102, 3.5; V98, 2.3;
2W84	100%	2	W103, 4.9; F107, 3.2;
2WAX	21%	2	F206, 2.3; L210, 1.6;
2Z2S	41%	2	S65, 1.0; L66, 2.9;
2ZNV	49%	2	E329, 1.4; F332, 3.0;
2ZSH	39%	2	L50, 2.1; E51, 2.7;
3A1G	70%	3	R3, 2.8; I4, 2.2; L7, 1.4;
3BLH	45%	2	F89, 2.2; K93, 3.1;
3BS5	53%	2	R57, 2.4; R61, 2.0;
3CJT	33%	2	W59, 4.5; W63, 3.5;
3CPH	55%	2	R248, 3.5; I252, 1.3;
3CQX	59%	2	Q156, 1.6; I160, 2.8;
3D24	85%	3	L210, 2.6; Y213, 2.1; L214, 1.7;
3D48	44%	3	R177, 4.6; H180, 1.1; K181, 1.5;
3DA7	49%	2	D36, 1.3; D40, 5.8;
3DAB	84%	2	F19, 3.3; W23, 3.6;
3EBA	63%	2	D91, 2.0; C95, 5.2;
3ECH	91%	2	W45, 7.0; Y48, 4.3;
3EG5	45%	3	R66, 4.7; L67, 1.3; L70, 1.8;
3F75	26%	2	R170, 2.6; F173, 2.5;
3F9K	72%	2	M128, 1.3; W131, 2.6;
3FMP	71%	3	D255, 1.7; Q256, 1.2; R259, 3.3;
3FUB	79%	2	R171, 2.5; I175, 1.7;
3GCG	32%	2	I156, 1.3; F159, 3.1;
3H2U	71%	2	L928, 1.2; E932, 3.9;
3H9R	59%	2	W245, 2.1; F246, 1.8;
1A93	100%	4	N10, 2.3; H13, 1.9; I17, 1.7; L20, 2.0;
1AVO	42%	4	H202, 1.4; Y209, 2.7; V216, 1.3; R220, 2.4;
1BCC	71%	2	F59, 3.8; F74, 7.2;
1BIQ	19%	3	D158, 3.2; Y166, 1.4; L169, 2.6;
1BIQ	20%	3	L82, 1.3; I86, 1.0; R89, 4.4;
1BP3	27%	2	H18, 1.0; F25, 2.9;
1CKK	44%	2	W7, 3.5; K14, 1.6;
1CP9	17%	4	L25, 2.4; F26, 2.3; Y29, 5.0; D36, 1.8;
1CUL	48%	2	V413, 1.9; D424, 2.6;
1DE4	73%	4	H74, 1.9; T77, 2.8; V78, 4.2; W81, 1.7;
1DKF	64%	2	E395, 1.7; Y402, 3.5;
1DML	76%	3	L1227, 1.2; F1231, 5.3; L1234, 2.7;

TABLE S1

Bullock, et. al

A. PDB CODE	L. HOTSPOT RESIDUE HELIX POSITIONS	M. HOTSPOT RESIDUE END TO END LENGTH	N. HELIX LENGTH	O. HELIX START RESIDUE #	P. HELIX END RESIDUE #
2K8B	i; i+1; i+4;	4	17	104	120
2OCF	i; i+4;	5	7	78	84
2OF5	i; i+3;	5	12	863	874
2OZN	i; i+3;	5	10	1588	1597
2P5T	i; i+4;	5	19	110	128
2PHE	i; i+1; i+4;	2	6	475	480
2PMS	i; i+1;	5	19	174	192
2POP	i; i+1; i+4;	2	11	2212	2222
2PQR	i; i+1;	4	9	97	105
2PV9	i; i+1;	3	6	14E	14F
2QB0	i; i+1;	4	14	78	91
2RHK	i; i+1;	5	6	97	102
2UZ6	i; i+3;	5	7	6	12
2V1S	i; i+4;	5	9	15	23
2V52	i; i+1; i+4;	5	9	116	124
2VGO	i; i+3;	5	5	833	837
2VZD	i; i+1;	4	10	2	11
2W2X	i; i+3;	4	9	65	73
2W2X	i; i+4;	5	16	98	113
2W84	i; i+4;	5	17	94	110
2WAX	i; i+4;	2	7	206	212
2Z2S	i; i+1;	5	5	65	69
2ZNV	i; i+3;	2	10	329	338
2ZSH	i; i+1;	4	16	43	58
3A1G	i; i+1; i+4;	2	8	3	10
3BLH	i; i+4;	2	16	80	95
3BS5	i; i+4;	2	7	56	62
3CJT	i; i+4;	4	8	59	66
3CPH	i; i+4;	5	15	239	253
3CQX	i; i+4;	3	10	153	162
3D24	i; i+3; i+4;	5	8	208	215
3D48	i; i+3; i+4;	4	34	161	194
3DA7	i; i+4;	2	9	35	43
3DAB	i; i+4;	5	8	19	26
3EBA	i; i+4;	5	11	90	100
3ECH	i; i+3;	2	7	44	50
3EG5	i; i+1; i+4;	4	9	65	73
3F75	i; i+3;	2	8	170	177
3F9K	i; i+3;	5	11	124	134
3FMP	i; i+1; i+4;	5	11	253	263
3FUB	i; i+4;	5	15	165	179
3GCG	i; i+3;	5	24	155	178
3H2U	i; i+4;	5	21	918	938
3H9R	i; i+1;	5	14	242	255
1A93	i; i+3; i+7; i+10;	11	29	6	34
1AVO	i; i+7; i+14; i+18;	19	39	195	233
1bcc	i; i+15;	16	23	55	77
1BIQ	i; i+8; i+11;	16	19	153	171
1BIQ	i; i+4; i+7;	13	32	67	98
1BP3	i; i+7;	12	30	6	35
1CKK	i; i+7;	8	11	7	17
1CP9	i; i+1; i+4; i+11;	8	16	22	37
1CUL	i; i+11;	12	22	409	430
1DE4	i; i+3; i+4; i+7;	16	28	59	86
1DKF	i; i+7;	8	23	391	413
1DML	i; i+4; i+7;	12	16	1220	1235

TABLE S1

Bullock, et. al

A. PDB CODE	Q. HELIX SEQUENCE	R. RESOLUTION
2K8B	PMFLDQVAKFIIDNTKG	NOT APP
2OCF	LRLMLAG	2.95
2OF5	QDVAEEVRAVLE	3.20
2OZN	IGDLAMVSKN	1.60
2P5T	PWILMSDDLSLDLIHTNIYL	3.20
2PHE	FEQMFT	NOT APP
2PMS	PQAKIAELENQVHRLEQEL	2.91
2POP	EDELFRLSQLG	3.10
2PQR	SATTFRILA	1.88
2PV9	EKELLD	3.50
2QB0	GDVLYELLQHILKQ	2.56
2RHK	YFYSKF	1.95
2UZ6	PPCILNN	2.40
2V1S	LSRLLSYAG	2.05
2V52	DYLKRKIRS	1.45
2VGO	LEELF	1.70
2VZD	DDLDALLADL	2.10
2W2X	DRLRPLSYP	2.30
2W2X	VEELFEWFQSIREITW	2.30
2W84	VADLALSENWAQEFLAA	NOT APP
2WAX	FEGNLAL	2.30
2Z2S	SLASV	2.70
2ZNV	EELFNVQDQH	1.60
2ZSH	MADVAQKLEQLEVMMMS	1.80
3A1G	RIKELRNL	1.70
3BLH	GNSVAPAAFLAAKVE	2.48
3BS5	GRALLRI	2.00
3CJT	WLEAWRRD	2.30
3CPH	LGEELPQGFARLSAIY	2.90
3CQX	QKFQSIVIGC	2.30
3D24	SELLKYLT	2.11
3D48	EESRLSAYYNLLHCLRRDSHKIDNYLKLLKCRII	2.50
3DA7	LDALWDCLT	2.25
3DAB	FSDLWKLL	1.90
3EBA	ADAVACAKRVV	1.85
3ECH	AWDLYGE	1.80
3EG5	DRLRPLSYP	2.70
3F75	RDEFRRKY	1.99
3F9K	QEVKMVAWWIG	3.20
3FMP	HQDQSIRIQRM	3.19
3FUB	DTCKKYRSAYITPC	2.35
3GCG	PITRFNTQTQMIEQVSQEIFERNF	2.30
3H2U	DIIAAAKRMALLMAEMSRLVR	2.75
3H9R	EKSWFRETELYNTV	2.35
1A93	MRRKNDTHQQDIDDLKRQNALLEQQVRAL	NOT APP
1AV0	GDYRQLVHELDEAEYRDIRLMVMEIRNAYAVLYDIILKN	2.80
1BCC	TEELFDLFLHARDHCVAHKLFNSL	3.16
1BIQ	ISSYYDELIEMTSYWHLLG	2.05
1BIQ	EHEKHIFISNLKYQTLLDSIQGRSPNVALLPL	2.05
1BP3	LSRLFDNAMLRAHRLHQAFDTYQEFEAY	2.90
1CKK	WTIVLVKMSL	NOT APP
1CP9	TYSLFYGYGYAVAQDR	2.50
1CUL	AQELVMTLNELFARFDKLAAEN	2.40
1DE4	SQMWLQLSQLSKGWDHMFTVDFWTIMEN	2.80
1DKF	PAEVEALREKVYASLEAYCKHKY	2.50
1DML	AEETRRMLHRAFDTLA	2.70

TABLE S1

Bullock, et. al

A. PDB CODE	B. INTERFACE CHAINS	C. CHAIN	D. TITLE
1E7P	E F	E	QUINOL:FUMARATE REDUCTASE FROM WOLINELLA SUCCINOGENES
1EFU	C D	D	ELONGATION FACTOR COMPLEX EF-TU/EF-TS FROM ESCHERICHIA COLI
1F80	A E	A	HOLO-(ACYL CARRIER PROTEIN) SYNTHASE IN COMPLEX WITH HOLO- (ACYL CARRIER PROTEIN
1FM6	A D	A	THE 2.1 ANGSTROM RESOLUTION CRYSTAL STRUCTURE OF THE HETERO-DIMER OF THE HUMAN
1G73	A C	A	CRYSTAL STRUCTURE OF SMAC BOUND TO XIAP-BIR3 DOMAIN
1GX7	A D	A	BEST MODEL OF THE ELECTRON TRANSFER COMPLEX BETWEEN CYTOCHROME C3 AND [FE]-HY-
1H4L	B E	E	STRUCTURE AND REGULATION OF THE CDK5-P25(NCK5A) COMPLEX
1HX1	A B	B	CRYSTAL STRUCTURE OF A BAG DOMAIN IN COMPLEX WITH THE HSC70 ATPASE DOMAIN
1I1R	A B	B	CRYSTAL STRUCTURE OF A CYTOKINE/RECEPTOR COMPLEX
1I2M	C D	C	RAN-RCC1-SO4 COMPLEX
1I5K	A C	C	STRUCTURE AND BINDING DETERMINANTS OF THE RECOMBINANT KRINGLE-2 DOMAIN OF HUM
1IBR	A B	B	COMPLEX OF RAN WITH IMPORTIN BETA
1J7D	A B	A	CRYSTAL STRUCTURE OF HMMS2-HUBC13
1JEK	A B	B	VISNA TM CORE STRUCTURE
1JYO	A F	A	STRUCTURE OF THE SALMONELLA VIRULENCE EFFECTOR SPTP IN COMPLEX WITH ITS SECRETIC
1LDK	A D	A	STRUCTURE OF THE CUL1-RBX1-SKP1-F BOXSKP2 SCF UBIQUITIN LIGASE COMPLEX
1LQB	A B	B	CRYSTAL STRUCTURE OF A HYDROXYLATED HIF-1 ALPHA PEPTIDE BOUND TO THE PVHL/ELONG
1M1E	A B	A	BETA-CATENIN ARMADILLO REPEAT DOMAIN BOUND TO ICAT
1N1J	A B	A	CRYSTAL STRUCTURE OF THE NF-YB/NF-YC HISTONE PAIR
1N1J	A B	A	CRYSTAL STRUCTURE OF THE NF-YB/NF-YC HISTONE PAIR
1NGM	E F	F	CRYSTAL STRUCTURE OF A YEAST BRF1-TBP-DNA TERNARY COMPLEX
1NH2	B D	B	CRYSTAL STRUCTURE OF A YEAST TFIIA/TBP/DNA COMPLEX
1NH2	B D	B	CRYSTAL STRUCTURE OF A YEAST TFIIA/TBP/DNA COMPLEX
1NH2	B D	D	CRYSTAL STRUCTURE OF A YEAST TFIIA/TBP/DNA COMPLEX
1NU7	B D	D	STAPHYLOCOAGULASE-THROMBIN COMPLEX
1NU9	D F	F	STAPHYLOCOAGULASE-PRETHROMBIN-2 COMPLEX
1NVM	G H	G	CRYSTAL STRUCTURE OF A BIFUNCTIONAL ALDOLASE-DEHYDROGENASE : SEQUESTERING A RE
1OR0	A B	A	CRYSTAL STRUCTURES OF GLUTARYL 7-AMINOCEPHALOSPORANIC ACID ACYLASE: INSIGHT INTI
1OR7	A C	C	CRYSTAL STRUCTURE OF ESCHERICHIA COLI SIGMAE WITH THE CYTOPLASMIC DOMAIN OF ITS
1OXK	A B	B	COMPLEX BETWEEN YPD1 AND SLN1 RESPONSE REGULATOR DOMAIN IN SPACE GROUP P3(2)
1R4M	A B	A	APPBP1-UBA3-NEDD8, AN E1-UBIQUITIN-LIKE PROTEIN COMPLEX
1TI2	A B	B	CRYSTAL STRUCTURE OF PYROGALLOL-PHLOROGLUCINOL TRANSHYDROXYLASE FROM PELOB
1TQY	A B	B	THE ACTINORHODIN KETOSYNTHASE/CHAIN LENGTH FACTOR
1TY4	A C	C	CRYSTAL STRUCTURE OF A CED-9/EGL-1 COMPLEX
1UKV	G Y	G	STRUCTURE OF RABGDP-DISSOCIATION INHIBITOR IN COMPLEX WITH PRENYLATED YPT1 GTPA <sup>S</sup>
1VF6	A C	C	2.1 ANGSTROM CRYSTAL STRUCTURE OF THE PALS-1-L27N AND PATJ L27 HETERO-DIMER COMPLE
1VG9	G H	G	THE CRYSTAL STRUCTURES OF THE REP-1 PROTEIN IN COMPLEX WITH C-TERMINALLY TRUNCAT
1WA8	A B	A	SOLUTION STRUCTURE OF THE CFP-10-ESAT-6 COMPLEX. MAJOR VIRULENCE DETERMINANTS OF
1WPX	A B	A	CRYSTAL STRUCTURE OF CARBOXYPEPTIDASE Y INHIBITOR COMPLEXED WITH THE COGNATE P
1WPX	A B	B	CRYSTAL STRUCTURE OF CARBOXYPEPTIDASE Y INHIBITOR COMPLEXED WITH THE COGNATE P
1XB2	A B	A	CRYSTAL STRUCTURE OF BOS TAURUS MITOCHONDRIAL ELONGATION FACTOR TU/TS COMPLEX
1XKP	B C	C	CRYSTAL STRUCTURE OF THE VIRULENCE FACTOR YOPN IN COMPLEX WITH ITS HETERO-DIMERI
1Y76	C B	C	SOLUTION STRUCTURE OF PATJ/PALS1 L27 DOMAIN COMPLEX
1YDI	A B	B	HUMAN VINCULIN HEAD DOMAIN (VH1, 1-258) IN COMPLEX WITH HUMAN ALPHA-ACTININ'S VIN
1YKE	C D	D	STRUCTURE OF THE MEDIATOR MED7/MED21 SUBCOMPLEX
1ZL8	A B	A	NMR STRUCTURE OF L27 HETERO-DIMER FROM C. ELEGANS LIN-7 AND H. SAPIENS LIN-2 SCAFFO
2A6Q	A E	A	CRYSTAL STRUCTURE OF YEFM-YOEB COMPLEX
2AFF	A B	B	THE SOLUTION STRUCTURE OF THE K167FHA/HNIFK(226-269)3P COMPLEX
2AVU	B E	E	STRUCTURE OF THE ESCHERICHIA COLI FLHDC COMPLEX, A PROKARYOTIC HETERO-MERIC REGI
2BGN	B E	E	HIV-1 TAT PROTEIN DERIVED N-TERMINAL NONAPEPTIDE TRP2-TAT (1-9) BOUND TO THE ACTIVE
2BNQ	A E	A	STRUCTURAL AND KINETIC BASIS FOR HEIGHTENED IMMUNOGENICITY OF T CELL VACCINES
2BYK	D C	D	HISTONE FOLD HETERO-DIMER OF THE CHROMATIN ACCESSIBILITY COMPLEX
2BYK	D C	D	HISTONE FOLD HETERO-DIMER OF THE CHROMATIN ACCESSIBILITY COMPLEX
2C5I	T P	P	N-TERMINAL DOMAIN OF TLG1 COMPLEXED WITH N-TERMINUS OF VPS51 IN DISTORTED CONFO
2C9W	B C	C	CRYSTAL STRUCTURE OF SOCS-2 IN COMPLEX WITH ELONGIN-B AND ELONGIN-C AT 1.9A RESOLU
2CJS	A C	A	STRUCTURAL BASIS FOR A MUNC13-1 DIMERIC - MUNC13-1 - RIM HETERO-DIMER SWITCH: C2-DO

TABLE S1

Bullock, et. al

A. PDB CODE	E. FUNCTION	F. $\Delta\Delta G_{AVG,HELIX}$ (KCAL/MOL)	G. $\Delta\Delta G_{SUM, HELIX}$ (KCAL/MOL)	H. $\Delta\Delta G_{SUM, CHAIN}$ (KCAL/MOL)
1E7P	OXIDOREDUCTASE	2.5	5.0	14.7
1EFU	COMPLEX (TWO ELONGATION FACTORS)	2.9	8.8	19.5
1F80	TRANSFERASE	2.3	9.2	12.3
1FM6	TRANSCRIPTION	2.0	6.1	7.6
1G73	APOPTOSIS/APOPTOSIS INHIBITOR	3.3	13.2	13.2
1GX7	OXIDOREDUCTASE	2.8	8.5	40.2
1H4L	KINASE/KINASE ACTIVATOR	2.3	6.9	9.1
1HX1	CHAPERONE/CHAPERONE INHIBITOR	2.5	4.9	11.1
1I1R	CYTOKINE	2.3	7.0	8.2
1I2M	CELL CYCLE	2.1	8.2	13.3
1I5K	BLOOD CLOTTING	2.7	8.0	8.0
1IBR	CELL CYCLE, TRANSLATION	2.1	4.1	20.4
1J7D	UNKNOWN FUNCTION	2.2	6.6	6.6
1JEK	VIRAL PROTEIN	2.2	8.6	12.5
1JYO	CHAPERONE	2.5	5.0	6.5
1LDK	LIGASE	2.3	6.9	6.9
1LQB	GENE REGULATION	2.3	9.0	12.1
1M1E	STRUCTURAL PROTEIN	2.4	4.8	15.4
1N1J	DNA BINDING PROTEIN	4.3	17.3	23.2
1N1J	DNA BINDING PROTEIN	2.0	4.0	23.2
1NGM	TRANSCRIPTION/DNA	2.6	5.2	15.8
1NH2	TRANSCRIPTION/DNA	2.2	8.7	20.3
1NH2	TRANSCRIPTION/DNA	2.5	10.0	20.3
1NH2	TRANSCRIPTION/DNA	2.3	6.8	9.3
1NU7	HYDROLASE/PROTEIN BINDING	2.0	6.1	15.2
1NU9	HYDROLASE/PROTEIN BINDING	3.2	6.3	7.4
1NVM	LYASE/OXIDOREDUCTASE	2.1	6.3	17.2
1OR0	HYDROLASE	2.2	10.8	58.0
1OR7	TRANSCRIPTION	2.0	5.9	33.3
1OXK	SIGNALING PROTEIN	2.7	8.2	11.7
1R4M	CELL CYCLE	2.1	6.3	24.4
1TI2	OXIDOREDUCTASE	2.1	6.3	52.3
1TQY	TRANSFERASE	2.2	8.8	30.6
1TY4	APOPTOSIS	2.1	8.4	13.8
1UKV	PROTEIN TRANSPORT	2.3	9.0	18.5
1VF6	PROTEIN BINDING/PROTEIN TRANSPORT	2.0	3.9	21.9
1VG9	PROTEIN BINDING/PROTEIN TRANSPORT	2.2	6.6	10.1
1WA8	TUBERCULOSIS	4.2	12.6	29.6
1WPX	HYDROLASE	2.4	4.7	16.8
1WPX	HYDROLASE	2.6	5.2	20.3
1XB2	TRANSLATION	2.2	6.7	10.7
1XKP	MEMBRANE PROTEIN/CHAPERON	2.1	8.5	12.2
1Y76	TRANSPORT PROTEIN	5.9	17.7	24.0
1YDI	CELL ADHESION, STRUCTURAL PROTEIN	2.4	16.6	16.6
1YKE	GENE REGULATION	2.9	8.7	11.9
1ZL8	PROTEIN BINDING	2.2	4.3	25.2
2A6Q	TOXIN INHIBITOR/TOXIN	2.1	8.5	15.0
2AFF	CELL CYCLE	3.0	11.9	11.9
2AVU	TRANSCRIPTION ACTIVATOR	2.8	5.5	8.4
2BGN	HYDROLASE	2.3	6.8	15.1
2BNQ	IMMUNE SYSTEM/RECEPTOR	2.2	6.6	6.6
2BYK	DNA-BINDING PROTEIN	2.5	10.1	26.1
2BYK	DNA-BINDING PROTEIN	2.7	5.4	26.1
2C5I	PROTEIN TRANSPORT	2.1	6.4	9.4
2C9W	TRANSCRIPTION REGULATION	2.4	4.7	12.0
2CJS	EXOCYTOSIS	2.1	6.2	11.6

TABLE S1

Bullock, et. al

A. PDB CODE	I. HELIX CONTRIBUTION	J. # HOTSPOT RESIDUES	K. HOTSPOT RESIDUES, RESIDUE # ΔΔG (KCAL/MOL)
1E7P	34%	2	Q225, 3.6; V236, 1.4;
1EFU	45%	3	F271, 4.4; V275, 3.4; M278, 1.0;
1F80	75%	4	R21, 1.7; R24, 2.4; F25, 1.2; R28, 3.9;
1FM6	80%	3	E394, 1.8; Y397, 3.1; E401, 1.2;
1G73	100%	4	H92, 5.3; Y95, 2.8; L96, 1.3; E99, 3.8;
1GX7	21%	3	F147, 2.5; W154, 4.1; E155, 1.9;
1H4L	76%	3	W258, 3.6; L262, 1.8; I265, 1.5;
1HX1	44%	2	R237, 2.8; D252, 2.1;
1I1R	85%	3	L11, 1.1; R15, 2.4; W18, 3.5;
1I2M	62%	4	N103, 1.0; R106, 3.2; D107, 2.0; R110, 2.0;
1I5K	100%	3	L310, 2.5; L313, 1.5; R317, 4.0;
1IBR	20%	2	E281, 2.7; D288, 1.4;
1J7D	100%	3	F13, 4.6; E17, 1.0; E20, 1.0;
1JEK	69%	4	W631, 1.7; I635, 1.3; H638, 3.1; L642, 2.5;
1JYO	77%	2	E111, 2.2; E118, 2.8;
1LDK	100%	3	M43, 1.3; Y46, 1.0; Y50, 4.6;
1LQB	74%	4	H68, 3.0; M75, 1.1; Y79, 1.4; R82, 3.5;
1M1E	31%	2	T653, 1.1; F660, 3.7;
1N1J	75%	4	Y128, 2.4; L132, 1.5; Y135, 1.4; L136, 12.0;
1N1J	17%	2	V84, 1.1; I92, 2.9;
1NGM	33%	2	S480, 1.5; W487, 3.7;
1NH2	43%	4	L38, 2.1; W42, 3.7; K45, 1.6; L46, 1.3;
1NH2	49%	4	V9, 1.0; Y10, 5.0; I13, 2.4; V17, 1.6;
1NH2	73%	3	I15, 3.3; L19, 2.0; L26, 1.5;
1NU7	40%	3	L67, 3.0; Q71, 2.1; L74, 1.0;
1NU9	85%	2	K59, 4.9; L67, 1.4;
1NVM	37%	3	M328, 1.6; D331, 3.6; D335, 1.1;
1OR0	19%	5	F39, 1.7; Y40, 2.8; Y42, 2.5; Q46, 2.5;
1OR7	18%	3	I55, 1.9; V59, 1.9; I63, 2.1;
1OXK	70%	3	V1098, 1.7; R1105, 2.9; M1106, 3.6;
1R4M	26%	3	T492, 1.3; F496, 1.5; Q503, 3.5;
1TI2	12%	3	N18, 1.4; D25, 1.5; E26, 3.4;
1TQY	29%	4	F109, 1.0; F116, 3.8; L119, 1.7; W120, 2.3;
1TY4	61%	4	I50, 1.5; I54, 3.3; K57, 1.1; L58, 2.5;
1UKV	49%	4	E241, 1.9; Q244, 2.2; R248, 3.9; I252, 1.0;
1VF6	18%	2	F159, 1.4; H166, 2.5;
1VG9	65%	3	Q382, 1.0; R386, 3.0; V390, 2.6;
1WA8	43%	3	F17, 1.9; D23, 1.0; L24, 9.7;
1WPX	28%	2	W231, 3.5; Y239, 1.2;
1WPX	26%	2	F507, 4.0; S514, 1.2;
1XB2	63%	3	E193, 2.6; L194, 1.7; E198, 2.4;
1XKP	70%	4	R66, 1.6; M69, 2.9; Q70, 1.3; L73, 2.7;
1Y76	74%	3	L35, 3.7; F38, 11.8; L42, 2.2;
1YDI	100%	7	W743, 5.8; L746, 1.5; L747, 2.6; I750, 1.8; I754, 1.7; E758, 1.2; I761, 2.0;
1YKE	73%	3	M15, 2.6; F19, 4.4; L23, 1.7;
1ZL8	17%	2	L5, 1.6; L15, 2.7;
2A6Q	57%	4	E53, 1.0; E59, 2.9; Y62, 2.6; L63, 2.0;
2AFF	100%	4	F241, 1.8; L242, 3.9; R245, 2.8; V249, 3.4;
2AVU	65%	2	V71, 2.1; F82, 3.4;
2BGN	45%	3	L132, 2.1; Q135, 2.4; E139, 2.3;
2BNQ	100%	3	R65, 1.7; Q72, 3.3; T73, 1.6;
2BYK	39%	4	F81, 3.6; L85, 2.1; L89, 1.1; Y92, 3.3;
2BYK	21%	2	I37, 1.9; F44, 3.5;
2C5I	68%	3	R20, 2.3; L23, 2.5; F27, 1.6;
2C9W	39%	2	H68, 3.6; R82, 1.1;
2CJS	53%	3	E137, 2.1; W141, 2.4; L145, 1.7;

TABLE S1

Bullock, et. al

A. PDB CODE	L. HOTSPOT RESIDUE HELIX POSITIONS	M. HOTSPOT RESIDUE END TO END LENGTH	N. HELIX LENGTH	O. HELIX START RESIDUE #	P. HELIX END RESIDUE #
1E7P	i; i+11;	12	14	224	237
1EFU	i; i+4; i+7;	8	9	271	279
1F80	i; i+3; i+4; i+7;	8	10	21	30
1FM6	i; i+3; i+7;	8	23	386	408
1G73	i; i+3; i+4; i+7;	8	48	72	119
1GX7	i; i+7; i+8;	19	20	146	165
1H4L	i; i+4; i+7;	8	15	254	268
1HX1	i; i+15;	6	27	231	257
1I1R	i; i+4; i+7;	7	27	9	35
1I2M	i; i+3; i+4; i+7;	14	13	101	113
1I5K	i; i+3; i+7;	12	22	306	327
1IBR	i; i+7;	6	26	273	298
1J7D	i; i+4; i+7;	8	15	11	25
1JEK	i; i+4; i+7; i+11;	11	33	629	661
1JYO	i; i+7;	6	22	103	124
1LDK	i; i+3; i+7;	8	14	40	53
1LQB	i; i+7; i+11; i+14;	8	17	67	83
1M1E	i; i+7;	6	15	649	663
1N1J	i; i+4; i+7; i+8;	7	15	126	140
1N1J	i; i+8;	7	29	78	106
1NGM	i; i+7;	8	15	477	491
1NH2	i; i+4; i+7; i+8;	9	17	32	48
1NH2	i; i+1; i+4; i+8;	12	18	4	21
1NH2	i; i+4; i+11;	7	16	14	29
1NU7	i; i+4; i+7;	6	40	56	95
1NU9	i; i+8;	6	40	56	95
1NVM	i; i+3; i+7;	8	15	326	340
1OR0	i; i+1; i+3; i+7;	6	16	35	50
1OR7	i; i+4; i+8;	17	11	55	65
1OXK	i; i+7; i+8;	16	14	1097	1110
1R4M	i; i+4; i+11;	8	21	491	511
1TI2	i; i+7; i+8;	8	12	18	29
1TQY	i; i+7; i+10; i+11;	8	15	109	123
1TY4	i; i+4; i+7; i+8;	8	11	50	60
1UKV	i; i+3; i+7; i+11;	8	15	239	253
1VF6	i; i+7;	18	13	157	169
1VG9	i; i+4; i+8;	6	15	377	391
1WA8	i; i+6; i+7;	8	34	7	40
1WPX	i; i+8;	12	22	230	251
1WPX	i; i+7;	11	12	507	518
1XB2	i; i+1; i+5;	7	14	193	206
1XKP	i; i+3; i+4; i+7;	16	14	62	75
1Y76	i; i+3; i+7;	8	15	30	44
1YDI	i; i+3; i+4; i+7; i+11; i+15; i+18;	8	22	743	764
1YKE	i; i+4; i+8;	8	22	4	25
1ZL8	i; i+10;	15	17	4	20
2A6Q	i; i+6; i+9; i+10;	9	16	51	66
2AFF	i; i+1; i+4; i+8;	8	14	239	252
2AVU	i; i+11;	12	20	67	86
2BGN	i; i+3; i+7;	9	19	126	144
2BNQ	i; i+7; i+8;	19	29	57	85
2BYK	i; i+4; i+8; i+11;	9	19	79	97
2BYK	i; i+7;	9	29	31	59
2C5I	i; i+3; i+7;	19	14	16	29
2C9W	i; i+14;	12	17	67	83
2CJS	i; i+4; i+8;	11	20	135	154

TABLE S1

Bullock, et. al

A. PDB CODE	Q. HELIX SEQUENCE	R. RESOLUTION
1E7P	LQSKIAYLRRKMVS	3.10
1EFU	FAAEVAAMS	2.50
1F80	RQKRFAERIL	2.30
1FM6	PAEVEALREKVYASLEAYCKHY	2.10
1G73	EEEDEVWQVIIGARAEMTSKHQEYLKLETTWMTAVGLSEMAEAAYQT	2.00
1GX7	EFTADVTIWEEGSEFVERLT	NOT APP
1H4L	KEAFWDRCLSVINLM	2.65
1HX1	KDSRLKRKGKLVKKVQAFLAECDTVEQN	1.90
1I1R	KDLLIQRLNWLWVIDCFRDLCYRTG	2.40
1I2M	VPNWHRDLVRVCE	1.76
1I5K	ADAELQRLKNERHEEAELERLK	2.70
1IBR	DEVALQGIEFWSNVCDEEMDLAIEAS	2.30
1J7D	RNFRLLEELEEGQKG	1.85
1JEK	QQWEEEIEQHEGNLSLLLREAALQVHIAQRDAR	1.50
1JYO	TYHIISQLESFVNQQEALKNIL	1.90
1LDK	SRYMELYTHVYNYC	3.10
1LQB	SHVLSKVCMYFTYKVRY	2.00
1M1E	EGVATYAAAVLFRMS	2.10
1N1J	DSYVEPLKLYLQKFR	1.67
1N1J	KDAKECVQECVSEFISFITSEASERCHQE	1.67
1NGM	EEASKLKERIWIGLN	2.95
1NH2	EQTLQDLKNIWQKKLTE	1.90
1NH2	AEASRVYEIIIVESVVNEV	1.90
1NH2	TIGNSLVDALDTLISD	1.90
1NU7	KDAKDKLMTRILGEDQYLLERKKVQYEYKKLYKKYKEEN	2.20
1NU9	KDAKDKLMTRILGEDQYLLERKKVQYEYKKLYKKYKEEN	2.20
1NVM	EDMIVDVALDLLAAH	1.70
1OR0	APSAFYGYGWAQARSH	2.00
1OR7	ISSRVMAAIEE	2.00
1OXK	HVNQEVIKRLMLNLE	2.10
1R4M	HTIAFLGGAAAQEVIKIITK	3.00
1TI2	NCFMGCMDEHEL	2.35
1TQY	FDFTHREFRKLWSEG	2.00
1TY4	IGYEIGSKLAA	2.20
1UKV	LGEQPQGFARLSAIY	1.50
1VF6	RDFQNAFKIHNAV	2.10
1VG9	QGELPQFCFCRMCAVF	2.50
1WA8	AATLAQEAGNFERISGDLKTQIDQVESTAGSLQG	NOT APP
1WPX	VWSCVPATIYCNNAQLAPYQRT	2.70
1WPX	FAQASIDSYKKH	2.70
1XB2	ELVELEIRELLTEF	2.20
1XKP	VTLLRSLMQQALAW	1.70
1Y76	TQNEKLSAFYETLKS	NOT APP
1YDI	WEQLLTTIARTINEVENQILTR	1.80
1YKE	RLTQLQICLDQMTEQFCATLNY	3.30
1ZL8	NLERDVQRILELMEHVQ	NOT APP
2A6Q	LEEYNSLEETAYLLRS	2.05
2AFF	PTFLERRKSQVAEL	NOT APP
2AVU	WEQNVHASMFCAWQFLLKT	3.00
2BGN	PDEVVSLVNQGLQEGERDF	3.15
2BNQ	PEYWDGETRKVKAHSQTHRVDLGLTRGLYY	1.70
2BYK	ESFVPSLTQDLEVYRKVVK	2.40
2BYK	KEARAAIARAASVFAIFVTSSSTALAHKQ	2.40
2C5I	LNKDRRLLLREFYN	2.30
2C9W	SHVLSKVCMYFTYKVRY	1.90
2CJS	EEEARYWAKKLEQLNAKLNS	1.78

TABLE S1

Bullock, et. al

A. PDB CODE	B. INTERFACE CHAINS	C. CHAIN	D. TITLE
2D10	A E	E	CRYSTAL STRUCTURE OF THE RADIXIN FERM DOMAIN COMPLEXED WITH THE NHERF-1 C-TERM
2DOI	X C	C	THE X-RAY CRYSTALLOGRAPHIC STRUCTURE OF THE ANGIOGENESIS INHIBITOR, ANGIOSTATIN,
2DSR	B I	I	STRUCTURAL BASIS FOR THE INHIBITION OF INSULIN-LIKE GROWTH FACTORS BY IGF BINDING ]
2E9X	A C	A	THE CRYSTAL STRUCTURE OF HUMAN GINS CORE COMPLEX
2E9X	A D	A	THE CRYSTAL STRUCTURE OF HUMAN GINS CORE COMPLEX
2E9X	A D	D	THE CRYSTAL STRUCTURE OF HUMAN GINS CORE COMPLEX
2E9X	A D	D	THE CRYSTAL STRUCTURE OF HUMAN GINS CORE COMPLEX
2E9X	B C	B	THE CRYSTAL STRUCTURE OF HUMAN GINS CORE COMPLEX
2E9X	B C	C	THE CRYSTAL STRUCTURE OF HUMAN GINS CORE COMPLEX
2EFC	A B	A	ARA7-GDP/ATVP9A
2EHB	A D	A	THE STRUCTURE OF THE C-TERMINAL DOMAIN OF THE PROTEIN KINASE ATSOS2 BOUND TO THE
2EHO	B D	B	CRYSTAL STRUCTURE OF HUMAN GINS COMPLEX
2EHO	E F	E	CRYSTAL STRUCTURE OF HUMAN GINS COMPLEX
2EQB	A B	B	CRYSTAL STRUCTURE OF THE RAB GTPASE SEC4P, THE SEC2P GEF DOMAIN, AND PHOSPHATE CO
2ES4	A D	D	CRYSTAL STRUCTURE OF THE BURKHOLDERIA GLUMAE LIPASE- SPECIFIC FOLDASE IN COMPLE
2FK0	Q R	R	CRYSTAL STRUCTURE OF A H5N1 INFLUENZA VIRUS HEMAGGLUTININ.
2FO1	A D	D	CRYSTAL STRUCTURE OF THE CSL-NOTCH-MASTERMIND TERNARY COMPLEX BOUND TO DNA
2G38	A B	B	A PE/PPE PROTEIN COMPLEX FROM MYCOBACTERIUM TUBERCULOSIS
2GMI	A B	B	MMS2/UBC13~UBIQUITIN
2GOX	C D	D	CRYSTAL STRUCTURE OF EFB-C / C3D COMPLEX
2HQW	A B	B	CRYSTAL STRUCTURE OF CA2+/CALMODULIN BOUND TO NMDA RECEPTOR NR1C1 PEPTIDE
2HUE	B C	B	STRUCTURE OF THE H3-H4 CHAPERONE ASF1 BOUND TO HISTONES H3 AND H4
2HV8	A D	D	CRYSTAL STRUCTURE OF GTP-BOUND RAB11 IN COMPLEX WITH FIP3
2I2R	B F	F	CRYSTAL STRUCTURE OF THE KCHIP1/KV4.3 T1 COMPLEX
2IZV	B C	C	CRYSTAL STRUCTURE OF SOCS-4 IN COMPLEX WITH ELONGIN-B AND ELONGIN-C AT 2.55A RESOI
2JFA	A P	P	ESTROGEN RECEPTOR ALPHA LBD IN COMPLEX WITH AN AFFINITY- SELECTED COREPRESSOR PE
2JRI	A C	A	SOLUTION STRUCTURE OF THE JOSEPHIN DOMAIN OF ATAXIN-3 IN COMPLEX WITH UBIQUITIN M
2K2I	A B	B	NMR SOLUTION STRUCTURE OF THE C-TERMINAL DOMAIN (T94-Y172) OF THE HUMAN CENTRIN
2NNU	A B	B	CRYSTAL STRUCTURE OF THE PAPILLOMAVIRUS DNA TETHERING COMPLEX E2:BRD4
2NOJ	A B	B	CRYSTAL STRUCTURE OF EHP / C3D COMPLEX
2O8A	B J	J	RAT PP1CGAMMA COMPLEXED WITH MOUSE INHIBITOR-2
2OF5	E K	E	OLIGOMERIC DEATH DOMAIN COMPLEX
2OT3	A B	A	CRYSTAL STRUCTURE OF RABEX-5 VPS9 DOMAIN IN COMPLEX WITH NUCLEOTIDE FREE RAB21
2PBI	A B	A	THE MULTIFUNCTIONAL NATURE OF GBETA5/RGS9 REVEALED FROM ITS CRYSTAL STRUCTURE
2PJW	H V	H	THE VPS27/HSE1 COMPLEX IS A GAT DOMAIN-BASED SCAFFOLD FOR UBIQUITIN-DEPENDENT SOI
2PQN	A B	B	CRYSTAL STRUCTURE OF YEAST FIS1 COMPLEXED WITH A FRAGMENT OF YEAST MDV1
2PQR	A C	C	CRYSTAL STRUCTURE OF YEAST FIS1 COMPLEXED WITH A FRAGMENT OF YEAST CAF4
2QIY	A C	C	YEAST DEUBIQUITINASE UBP3 AND BRE5 COFACTOR COMPLEX
2QLV	A B	A	CRYSTAL STRUCTURE OF THE HETEROTRIMER CORE OF THE S. CEREVISIAE AMPK HOMOLOG SN
2R17	A C	C	FUNCTIONAL ARCHITECTURE OF THE RETROMER CARGO-RECOGNITION COMPLEX
2SIV	C D	C	SIV GP41 CORE STRUCTURE
2VID	A B	A	STRUCTURAL BASIS OF LSD1-COREST SELECTIVITY IN HISTONE H3 RECOGNITION
2VE7	A C	A	CRYSTAL STRUCTURE OF A BONSAI VERSION OF THE HUMAN NDC80 COMPLEX
2VE7	A C	A	CRYSTAL STRUCTURE OF A BONSAI VERSION OF THE HUMAN NDC80 COMPLEX
2VE7	A C	C	CRYSTAL STRUCTURE OF A BONSAI VERSION OF THE HUMAN NDC80 COMPLEX
2VGO	A D	D	CRYSTAL STRUCTURE OF AURORA B KINASE IN COMPLEX WITH REVERSINE INHIBITOR
2WAX	A B	B	STRUCTURE OF THE HUMAN DDX6 C-TERMINAL DOMAIN IN COMPLEX WITH AN EDC3-FDF PEPTI
2WIN	H N	N	C3 CONVERTASE (C3BBB) STABILIZED BY SCIN
2WME	D C	D	CRYSTALLOGRAPHIC STRUCTURE OF BETAINE ALDEHYDE DEHYDROGENASE FROM PSEUDOMO
2Z2T	A D	A	CRYSTAL STRUCTURE OF THE COMPLEX BETWEEN GP41 FRAGMENT N36 AND FUSION INHIBITO
2Z3R	C D	C	CRYSTAL STRUCTURE OF THE IL-15/IL-15RA COMPLEX
2ZL1	A B	B	MP1-P14 SCAFFOLDING COMPLEX
3BEG	A B	A	CRYSTAL STRUCTURE OF SR PROTEIN KINASE 1 COMPLEXED TO ITS SUBSTRATE ASF/SF2
3BOW	B C	B	STRUCTURE OF M-CALPAIN IN COMPLEX WITH CALPASTATIN
3BRT	A B	B	NEMO/IKK ASSOCIATION DOMAIN STRUCTURE
3BRV	A B	B	NEMO/IKKB ASSOCIATION DOMAIN STRUCTURE

TABLE S1

Bullock, et. al

A. PDB CODE	E. FUNCTION	F. $\Delta\Delta G_{AVG,HELIX}$ (KCAL/MOL)	G. $\Delta\Delta G_{SUM, HELIX}$ (KCAL/MOL)	H. $\Delta\Delta G_{SUM, CHAIN}$ (KCAL/MOL)
2D10	CELL ADHESION	2.9	8.6	9.9
2DOI	HYDROLASE	2.0	6.1	6.1
2DSR	PROTEIN BINDING/HORMONE/GROWTH FACTOR	2.4	4.7	8.0
2E9X	REPLICATION	2.0	8.0	13.1
2E9X	REPLICATION	2.2	4.3	15.1
2E9X	REPLICATION	2.6	10.4	21.8
2E9X	REPLICATION	2.5	7.4	21.8
2E9X	REPLICATION	2.1	4.1	27.3
2E9X	REPLICATION	2.4	14.2	32.0
2EFC	TRANSPORT PROTEIN	2.7	8.0	15.5
2EHB	SIGNALLING PROTEIN/TRANSFERASE	2.0	5.9	17.9
2EHO	REPLICATION	3.6	10.7	14.4
2EHO	REPLICATION	2.4	4.7	15.7
2EQB	ENDOCYTOSIS/EXOCYTOSIS	2.3	6.9	6.9
2ES4	HYDROLASE	2.0	4.0	9.5
2FK0	VIRAL PROTEIN	2.0	3.9	10.6
2FO1	GENE REGULATION/SIGNALLING PROTEIN/DNA	2.2	4.4	5.4
2G38	STRUCTURAL GENOMICS, UNKNOWN FUNCTION	2.4	7.2	22.9
2GMI	LIGASE, HUMAN PROTEIN	2.6	7.9	9.5
2GOX	CELL ADHESION/TOXIN	2.3	6.8	8.0
2HQW	METAL BINDING PROTEIN	3.2	12.6	14.5
2HUE	DNA BINDING PROTEIN	3.1	9.3	24.8
2HV8	PROTEIN TRANSPORT	2.4	7.2	7.2
2I2R	TRANSPORT PROTEIN	3.7	7.3	46.4
2IZV	TRANSCRIPTION	2.0	6.1	10.3
2JFA	TRANSCRIPTION	2.3	6.8	6.8
2JRI	HYDROLASE/SIGNALING PROTEIN	2.0	6.0	17.9
2K2I	CELL CYCLE	4.6	9.2	9.2
2NNU	TRANSCRIPTION	2.6	10.2	14.3
2NOJ	IMMUNE SYSTEM	2.0	6.1	6.1
2O8A	HYDROLASE/INHIBITOR	2.1	6.4	25.3
2OF5	APOPTOSIS	2.8	5.5	9.3
2OT3	PROTEIN TRANSPORT	2.7	5.4	11.2
2PBI	SIGNALING PROTEIN	2.4	7.1	45.7
2PJW	ENDOCYTOSIS/EXOCYTOSIS	2.2	6.6	28.3
2PQN	APOPTOSIS	2.4	12.2	14.1
2PQR	APOPTOSIS	3.2	12.6	12.6
2QIY	SIGNALING PROTEIN/HYDROLASE	2.4	7.1	14.8
2QLV	TRANSFERASE/PROTEIN BINDING	2.6	5.1	11.9
2R17	PROTEIN TRANSPORT	2.3	4.5	9.5
2SIV	ENVELOPE GLYCOPROTEIN	2.1	8.2	9.6
2VID	OXIDOREDUCTASE/REPRESSOR	2.0	5.9	23.3
2VE7	CELL CYCLE	2.4	7.2	30.1
2VE7	CELL CYCLE	2.0	4.0	30.1
2VE7	CELL CYCLE	2.6	5.1	28.9
2VGO	TRANSFERASE	2.5	4.9	20.1
2WAX	HYDROLASE	2.3	6.8	18.7
2WIN	IMMUNE SYSTEM	2.0	6.1	10.8
2WME	OXIDOREDUCTASE	2.3	4.5	18.4
2Z2T	VIRAL PROTEIN/INHIBITOR	2.4	9.4	9.4
2Z3R	CYTOKINE/CYTOKINE RECEPTOR	2.8	8.3	10.4
2ZL1	PROTEIN BINDING	2.0	6.1	14.4
3BEG	TRANSFERASE/SPlicing	3.5	7.0	12.4
3BOW	HYDROLASE/HYDROLASE INHIBITOR	2.0	5.9	13.7
3BRT	TRANSFERASE/TRANSCRIPTION	2.5	4.9	7.8
3BRV	TRANSFERASE/TRANSCRIPTION	2.0	8.0	12.7

TABLE S1

Bullock, et. al

A. PDB CODE	I. HELIX CONTRIBUTION	J. # HOTSPOT RESIDUES	K. HOTSPOT RESIDUES, RESIDUE # ΔΔG (KCAL/MOL)
2D10	87%	3	W348, 2.8; K351, 1.7; F355, 4.1;
2DOI	100%	3	L310, 3.1; K314, 1.9; H318, 1.1;
2DSR	59%	2	E9, 1.4; F16, 3.3;
2E9X	61%	4	R71, 3.3; R74, 1.9; Y81, 1.3; R86, 1.5;
2E9X	28%	2	W113, 2.2; Y124, 2.1;
2E9X	48%	4	F129, 3.3; F133, 2.8; Y140, 3.1; L141, 1.2;
2E9X	34%	3	Y87, 3.4; R94, 2.5; L97, 1.5;
2E9X	15%	2	W121, 1.9; R129, 2.2;
2E9X	44%	6	M1171, 1.3; L1175, 3.6; K1181, 1.2; D1185, 1.3; F1186, 2.8; W1189, 4.0;
2EFC	52%	3	Y225, 4.7; T228, 1.0; F236, 2.3;
2EHB	33%	3	L132, 1.6; L139, 2.0; E142, 2.3;
2EHO	74%	3	R74, 1.0; D82, 1.1;
2EHO	30%	2	Y87, 3.3; R94, 1.4;
2EQB	100%	3	E102, 2.4; D103, 1.3; F109, 3.2;
2ES4	42%	2	R268, 1.0; D276, 3.0;
2FK0	37%	2	V100, 1.9; H111, 2.0;
2FO1	81%	2	R71, 2.3; Y81, 2.1;
2G38	31%	3	W31, 3.5; E37, 2.0; F45, 1.7;
2GMI	83%	3	L11, 1.0; E18, 1.4; F8, 5.5;
2GOX	85%	3	H130, 2.1; R131, 1.9; N138, 2.8;
2HQW	87%	4	T879, 1.5; F880, 5.0; L887, 4.6; S890, 1.5;
2HUE	38%	3	F67, 4.9; I74, 1.4; F78, 3.0;
2HV8	100%	3	Q735, 1.0; D739, 4.0; M746, 2.2;
2I2R	16%	2	F111, 6.2; L118, 1.1;
2IZV	59%	3	S67, 1.3; H68, 3.6; R82, 1.2;
2JFA	100%	3	L13, 2.1; L5, 1.2; I9, 3.5;
2JRI	34%	3	V31, 1.4; S34, 1.5; H38, 3.1;
2K2I	100%	2	L651, 2.2; W658, 7.0;
2NNU	71%	4	I1345, 2.2; F1349, 3.3; D1352, 2.3; L1353, 2.4;
2NOJ	100%	3	H74, 1.7; R75, 1.3; N82, 3.1;
2O8A	25%	3	K137, 2.1; F141, 2.4; H148, 1.9;
2OF5	59%	2	R118, 3.1; Q125, 2.4;
2OT3	48%	2	Y354, 3.6; F365, 1.8;
2PBI	16%	3	E69, 2.8; L73, 1.0; F76, 3.3;
2PJW	23%	3	L359, 2.6; E363, 1.6; Y366, 2.4;
2PQN	87%	5	L148, 1.6; F149, 4.0; F152, 3.9; Y155, 1.5; L156, 1.2;
2PQR	100%	4	L126, 2.3; F127, 4.6; F130, 4.0; I137, 1.7;
2QIY	48%	3	E216, 1.8; F217, 2.4; R224, 2.9;
2QLV	43%	2	L516, 2.5; Y523, 2.6;
2R17	47%	2	F534, 3.4; F541, 1.1;
2SIV	85%	4	V558, 1.0; L565, 1.8; W571, 2.3; L576, 3.1;
2V1D	25%	3	F478, 2.8; R485, 1.9; D486, 1.2;
2VE7	24%	3	L1128, 1.0; Y1138, 3.8; L1142, 2.4;
2VE7	13%	2	W187, 2.1; I194, 1.9;
2VE7	18%	2	F82, 3.5; I98, 1.6;
2VGO	24%	2	L807, 1.2; Y815, 3.7;
2WAX	36%	3	K215, 1.9; F219, 3.4; I222, 1.5;
2WIN	56%	3	F60, 2.7; K61, 1.5; Y68, 1.9;
2WME	24%	2	R269, 2.8; M276, 1.7;
2Z2T	100%	4	Q1551, 1.0; L1565, 4.2; L1568, 2.2; W1571, 2.0;
2Z3R	80%	3	E46, 3.6; V49, 1.0; E53, 3.7;
2ZL1	42%	3	I48, 1.5; I52, 1.8; Y56, 2.8;
3BEG	56%	2	D564, 3.6; E571, 3.4;
3BOW	43%	3	F103, 1.4; L106, 2.7; L110, 1.8;
3BRT	63%	2	R75, 2.0; L93, 2.9;
3BRV	63%	4	R75, 2.4; F82, 2.1; E89, 1.3; F92, 2.2;

TABLE S1

Bullock, et. al

A. PDB CODE	L. HOTSPOT RESIDUE HELIX POSITIONS	M. HOTSPOT RESIDUE END TO END LENGTH	N. HELIX LENGTH	O. HELIX START RESIDUE #	P. HELIX END RESIDUE #
2D10	i; i+3; i+7;	8	10	348	357
2DOI	i; i+4; i+8;	12	20	307	326
2DSR	i; i+7;	8	12	8	19
2E9X	i; i+3; i+10; i+15;	9	37	58	94
2E9X	i; i+11;	8	22	108	129
2E9X	i; i+4; i+11; i+12;	7	24	124	147
2E9X	i; i+7; i+10;	17	32	72	103
2E9X	i; i+8;	8	29	110	138
2E9X	i; i+4; 11; 15; 16; 19;	7	22	1170	1191
2EFC	i; i+3; i+11;	8	18	222	239
2EHB	i; i+7; i+10;	8	15	129	143
2EHO	i; i+8;	6	35	58	92
2EHO	i; i+7;	9	14	84	97
2EQB	i; i+1; i+7;	11	54	84	137
2ES4	i; i+8;	9	35	263	297
2FK0	i; i+11;	17	24	94	117
2FO1	i; i+10;	7	17	68	84
2G38	i; i+6; i+14;	19	29	22	50
2GMI	i; i+3; i+10;	6	14	6	19
2GOX	i; i+1; i+8;	11	14	127	140
2HQW	i; i+1; i+8; i+11;	12	16	877	892
2HUE	i; i+7; i+11;	7	16	64	79
2HV8	i; i+4; i+11;	8	31	717	747
2I2R	i; i+7;	6	14	108	121
2IZV	i; i+1; i+15;	9	17	67	83
2JFA	i; i+4; i+8;	13	13	2	14
2JRI	i; i+3; i+7;	17	22	30	51
2K2I	i; i+7;	11	10	651	660
2NNU	i; i+4; i+7; i+8;	9	11	1345	1355
2NOJ	i; i+1; i+8;	6	14	71	84
2O8A	i; i+4; i+11;	11	18	132	149
2OF5	i; i+7;	17	11	117	127
2OT3	i; i+11;	21	18	351	368
2PBI	i; i+4; i+7;	9	14	67	80
2PJW	i; i+4; i+7;	7	16	354	369
2PQN	i; i+1; i+4; i+7; i+8;	12	16	148	163
2PQR	i; i+1; i+4; i+11;	6	15	126	140
2QIY	i; i+1; i+8;	6	16	214	229
2QLV	i; i+7;	6	14	516	529
2R17	i; i+7;	9	22	524	545
2SIV	i; i+7; i+13; i+18;	6	35	547	581
2V1D	i; i+7; i+8;	12	34	474	507
2VE7	i; 11; 15;	12	20	1124	1143
2VE7	i; i+7;	8	22	177	198
2VE7	i; i+16;	9	21	79	99
2VGO	i; i+8;	12	13	805	817
2WAX	i; i+4; i+7;	8	12	215	226
2WIN	i; i+1; i+8;	12	24	60	83
2WME	i; i+7;	9	11	267	277
2Z2T	i; i+14; i+17; i+20;	8	35	1547	1581
2Z3R	i; i+3; i+7;	6	20	36	55
2ZL1	i; i+4; i+8;	8	20	42	61
3BEG	i; i+7;	8	13	561	573
3BOW	i; i+3; i+7;	6	14	99	112
3BRT	i; i+18;	15	60	50	109
3BRV	i; i+7; i+14; i+17;	8	60	50	109

TABLE S1

Bullock, et. al

A. PDB CODE	Q. HELIX SEQUENCE	R. RESOLUTION
2D10	WSKKNELFSN	2.50
2DOI	DAELQRLKNERHEEALERL	3.10
2DSR	AELVDALQFVCG	2.10
2E9X	LIPTIKFRHCSLLRNRRCTVAYLYDRLLRIRALRWEY	2.30
2E9X	AEEMEFNFNNYKRSLATYMRSLG	2.30
2E9X	PEELAFAREFMANTESYLNVALK	2.30
2E9X	DLKVSIHQMEMERIRYVLSSYLRCRLMKIEKF	2.30
2E9X	ADEIRTLVKDMWDTRIAKLRVSADSFVRQ	2.30
2E9X	EMERGLFQTGQKGLNDFQCWEK	2.30
2EFC	EAAYFFTNILSAESFISN	2.09
2EHB	REELKEMVVALLHES	2.10
2EHO	LIPTIKFRHCSLLRNRRCTVAYLYDRLLRIRALRW	3.00
2EHO	RIRYVLSSYLRCRL	3.00
2EQB	NELRTKAAEEEADKLNKEVEDLTASLFDEANNMVADARKEKYAIEILNKRLTEQL	2.70
2ES4	PEAAARAQMQQDDEAWQTRYQAYAAERDRIAAGQ	1.85
2FK0	YNAELLVLMENERTLDFHDSNVKN	2.95
2FO1	ELHRQRSELARANYEKA	3.12
2G38	DSMLAAARAWRSLDVEMTAVQRSFNRTLL	2.20
2GMI	RNFRLLEELEKGEK	2.50
2GOX	VSAHRKAQKAVNLV	2.20
2HQW	KATFRAITSTLASSFK	1.90
2HUE	KLPFQRLVREIAQDFK	1.70
2HV8	RDELMEAIQKQEEINFRLQDYIDRIIIVAIME	1.86
2I2R	FEDFVTALSILLRG	3.35
2IZV	SHVLSKVCMYFTYKVRY	2.55
2JFA	AFQLRQLILRGLQ	2.55
2JRI	PVELSSIAHQLDEEERMMAEG	NOT APP
2K2I	LHRALQAWVT	NOT APP
2NNU	IDMNFQSDLLS	1.59
2NOJ	VATHRKAQRAVNLI	2.70
2O8A	PEEREKKRQFEMKRKLHY	2.61
2OF5	DRQINQLAQRL	3.20
2OT3	EDGYYFTNLCCAVAFIEK	2.10
2PBI	NLEAQNLGNFIVKY	1.95
2PJW	SLRQVLANAERSYNQL	3.01
2PQN	LFQGFKSYLPIAELAI	2.15
2PQR	LFEFGFKATVSIQQQR	1.88
2QIY	EAEEFAASVQRYELNM	1.69
2QLV	LDVMGEIYIALKNL	2.60
2R17	RIRFTLPLVFAAYQLAFRYKE	2.80
2SIV	GIVQQQQQLLDVVKRQQELLRLTVWGTKNLQTRVT	2.20
2VID	ITAEFLVSKHRDLTALCKEYDELAETQGKLEEK	3.10
2VE7	NAERLKRLQKSADLYKDRLG	2.88
2VE7	TWPHIVAALVWLIDCIKIHTAM	2.88
2VE7	MEGLPLFSNLVTHLDSFLPIC	2.88
2VGO	NLLTQAIRQQYYK	1.70
2WAX	KAASFEEIDTYE	2.30
2WIN	FKKMSEAKYQLQKIYNEIDEALKS	3.90
2WME	LDRAADIAVMA	2.10
2Z2T	DIVQQQNLLRAIEAQHQHLLQLTVWGIKQLQARIL	2.10
2Z3R	KVTAMKCFLLELQVISLESG	2.00
2ZL1	ARVTAIASNIWAAYDRNGN	2.00
3BEG	RDEDHIALIHELL	2.90
3BOW	EERQFRKLGVQLAG	2.40
3BRT	TLQRCLEENQELRDAIRQSNQILRERCEELLHFQASQREEKEFLMCKFQEARKLVERLGL	2.25
3BRV	TLQRCLEENQELRDAIRQSNQILRERCEELLHFQASQREEKEFLMCKFQEARKLVERLGL	2.20

**TABLE S1**

Bullock, et. al

A. PDB CODE	B. INTERFACE CHAINS	C. CHAIN	D. TITLE
3C59	A B	A	CRYSTAL STRUCTURE OF THE LIGAND-BOUND GLUCAGON-LIKE PEPTIDE- 1 RECEPTOR EXTRAC
3DCG	A B	B	CRYSTAL STRUCTURE OF THE HIV VIF BC-BOX IN COMPLEX WITH HUMAN ELONGINB AND ELON
3EAB	B H	B	CRYSTAL STRUCTURE OF SPASTIN MIT IN COMPLEX WITH ESCRT III
3EX7	A B	A	THE CRYSTAL STRUCTURE OF EJC IN ITS TRANSITION STATE
3EZQ	K L	K	CRYSTAL STRUCTURE OF THE FAS/FADD DEATH DOMAIN COMPLEX
3G9V	C D	D	CRYSTAL STRUCTURE OF A SOLUBLE DECOY RECEPTOR IL-22BP BOUND TO INTERLEUKIN-22
3GJX	B A	A	CRYSTAL STRUCTURE OF THE NUCLEAR EXPORT COMPLEX CRM1- SNURPORTINI-RANGTP
3GJX	B A	B	CRYSTAL STRUCTURE OF THE NUCLEAR EXPORT COMPLEX CRM1- SNURPORTINI-RANGTP
3H6P	A C	C	CRYSTAL STRUCTURE OF RV3019C-RV3020C FROM MYCOBACTERIUM TUBERCULOSIS

**TABLE S1**

Bullock, et. al

A. PDB CODE	E. FUNCTION	F. $\Delta\Delta G_{AVG, HELIX}$ (KCAL/MOL)	G. $\Delta\Delta G_{SUM, HELIX}$ (KCAL/MOL)	H. $\Delta\Delta G_{SUM, CHAIN}$ (KCAL/MOL)
3C59	SIGNALING PROTEIN/SIGNALING PROTEIN	2.2	4.3	8.6
3DCG	LIGASE/VIRAL PROTEIN	2.0	3.9	7.9
3EAB	CELL CYCLE	2.8	8.3	9.6
3EX7	HYDROLASE/RNA BINDING PROTEIN/RNA	2.4	12.1	14.7
3EZQ	APOPTOSIS	2.6	7.7	9.2
3G9V	CYTOKINE/CYTOKINE RECEPTOR	2.2	4.3	8.6
3GJX	PROTEIN TRANSPORT	2.7	5.3	13.1
3GJX	PROTEIN TRANSPORT	2.1	8.3	14.9
3H6P	STRUCTURAL GENOMICS, UNKNOWN FUNCTION	2.1	6.4	7.5

**TABLE S1**

Bullock, et. al

A. PDB CODE	I. HELIX CONTRIBUTION	J. # HOTSPOT RESIDUES	K. HOTSPOT RESIDUES, RESIDUE # $\Delta\Delta G$ (kcal/mol)
3C59	50%	2	L32, 1.7; W39, 2.6;
3DCG	49%	2	H68, 2.6; M75, 1.3;
3EAB	86%	3	R117, 1.5; H120, 2.1; F124, 4.7;
3EX7	82%	5	Y124, 2.1; D128, 1.7; S135, 2.4; L139, 1.9; H140, 4.0;
3EZQ	84%	3	Y291, 2.2; I295, 4.5; T305, 1.0;
3G9V	50%	2	P50, 1.4; F57, 2.9;
3GJX	40%	2	F561, 2.4; K568, 2.9;
3GJX	56%	4	M1, 1.5; E2, 1.1; L4, 2.9; L8, 2.8;
3H6P	85%	3	Y21, 3.0; L25, 1.2; I32, 2.2;

**TABLE S1**

Bullock, et. al

A. PDB CODE	L. HOTSPOT RESIDUE HELIX POSITIONS	M. HOTSPOT RESIDUE END TO END LENGTH	N. HELIX LENGTH	O. HELIX START RESIDUE #	P. HELIX END RESIDUE #
3C59	i; i+7;	19	22	32	53
3DCG	i; i+7;	6	17	67	83
3EAB	i; i+3; i+7;	9	28	110	137
3EX7	i; i+4; i+11; i+15; i+16;	7	27	116	142
3EZQ	i; i+4; i+14;	9	32	287	318
3G9V	i; i+7;	6	17	50	66
3GJX	i; i+7;	11	14	559	572
3GJX	i; i+1; i+3; i+7;	14	11	0	10
3H6P	i; i+4; i+11;	14	19	21	39

**TABLE S1**

Bullock, et. al

A. PDB CODE	Q. HELIX SEQUENCE	R. RESOLUTION
3C59	LWETVQKWREYRRQCQRSLTE	2.30
3DCG	SHVLSKVCMYFTYKVRY	2.40
3EAB	SMEAERVVFHKQAFYEYISIALRIDEDE	2.50
3EX7	PEGLRVFFYLVQDLKCLVFSLIGLHF	2.30
3EZQ	KKEAYDTLIKDLKKANLCTLAEKIQTIILKDI	2.73
3G9V	PYITNRTFMLAKEASLA	2.76
3GJX	WKFLKTVVNKLFEF	2.50
3GJX	SMEELSQALAS	2.50
3H6P	YAGTLQSLGADIASEQAVL	1.91

**Table S2.** Dataset of HIPP interactions with hotspots on two helical faces

## Description of Entries:

- A. PDB code of predicted target.
- B. Chains in the complex featuring a helix at the interface.
- C. Candidate helix to be mimicked is part of the indicated chain.
- D. Title of PDB entry.
- E. Function of protein complex.
- F.  $\Delta\Delta G_{\text{avg}}$ /helix is derived from Rosetta computational alanine mutagenesis studies and indicates the average free energy penalty for mutating two or more key residues in the helix at the interface to alanine.
- G.  $\Delta\Delta G_{\text{sum}}$ /helix is derived from Rosetta computational alanine mutagenesis studies and indicates the average free energy penalty for mutating two or more key residues at the interface to alanine.
- H.  $\Delta\Delta G_{\text{sum}}$ /chain is derived from Rosetta computational alanine mutagenesis studies and indicates the sum free energy penalty for mutating two or more key residues in the helix at the interface to alanine.
- I. Helix contribution refers to the proportion of key contact residues positioned on the candidate helix as compared to the chain (see text for a detailed explanation).
- J. Number of hot spot residues in helix.
- K. Relative positioning of the hot spot residues on a helix.
- L. Hot spot residues derived from Rosetta computational alanine scanning mutagenesis.
- M. Number of residues separating end hot spot residues (see Methods for more details).
- N. Length of candidate helix to be mimicked.
- O. First residue of the candidate helix segment.
- P. Last residue of the candidate helix segment.
- Q. Sequence of candidate helix to be mimicked.
- R. Resolution of PDB structure (NOT APP indicates NMR structure).

TABLE S2

Bullock, et. al

A. PDB CODE	B. INTERFACE CHAINS	C. CHAIN	D. TITLE
1DOA	A B	A	STRUCTURE OF THE RHO FAMILY GTP-BINDING PROTEIN CDC42 IN COMPLEX WITH THE MULTIFUNCTIONAL PROTEIN KINASE Cdc42-binding protein 1 (CDC42BP1)
1FQV	E F	E	INSIGHTS INTO SCF UBIQUITIN LIGASES FROM THE STRUCTURE OF THE SKP1-SKP2 COMPLEX
1LQB	B C	C	CRYSTAL STRUCTURE OF A HYDROXYLATED HIF-1 ALPHA PEPTIDE BOUND TO THE PVHL/ELONGIN B/CDP COMPLEX
1MDU	A B	A	CRYSTAL STRUCTURE OF THE CHICKEN ACTIN TRIMER COMPLEXED WITH HUMAN GELSOLIN SE
1MF8	A B	A	CRYSTAL STRUCTURE OF HUMAN CALCINEURIN COMPLEXED WITH CYCLOSPORIN A AND HUMA
1TY4	A C	C	CRYSTAL STRUCTURE OF A CED-9/EGL-1 COMPLEX
1U0S	Y A	A	CHEMOTAXIS KINASE CHEA P2 DOMAIN IN COMPLEX WITH RESPONSE REGULATOR CHEY FROM
1XIU	A E	E	CRYSTAL STRUCTURE OF THE AGONIST-BOUND LIGAND-BINDING DOMAIN OF BIOMPHALARIA G
1Z56	A C	A	CO-CRYSTAL STRUCTURE OF LIF1P-LIG4P
2C9W	A C	C	CRYSTAL STRUCTURE OF SOCS-2 IN COMPLEX WITH ELONGIN-B AND ELONGIN-C AT 1.9A RESOLU
2EHB	A D	D	THE STRUCTURE OF THE C-TERMINAL DOMAIN OF THE PROTEIN KINASE ATSOS2 BOUND TO THE
2I3S	C D	D	BUB3 COMPLEX WITH BUB1 GLEBS MOTIF
2I3T	C D	D	BUB3 COMPLEX WITH MAD3 (BUBR1) GLEBS MOTIF
2KA6	A B	B	NMR STRUCTURE OF THE CBP-TAZ2/STAT1-TAD COMPLEX
2V1Y	A B	B	STRUCTURE OF A PHOSPHOINOSITIDE 3-KINASE ALPHA ADAPTOR- BINDING DOMAIN (ABD) IN A
3DAW	A B	B	STRUCTURE OF THE ACTIN-DEPOLYMERIZING FACTOR HOMOLOGY DOMAIN IN COMPLEX WITH
3EJB	G H	G	CRYSTAL STRUCTURE OF P450BIO1 IN COMPLEX WITH TETRADECANOIC ACID LIGATED ACYL CA
3G9V	A B	A	CRYSTAL STRUCTURE OF A SOLUBLE DECOY RECEPTOR IL-22BP BOUND TO INTERLEUKIN-22
1AVO	E F	E	PROTEASOME ACTIVATOR REG(ALPHA)
1BH8	A B	B	HTAFII18/HTAFII28 HETERODIMER CRYSTAL STRUCTURE
1BPL	A B	B	GLYCOSYLTRANSFERASE
1D8D	A B	A	CO-CRYSTAL STRUCTURE OF RAT PROTEIN FARNESYLTRANSFERASE COMPLEXED WITH A K-RAS
1DP5	A B	B	THE STRUCTURE OF PROTEINASE A COMPLEXED WITH A IA3 MUTANT INHIBITOR
1DX5	A M	A	CRYSTAL STRUCTURE OF THE THROMBIN-THROMBOMODULIN COMPLEX
1EOF	A D	A	CRYSTAL STRUCTURE OF THE HUMAN ALPHA-THROMBIN-HAEMADIN COMPLEX: AN EXOSITE II-
1EER	A C	A	CRYSTAL STRUCTURE OF HUMAN ERYTHROPOIETIN COMPLEXED TO ITS RECEPTOR AT 1.9 ANGS'
1F51	D H	D	A TRANSIENT INTERACTION BETWEEN TWO PHOSPHORELAY PROTEINS TRAPPED IN A CRYSTAL
1F6F	A B	A	CRYSTAL STRUCTURE OF THE TERNARY COMPLEX BETWEEN OVINE PLACENTAL LACTOGEN AN
1FM6	U V	V	THE 2.1 ANGSTROM RESOLUTION CRYSTAL STRUCTURE OF THE HETERODIMER OF THE HUMAN I
1FQJ	A B	A	CRYSTAL STRUCTURE OF THE HETEROTrIMERIC COMPLEX OF THE RGS DOMAIN OF RGS9, THE C
1G5J	A B	B	COMPLEX OF BCL-XL WITH PEPTIDE FROM BAD
1GX7	A D	D	BEST MODEL OF THE ELECTRON TRANSFER COMPLEX BETWEEN CYTOCHROME C3 AND [FE]-HY
1GZL	A C	A	CRYSTAL STRUCTURE OF C14LINKMID/IQN17: A CROSS-LINKED INHIBITOR OF HIV-1 ENTRY BOU
1H2S	A B	A	MOLECULAR BASIS OF TRANSMEMBRANE SIGNALLING BY SENSORY RHODOPSIN II-TRANSDUCE
1H3O	A B	B	CRYSTAL STRUCTURE OF THE HUMAN TAF4-TAF12 (TAFII135-TAFII20) COMPLEX
1HIA	A B	B	KALLIKREIN COMPLEXED WITH HIRUSTASIN
1HL6	A B	B	A NOVEL MODE OF RBD-PROTEIN RECOGNITION IN THE Y14-MAGO COMPLEX
1ID5	L H	L	CRYSTAL STRUCTURE OF BOVINE THROMBIN COMPLEX WITH PROTEASE INHIBITOR ECOTIN
1IHf	A B	A	INTEGRATION HOST FACTOR/DNA COMPLEX
1JFI	A B	B	CRYSTAL STRUCTURE OF THE NC2-TBP-DNA TERNARY COMPLEX
1JM7	A B	A	SOLUTION STRUCTURE OF THE BRCA1/BARD1 RING-DOMAIN HETERODIMER
1JYO	C F	F	STRUCTURE OF THE SALMONELLA VIRULENCE EFFECTOR SPTP IN COMPLEX WITH ITS SECRETIC
1LUJ	A B	A	CRYSTAL STRUCTURE OF THE BETA-CATENIN/ICAT COMPLEX
1M63	A B	A	CRYSTAL STRUCTURE OF CALCINEURIN-CYCLOPHILIN-CYCLOSPORIN SHOWS COMMON BUT DIS
1MF8	A B	A	CRYSTAL STRUCTURE OF HUMAN CALCINEURIN COMPLEXED WITH CYCLOSPORIN A AND HUMA
1N4Q	E F	F	PROTEIN GERANYLGERANYLTRANSFERASE TYPE-I COMPLEXED WITH A GGPP ANALOG AND A K
1NX0	A C	C	STRUCTURE OF CALPAIN DOMAIN 6 IN COMPLEX WITH CALPASTATIN DIC
1OO0	A B	A	CRYSTAL STRUCTURE OF THE DROSOPHILA MAGO NASHI-Y14 COMPLEX
1OQP	A B	B	STRUCTURE OF THE CA2+-C-TERMINAL DOMAIN OF CALTRACTIN IN COMPLEX WITH THE CDC31
1OQS	A B	A	CRYSTAL STRUCTURE OF RV4/RV7 COMPLEX
1OR0	A B	A	CRYSTAL STRUCTURES OF GLUTARYL 7-AMINOCEPHALOSPORANIC ACID ACYLASE: INSIGHT INT
1OR0	C D	C	CRYSTAL STRUCTURES OF GLUTARYL 7-AMINOCEPHALOSPORANIC ACID ACYLASE: INSIGHT INT
1P27	A B	A	CRYSTAL STRUCTURE OF THE HUMAN Y14/MAGOH COMPLEX
1PGR	E F	E	2:2 COMPLEX OF G-CSF WITH ITS RECEPTOR
1PZL	A B	B	CRYSTAL STRUCTURE OF HNF4A LBD IN COMPLEX WITH THE LIGAND AND THE COACTIVATOR S
1QZ7	A B	B	BETA-CATENIN BINDING DOMAIN OF AXIN IN COMPLEX WITH BETA- CATENIN

TABLE S2

Bullock, et. al

A. PDB CODE	E. FUNCTION	F. ΔΔG <sub>AVG,HELIX</sub> (KCAL/MOL)	G. ΔΔG <sub>SUM, HELIX</sub> (KCAL/MOL)	H. ΔΔG <sub>SUM, CHAIN</sub> (KCAL/MOL)	I. HELIX CONTRIBUTION
1DOA	CELL CYCLE	2.0	6.0	8.4	71%
1FQV	LIGASE	3.3	6.6	12.5	53%
1LQB	GENE REGULATION	2.5	7.6	10.6	72%
1MDU	STRUCTURAL PROTEIN	2.2	6.5	11.0	59%
1MF8	HYDROLASE, LIGASE	2.9	8.6	33.6	26%
1TY4	APOPTOSIS	2.0	6.0	13.8	43%
1U0S	SIGNALING PROTEIN	2.5	7.4	7.4	100%
1XIU	TRANSCRIPTION/TRANSFERASE	2.2	8.8	8.8	100%
1Z56	LIGASE	4.3	12.9	12.9	100%
2C9W	TRANSCRIPTION REGULATION	2.1	6.3	9.1	69%
2EHB	SIGNALLING PROTEIN/TRANSFERASE	3.0	8.9	17.9	50%
2I3S	CELL CYCLE	2.8	8.4	15.4	55%
2I3T	CELL CYCLE	2.8	5.5	17.7	31%
2KA6	TRANSCRIPTION REGULATOR	2.6	10.5	19.6	54%
2V1Y	TRANSFERASE	2.7	5.3	7.8	68%
3DAW	STRUCTURAL PROTEIN/STRUCTURAL PROTEIN RE	2.4	7.3	8.3	88%
3EJB	OXIDOREDUCTASE/LIPID TRANSPORT	2.3	9.3	13.5	69%
3G9V	CYTOKINE/CYTOKINE RECEPTOR	2.7	5.4	12.8	42%
1AV0	PROTEASOME ACTIVATOR	2.8	19.9	19.9	100%
1BH8	TRANSCRIPTION REGULATION COMPLEX	2.0	9.8	16.0	61%
1BPL	GLYCOSYLTRANSFERASE	2.9	17.1	48.5	35%
1D8D	TRANSFERASE	2.1	10.7	49.1	22%
1DP5	HYDROLASE/HYDROLASE INHIBITOR	2.0	16.0	22.0	73%
1DX5	SERINE PROTEINASE	2.2	8.7	10.7	81%
1E0F	COAGULATION/CRYSTAL STRUCTURE/HEPARIN-B	2.0	3.9	6.1	64%
1EER	COMPLEX (CYTOKINE/RECEPTOR)	2.1	4.1	4.1	100%
1F51	TRANSFERASE	2.2	8.9	8.9	100%
1F6F	HORMONE/GROWTH FACTOR/HORMONE RECEPTOR	2.3	9.0	10.7	84%
1FM6	TRANSCRIPTION	2.1	6.4	6.4	100%
1FQJ	SIGNALING PROTEIN	2.0	5.9	5.9	100%
1G5J	APOPTOSIS	2.3	4.6	4.6	100%
1GX7	OXIDOREDUCTASE	2.2	13.3	51.0	26%
1GZL	GLYCOPROTEIN	2.6	5.1	5.1	100%
1H2S	MEMBRANE PROTEIN	2.0	4.0	9.0	44%
1H3O	TRANSCRIPTION/TBP-ASSOCIATED FACTORS	2.0	5.9	14.3	41%
1HIA	COMPLEX (PROTEASE/INHIBITOR)	2.9	5.8	27.9	21%
1HL6	SIGNAL PROTEIN	3.0	11.9	26.6	45%
1ID5	HYDROLASE	2.7	13.5	13.5	100%
1IHF	TRANSCRIPTION/DNA	2.0	18.3	38.1	48%
1JFI	TRANSCRIPTION/DNA	2.3	9.0	16.5	55%
1JM7	ANTITUMOR	3.0	12.0	15.8	76%
1JYO	CHAPERONE	2.3	9.3	26.1	36%
1LUJ	STRUCTURAL PROTEIN	2.0	7.9	10.0	79%
1M63	HYDROLASE/ISOMERASE	2.0	9.9	22.4	44%
1MF8	HYDROLASE, LIGASE	2.1	10.4	33.6	31%
1N4Q	TRANSFERASE	2.0	7.9	46.8	17%
1NX0	HYDROLASE	2.2	6.7	9.8	68%
1OO0	SIGNALING PROTEIN	2.2	13.0	20.8	63%
1OQP	PROTEIN BINDING	2.5	12.7	12.7	100%
1OQS	HYDROLASE	3.0	5.9	17.4	34%
1OR0	HYDROLASE	4.0	7.9	58.0	14%
1OR0	HYDROLASE	3.2	9.7	63.2	15%
1P27	RNA BINDING PROTEIN	2.3	7.0	15.0	47%
1PGR	CYTOKINE	2.2	6.5	7.9	82%
1PZL	TRANSCRIPTION	2.2	8.7	8.7	100%
1QZ7	CELL ADHESION	2.0	10.1	10.1	100%

**TABLE S2**

Bullock, et. al

A. PDB CODE	J. # HOTSPOT RESIDUES	K. HOTSPOT RESIDUES, RESIDUE # ΔΔG (KCAL/MOL)
1DOA	3	R66, 2.8; L67, 2.2; R68, 1.0;
1FQV	2	K131, 2.8; S133, 3.8;
1LQB	3	L158, 3.5; K159, 1.2; R161, 2.9;
1MDU	3	I79, 2.3; F80, 3.2; V82, 1.0;
1MF8	3	F350, 4.8; W352, 1.4; L354, 2.4;
1TY4	3	D63, 2.5; F65, 2.5; D66, 1.0;
1U0S	3	R195, 2.5; Y197, 2.9; L198, 2.0;
1XIU	4	L690, 1.8; H691, 2.2; L693, 1.9; L694, 2.9;
1Z56	3	R209, 1.4; M211, 1.3; M212, 10.2;
2C9W	3	L101, 2.2; L103, 1.0; L104, 3.1;
2EHB	3	F313, 5.6; M315, 1.3; I316, 2.0;
2I3S	3	E337, 3.5; E338, 1.9; L340, 3.0;
2I3T	2	E383, 2.3; L385, 3.2;
2KA6	4	E730, 1.8; F731, 4.5; E733, 3.0; V734, 1.2;
2V1Y	2	F494, 4.3; E496, 1.0;
3DAW	3	R267, 1.2; R269, 4.7; M270, 1.4;
3EJB	4	L57, 3.4; D58, 1.9; V60, 1.3; E61, 2.7;
3G9V	2	W123, 1.3; E125, 4.1;
1AVO	7	L29, 1.3; Y32, 4.0; F33, 2.7; K36, 6.9; I37, 1.6; L40, 1.2; L44, 2.2;
1BH8	5	M154, 1.1; K159, 1.0; F161, 4.5; V162, 1.7; V166, 1.5;
1BPL	6	E211, 1.0; I212, 1.3; W215, 3.5; W218, 5.1; Y219, 4.4; E222, 1.8;
1D8D	5	N234, 3.2; S235, 2.9; W237, 1.9; N238, 1.6; H241, 1.1;
1DP5	8	V8, 2.9; I11, 1.5; F12, 2.8; L19, 1.6; D22, 2.0; V25, 1.0; V26, 1.9; F30, 2.3;
1DX5	4	E14, 2.0; E14, 2.1; L14, 1.0; Y14, 3.6;
1EOF	2	E14, 1.0; Y14, 2.9;
1EER	2	R103, 2.9; L108, 1.2;
1F51	4	H630, 3.4; N634, 2.6; L638, 1.4; K640, 1.5;
1F6F	4	H177, 1.7; R178, 4.6; S181, 1.5; K182, 1.2;
1FM6	3	I632, 3.2; L636, 1.2; L637, 2.0;
1FQJ	3	E203, 1.1; K206, 3.5; H209, 1.3;
1G5J	2	R313, 1.0; F319, 3.6;
1GX7	6	K40, 1.3; Y42, 2.7; M43, 1.4; R46, 1.9; I47, 1.0; Y51, 5.0;
1GZL	2	L29, 1.0; W35, 4.1;
1H2S	2	T191, 1.2; L196, 2.8;
1H3O	3	F91, 2.3; I92, 1.8; V96, 1.8;
1HIA	2	W237, 2.8; I242, 3.0;
1HL6	4	Y125, 2.7; S136, 1.7; L140, 2.6; H141, 4.9;
1ID5	5	E14, 2.4; E14, 2.6; F14, 1.7; L14, 3.0; Y14, 3.8;
1IHF	9	D22, 1.4; E25, 1.4; L26, 1.4; F30, 2.9; F31, 4.0; E33, 1.0; R35, 2.7; L38, 1.8; E39, 1.7;
1JFI	4	L138, 2.0; F146, 3.4; I147, 2.6; H148, 1.0;
1JM7	4	Q81, 1.1; E85, 2.2; L86, 7.7; D96, 1.0;
1JYO	4	F83, 4.5; H85, 1.1; E89, 1.3; K90, 2.4;
1LUJ	4	T653, 1.3; Y654, 1.8; F660, 2.7; R661, 2.1;
1M63	5	F350, 4.8; W352, 1.5; L354, 1.1; K360, 1.1; V361, 1.4;
1MF8	5	V361, 1.6; M364, 3.7; L365, 1.8; V368, 1.8; L369, 1.5;
1N4Q	4	K243, 1.7; R250, 2.1; W251, 2.2; I253, 1.9;
1NX0	3	I603, 2.4; L606, 2.9; D609, 1.4;
1OO0	6	Y125, 1.9; D129, 1.8; L133, 1.2; S136, 1.7; L140, 2.5; H141, 3.9;
1OQP	5	E245, 1.4; K247, 1.0; W248, 5.7; L251, 2.4; L252, 2.2;
1OQS	2	F3, 4.4; I9, 1.5;
1OR0	2	F100, 3.8; F107, 4.1;
1OR0	3	E74, 1.8; V78, 1.0; W79, 6.9;
1P27	3	Y124, 2.6; S135, 2.2; H140, 2.2;
1PGR	3	K17, 1.3; E20, 3.4; R23, 1.8;
1PZL	4	L10, 2.3; H11, 1.1; L14, 3.5; Q15, 1.8;
1QZ7	5	E470, 1.0; L473, 2.9; D474, 2.3; H476, 2.9; V480, 1.0;

TABLE S2

Bullock, et. al

A. PDB CODE	L. HOTSPOT RESIDUE HELIX POSITIONS	M. HOTSPOT RESIDUE END TO END LENGTH	N. HELIX LENGTH	O. HELIX START RESIDUE #	P. HELIX END RESIDUE #
1DOA	i; i+1; i+2;	5	5	65	69
1FQV	i; i+2;	5	9	126	134
1LQB	i; i+1; i+3;	5	11	158	168
1MDU	i; i+1; i+3;	5	18	71	88
1MF8	i; i+2; i+4;	5	10	349	358
1TY4	i; i+2; i+3;	4	6	63	68
1U0S	i; i+2; i+3;	5	15	192	206
1XIU	i; i+1; i+3; i+4;	5	10	688	697
1Z56	i; i+2; i+3;	4	6	209	214
2C9W	i; i+2; i+3;	5	11	100	110
2EHB	i; i+2; i+3;	5	6	312	317
2I3S	i; i+1; i+3;	5	9	336	344
2I3T	i; i+2;	4	9	381	389
2KA6	i; i+1; i+3; i+4;	4	12	728	739
2V1Y	i; i+2;	5	25	481	505
3DAW	i; i+2; i+3;	5	10	266	275
3EJB	i; i+1; i+3; i+4;	3	14	57	70
3G9V	i; i+2;	4	5	122	126
1AVO	i; i+3; i+4; i+7; i+8; i+11; i+15;	16	38	8	45
1BH8	i; i+5; i+7; i+8; i+12;	11	29	148	176
1BPL	i; i+1; i+4; i+7; i+8; i+11;	12	18	206	223
1D8D	i; i+1; i+3; i+4; i+7;	6	13	234	246
1DP5	i; i+3; i+4; i+11; i+14; i+17; i+18; i+22 ;	23	29	3	31
1DX5	i; i+2 ; i+3 ; i+7;	7	9	14	14
1E0F	i; i+5;	12	11	14A	14J
1EER	i; i+5;	7	25	89	113
1F51	i; i+4; i+8; i+10;	6	23	620	642
1F6F	i; i+1; i+4; i+5;	14	34	162	195
1FM6	i; i+4; i+5;	11	9	631	639
1FQJ	i; i+3; i+6;	8	10	201	210
1G5J	i; i+6;	9	15	306	320
1GX7	i; i+2; i+3; i+6; i+7; i+11;	12	18	39	56
1GZL	i; i+6;	8	43	2	44
1H2S	i; i+5;	13	34	190	223
1H3O	i; i+1; i+5;	7	22	85	106
1HIA	i; i+5;	8	11	235	245
1HL6	i; i+11; i+15; i+16;	15	27	117	143
1ID5	i; i+2 ; i+3 ; i+4 ; i+7;	9	9	14	14
1IHF	i; i+3; i+4; i+8; i+9; i+11; i+13; i+16; i+17;	8	21	20	40
1JFI	i; i+8; i+9; i+10;	9	29	133	161
1JM7	i; i+4; i+5; i+15;	8	19	80	98
1JYO	i; i+2; i+6; i+7;	8	15	77	91
1LUJ	i; i+1; i+7; i+8;	9	14	649	662
1M63	i; i+2; i+4; i+10; i+11;	9	15	349	363
1MF8	i; i+3; i+4; i+7; i+8;	14	12	359	370
1N4Q	i; i+7; i+8; i+10;	8	13	242	254
1NX0	i; i+3; i+6;	12	9	602	610
1OO0	i; i+4; i+8; i+11; i+15; i+16;	14	26	117	142
1OQP	i; i+2; i+3; i+6; i+7;	16	14	240	253
1OQS	i; i+6;	12	13	2	14
1OR0	i; i+7;	13	21	98	118
1OR0	i; i+4; i+5;	11	10	74	83
1P27	i; i+11; i+16;	9	26	116	141
1PGR	i; i+3; i+6;	19	29	12	40
1PZL	i; i+1; i+4; i+5;	15	11	8	18
1QZ7	i; i+3; i+4; i+6; i+10;	12	12	470	481

TABLE S2

Bullock, et. al

A. PDB CODE	B. HELIX SEQUENCE	C. RESOLUTION
1DOA	DRLRP	2.60
1FQV	LPELLKVSG	2.80
1LQB	LKERCLQVVRS	2.00
1MDU	QDESGAAIAIFTVQLDDYL	2.20
1MF8	VFTWSLPFVG	3.10
1TY4	DDFDAQ	2.20
1U0S	KSARIYLVFHKLEEL	1.90
1XIU	KILHRLLQEGL	2.50
1Z56	RAMMVT	3.92
2C9W	ALELLMAANFL	1.90
2EHB	AFEMIT	2.10
2I3S	TEEILAMIK	1.90
2I3T	LEEVLAISR	2.80
2KA6	PEEFDEVSRIVG	NOT APP
2V1Y	RTAIEAFNETIKIFEEQCQTQERYS	2.40
3DAW	IRERMLYSSC	2.55
3EJB	LDTVELVMALEEEF	2.00
3G9V	PWWET	2.76
1AV0	PEAQAKVDVFREDLCTKTENLLGSYFPKKISELDAFLK	2.80
1BH8	QNVVIAMSGISKVFVGEVVEALDVCEKW	3.00
1BPL	PDVAAEIKRWTWYANEL	2.20
1D8D	NSVWNQRHFVISN	2.00
1DP5	TDQQKVSEIFQSSKEKLQGDAKVVSDAFM	2.20
1DX5	ERELLESYI	2.30
1E0F	KTERELLESYI	3.10
1EER	EPLQLHVDKAVGLRSLLTLLRALG	1.90
1F51	ELIHLLGHSRHDWMNKLQLIKGN	3.00
1F6F	ENVRRVAFYRLFHCLHRDSSKIYTYLRLIKCRLT	2.30
1FM6	KILHRLLQE	2.10
1FQJ	RSERKKWIHC	2.02
1G5J	QRYGRELRRMSDEFV	NOT APP
1GX7	IKDYMUDRINGVYGADAK	NOT APP
1GZL	MKQIEDKIEEIESKQKKIENEIARIKKLLQLTVWGIKQLQARI	1.80
1H2S	PTVDVALIVYLDLVTKVGFGLDAATLRAEH	1.93
1H3O	LQIADDFIESVVTAAACQLARHR	2.30
1HIA	LDWIDDITEN	2.40
1HL6	PEGLRCFYYLVQDLKCLVFSLIGLHF	2.50
1ID5	EKELFESYI	2.50
1IHF	KRDAKELVELFFEEIRRALEN	2.20
1JFI	NDARELVNCCTEFIHLISSEANEICNKS	2.62
1JM7	SQLVEELLKIICAFQLDTG	NOT APP
1JYO	QKILQTFLHALTEKY	1.90
1LUJ	EGVATYAAAVLFRM	2.50
1M63	VFTWSLPFVGKVT	2.80
1MF8	EKVTEMLVNLN	3.10
1N4Q	EKELNRIKRWCIM	2.40
1NX0	AIDALSSDF	2.30
1OO0	PEGLRCFYYLVQDLKCLVFSLIGLHF	1.85
1OQP	KRELIESKWHRLLF	NOT APP
1OQS	LFQFGEMILQKTG	1.90
1OR0	PDFRANLDAFAAGINAYAQQN	2.00
1OR0	EQTTVWLTTN	2.00
1P27	PEGLRVFFYLVQDLKCLVFSLIGLHF	2.00
1PGR	QSFLLKCLEQVRKIQGDGAALQEKLCA	3.50
1PZL	KILHRLLQEGL	2.10
1QZ7	ESILDEHVQRVM	2.20

TABLE S2

Bullock, et. al

A. PDB CODE	B. INTERFACE CHAINS	C. CHAIN	D. TITLE
1R8U	A B	A	NMR STRUCTURE OF CBP TAZ1/CITED2 COMPLEX
1RF8	A B	B	SOLUTION STRUCTURE OF THE YEAST TRANSLATION INITIATION FACTOR EIF4E IN COMPLEX WITH
1RIW	B C	C	THROMBIN IN COMPLEX WITH NATURAL PRODUCT INHIBITOR OSCILLARIN
1RK8	A B	B	STRUCTURE OF THE CYTOSOLIC PROTEIN PYM BOUND TO THE MAGO- Y14 CORE OF THE EXON J
1RM1	B C	B	STRUCTURE OF A YEAST TFIIA/TBP/TATA-BOX DNA COMPLEX
1RM1	B C	B	STRUCTURE OF A YEAST TFIIA/TBP/TATA-BOX DNA COMPLEX
1RP3	A B	B	COCRYSTAL STRUCTURE OF THE FLAGELLAR SIGMA/ANTI-SIGMA COMPLEX, SIGMA-28/FLGM
1SA0	C D	C	TUBULIN-COLCHICINE: STATHMIN-LIKE DOMAIN COMPLEX
1SB0	A B	B	SOLUTION STRUCTURE OF THE KIX DOMAIN OF CBP BOUND TO THE TRANSACTIVATION DOMAIN
1SYQ	A B	B	HUMAN VINCULIN HEAD DOMAIN VH1, RESIDUES 1-258, IN COMPLEX WITH HUMANTALIN'S VINC
1TCO	A B	A	TERNARY COMPLEX OF A CALCINEURIN A FRAGMENT, CALCINEURIN B, FKBP12 AND THE IMMUN
1TN6	A B	A	PROTEIN FARNESYLTRANSFERASE COMPLEXED WITH A RAP2A PEPTIDE SUBSTRATE AND A FPP A
1TQY	C D	C	THE ACTINORHODIN KETOSYNTHASE/CHAIN LENGTH FACTOR
1TQY	E F	E	THE ACTINORHODIN KETOSYNTHASE/CHAIN LENGTH FACTOR
1TUE	H J	J	THE X-RAY STRUCTURE OF THE PAPILLOMAVIRUS HELICASE IN COMPLEX WITH ITS MOLECULAR
1UKL	A C	C	CRYSTAL STRUCTURE OF IMPORTIN-BETA AND SREBP-2 COMPLEX
1VCB	K L	L	THE VHL-ELONGINC-ELONGINB STRUCTURE
1VYT	A E	E	BETA3 SUBUNIT COMPLEXED WITH AID
1WA8	A B	B	SOLUTION STRUCTURE OF THE CFP-10-LESAT-6 COMPLEX. MAJOR VIRULENCE DETERMINANTS OF
1XB2	A B	B	CRYSTAL STRUCTURE OF BOS TAURUS MITOCHONDRIAL ELONGATION FACTOR TU/TS COMPLEX
1XLS	E M	M	CRYSTAL STRUCTURE OF THE MOUSE CAR/RXR LBD HETERO-DIMER BOUND TO TCPOBOP AND 9C
1Y74	A D	A	SOLUTION STRUCTURE OF MLIN-2/MLIN-7 L27 DOMAIN COMPLEX
1YFN	D H	H	VERSATILE MODES OF PEPTIDE RECOGNITION BY THE AAA+ ADAPTOR PROTEIN SSPB- THE CRY
1YOV	A B	A	INSIGHTS INTO THE UBIQUITIN TRANSFER CASCADE FROM THE REFINED STRUCTURE OF THE AC
1Z8U	C D	C	CRYSTAL STRUCTURE OF OXIDIZED ALPHA HEMOGLOBIN BOUND TO AHSP
1ZDT	A P	P	THE CRYSTAL STRUCTURE OF HUMAN STEROIDOGENIC FACTOR-1
1ZUN	A B	A	CRYSTAL STRUCTURE OF A GTP-REGULATED ATP SULFURLASE HETERO-DIMER FROM PSEUDOM
1ZW3	A B	B	VINCULIN HEAD (0-258) IN COMPLEX WITH THE TALIN ROD RESIDUES 1630-1652
2A6Q	A E	A	CRYSTAL STRUCTURE OF YEFM-YOEB COMPLEX
2A6Q	C F	F	CRYSTAL STRUCTURE OF YEFM-YOEB COMPLEX
2AST	B C	C	CRYSTAL STRUCTURE OF SKP1-SKP2-CKS1 IN COMPLEX WITH A P27 PEPTIDE
2B87	A B	A	STRUCTURAL BASIS FOR MOLECULAR RECOGNITION IN AN AFFIBODY:AFFIBODY COMPLEX
2B9S	A B	B	CRYSTAL STRUCTURE OF HETERO-DIMERIC L. DONOVANI TOPOISOMERASE I-VANADATE-DNA CO
2BZW	A B	B	THE CRYSTAL STRUCTURE OF BCL-XL IN COMPLEX WITH FULL-LENGTH BAD
2C2V	B C	C	CRYSTAL STRUCTURE OF THE CHIP-UBC13-UEV1A COMPLEX
2D1P	G I	I	CRYSTAL STRUCTURE OF HETEROHEXAMERIC TUSBCD PROTEINS, WHICH ARE CRUCIAL FOR TH
2DOQ	A D	D	CRYSTAL STRUCTURE OF SFI1P/CDC31P COMPLEX
2DOQ	B D	D	CRYSTAL STRUCTURE OF SFI1P/CDC31P COMPLEX
2DYM	E F	F	THE CRYSTAL STRUCTURE OF SACCHAROMYCES CEREVISIAE ATG5- ATG16(1-46) COMPLEX
2E30	A B	B	SOLUTION STRUCTURE OF THE CYTOPLASMIC REGION OF NA+/H+ EXCHANGER 1 COMPLEXED W
2E9X	F G	G	THE CRYSTAL STRUCTURE OF HUMAN GINS CORE COMPLEX
2E9X	F G	G	THE CRYSTAL STRUCTURE OF HUMAN GINS CORE COMPLEX
2EHO	J L	L	CRYSTAL STRUCTURE OF HUMAN GINS COMPLEX
2EY4	A E	E	CRYSTAL STRUCTURE OF A CBF5-NOP10-GAR1 COMPLEX
2F66	A B	A	STRUCTURE OF THE ESCRT-I ENDOSOMAL TRAFFICKING COMPLEX
2FUG	A C	C	CRYSTAL STRUCTURE OF THE HYDROPHILIC DOMAIN OF RESPIRATORY COMPLEX I FROM THE R
2G38	A B	B	A PE/PPE PROTEIN COMPLEX FROM MYCOBACTERIUM TUBERCULOSIS
2GGM	A C	C	HUMAN CENTRIN 2 XERODERMA PIGMENTOSUM GROUP C PROTEIN COMPLEX
2GL7	D E	E	CRYSTAL STRUCTURE OF A BETA-CATENIN/BCL9/TCF4 COMPLEX
2HUE	B C	B	STRUCTURE OF THE H3-H4 CHAPERONE ASF1 BOUND TO HISTONES H3 AND H4
2HUE	B C	C	STRUCTURE OF THE H3-H4 CHAPERONE ASF1 BOUND TO HISTONES H3 AND H4
2IBF	A B	B	HUMAN VINCULIN'S HEAD DOMAIN (VH1, RESIDUES 1-258) IN COMPLEX WITH TWO VINCULIN BI
2IO5	B C	B	CRYSTAL STRUCTURE OF THE CIA- HISTONE H3-H4 COMPLEX
2J9U	C D	C	2 ANGSTROM X-RAY STRUCTURE OF THE YEAST ESCRT-I VPS28 C- TERMINUS IN COMPLEX WITH
2NLA	A B	B	CRYSTAL STRUCTURE OF THE MCL-1:MNOXAB BH3 COMPLEX
2NUP	B C	C	CRYSTAL STRUCTURE OF THE HUMAN SEC23A/24A HETERO-DIMER, COMPLEXED WITH THE SNAR

TABLE S2

Bullock, et. al

A. PDB CODE	E. FUNCTION	F. $\Delta\Delta G_{AVG,HELIX}$ (KCAL/MOL)	G. $\Delta\Delta G_{SUM, HELIX}$ (KCAL/MOL)	H. $\Delta\Delta G_{SUM, CHAIN}$ (KCAL/MOL)	I. HELIX CONTRIBUTION
1R8U	TRANSCRIPTION/TRANSCRIPTION ACTIVATOR	2.1	6.2	13.8	45%
1RF8	BIOSYNTHETIC PROTEIN, TRANSLATION	2.1	6.4	15.1	42%
1RIW	HYDROLASE/BLOOD CLOTTING	2.8	11.2	64.3	17%
1RK8	TRANSLATION	2.5	10.0	15.4	65%
1RM1	TRANSCRIPTION/DNA	2.1	8.5	29.3	29%
1RM1	TRANSCRIPTION/DNA	2.0	9.8	29.3	33%
1RP3	TRANSCRIPTION	2.2	17.7	31.0	57%
1SA0	CELL CYCLE	2.6	7.8	22.0	35%
1SB0	TRANSCRIPTION	2.2	6.5	6.5	100%
1SYQ	CELL ADHESION	2.0	14.1	14.1	100%
1TCO	COMPLEX (HYDROLASE/ISOMERASE)	2.3	16.1	22.5	72%
1TN6	TRANSFERASE	2.0	6.0	55.1	11%
1TQY	TRANSFERASE	2.0	3.9	38.9	10%
1TQY	TRANSFERASE	2.0	5.9	28.4	21%
1TUE	REPLICATION	3.3	10.0	10.0	100%
1UKL	PROTEIN TRANSPORT/DNA BINDING PROTEIN	2.0	3.9	6.8	57%
1VCB	TRANSCRIPTION	2.0	7.8	7.8	100%
1VYT	TRANSPORT PROTEIN	2.9	14.5	14.5	100%
1WA8	TUBERCULOSIS	4.4	8.7	13.6	64%
1XB2	TRANSLATION	2.5	5.0	23.0	22%
1XLS	TRANSCRIPTION	2.1	6.2	9.1	68%
1Y74	TRANSPORT PROTEIN	4.7	14.2	18.8	76%
1YFN	PROTEIN BINDING	2.4	4.7	11.7	40%
1YOV	SIGNALING PROTEIN	2.0	6.1	32.9	19%
1Z8U	ELECTRON TRANSPORT	2.0	8.0	8.0	100%
1ZDT	TRANSCRIPTION	2.0	8.1	8.1	100%
1ZUN	TRANSFERASE	2.0	6.0	14.8	41%
1ZW3	PROTEIN BINDING	2.2	8.6	10.0	86%
2A6Q	TOXIN INHIBITOR/TOXIN	2.4	9.5	15.0	63%
2A6Q	TOXIN INHIBITOR/TOXIN	2.2	6.7	22.9	29%
2AST	CELL CYCLE/LIGASE/PROTEIN TURNOVER	2.6	12.9	18.6	69%
2B87	PROTEIN BINDING	2.3	7.0	11.1	63%
2B9S	ISOMERASE/DNA	2.0	8.1	28.1	29%
2BZW	TRANSCRIPTION	2.4	12.2	18.3	67%
2C2V	CHAPERONE	5.5	16.4	16.4	100%
2D1P	TRANSLATION	2.6	15.5	15.5	100%
2DOQ	CELL CYCLE	2.5	7.6	7.6	100%
2DOQ	CELL CYCLE	3.4	13.7	13.7	100%
2DYM	PROTEIN TURNOVER/PROTEIN TURNOVER	2.2	13.0	25.8	50%
2E30	METAL BINDING PROTEIN/TRANSPORT PROTEIN	2.6	7.7	9.2	84%
2E9X	REPLICATION	3.2	9.6	16.9	57%
2E9X	REPLICATION	2.0	8.0	16.9	47%
2EHO	REPLICATION	2.1	6.2	13.7	45%
2EY4	ISOMERASE/BIOSYNTHETIC PROTEIN	2.0	7.8	18.6	42%
2F66	TRANSPORT PROTEIN	2.2	13.1	15.5	85%
2FUG	OXIDOREDUCTASE	3.4	6.8	7.9	86%
2G38	STRUCTURAL GENOMICS, UNKNOWN FUNCTION	2.5	4.9	22.9	21%
2GGM	CELL CYCLE	3.1	12.2	12.2	100%
2GL7	TRANSCRIPTION	2.1	6.3	13.6	46%
2HUE	DNA BINDING PROTEIN	2.1	10.3	24.8	42%
2HUE	DNA BINDING PROTEIN	2.5	17.2	22.5	76%
2IBF	CELL ADHESION, STRUCTURAL PROTEIN	3.3	19.8	27.9	71%
2IO5	CHAPERONE/STRUCTURAL PROTEIN	2.0	7.8	13.3	59%
2J9U	PROTEIN TRANSPORT	2.0	3.9	3.9	100%
2NLA	APOPTOSIS	2.2	8.6	8.6	100%
2NUP	PROTEIN TRANSPORT	2.5	10.1	14.1	72%

**TABLE S2**

Bullock, et. al

A. PDB CODE	J. # HOTSPOT RESIDUES	K. HOTSPOT RESIDUES, RESIDUE # $\Delta\Delta G_{(kcal/mol)}$
1R8U	3	E225, 1.7; L228, 2.1; L231, 2.4;
1RF8	3	F282, 6.6; K287, 2.5; K289, 2.4;
1RIW	4	W279, 6.0; I280, 1.6; V283, 1.7; I284, 1.9;
1RK8	4	L133, 1.0; S136, 2.0; L140, 2.7; H141, 4.3;
1RM1	4	T14, 1.2; I15, 4.0; L23, 1.2; L26, 2.1;
1RM1	5	L36, 3.0; R39, 1.6; V40, 1.3; V47, 1.9; L52, 2.0;
1RP3	8	D76, 1.8; K78, 1.5; V79, 1.4; V80, 1.7; L83, 2.3; I84, 1.7; F86, 2.5; F87, 4.8;
1SA0	3	H406, 2.1; W407, 4.5; E411, 1.2;
1SB0	3	E105, 1.1; L95, 2.0; L99, 3.4;
1SYQ	7	L608, 2.2; L609, 1.1; K613, 1.1; L615, 3.0; L622, 3.0; L623, 2.5; R624, 1.2;
1TCO	7	V349, 1.3; F350, 5.1; L354, 1.8; F356, 3.0; K360, 1.0; M364, 1.6; L369, 2.3;
1TN6	3	Y355, 1.8; Y358, 2.6; R361, 1.6;
1TQY	2	P149, 1.1; W154, 2.8;
1TQY	3	L114, 1.1; Y118, 3.8; L119, 1.0;
1TUE	3	I19, 2.4; Y23, 5.5; E24, 2.1;
1UKL	2	R371, 1.7; Y376, 2.2;
1VCB	4	L158, 3.4; R161, 2.4; V166, 1.0; L169, 1.0;
1VYT	5	L430, 1.0; L434, 1.1; Y437, 4.8; W440, 5.9; I441, 1.7;
1WA8	2	I625, 7.5; L636, 1.2;
1XB2	2	K60, 1.4; R67, 3.6;
1XLS	3	L744, 1.4; L745, 2.9; L749, 1.9;
1Y74	3	L19, 1.8; D22, 5.2; L33, 7.2;
1YFN	2	P6, 1.1; K11, 3.6;
1YOV	3	Y478, 1.2; E481, 1.3; R484, 3.6;
1Z8U	4	D43, 1.7; F47, 2.8; Y48, 1.0; Y51, 2.5;
1ZDT	4	L744, 1.9; L745, 2.8; L748, 1.2; L749, 2.2;
1ZUN	3	L11, 2.9; R20, 1.6; H7, 1.5;
1ZW3	4	L1633, 1.6; V1640, 1.6; L1647, 3.2; I1648, 2.2;
2A6Q	4	N69, 1.4; R72, 2.9; L73, 1.8; L80, 3.4;
2A6Q	3	W10, 2.5; Y13, 2.2; E8, 2.0;
2AST	5	E3040, 2.1; S3041, 1.4; E3042, 6.5; R3044, 1.7; N3045, 1.2;
2B87	3	W11, 1.2; W14, 3.5; F17, 2.3;
2B9S	4	R226, 2.1; I227, 1.6; I228, 1.0; W231, 3.4;
2BZW	5	Y105, 2.8; L109, 2.5; D114, 2.0; F116, 3.7; E117, 1.2;
2C2V	3	F42, 1.8; L45, 13.1; L48, 1.5;
2D1P	6	Y79, 3.5; T80, 1.4; F82, 3.7; V83, 3.3; R84, 1.3; V87, 2.3;
2DOQ	3	F237, 2.3; W240, 3.8; L245, 1.5;
2DOQ	4	F258, 3.2; L264, 2.6; F268, 2.2; W271, 5.7;
2DYM	6	L28, 1.8; I29, 1.5; R31, 1.8; L32, 2.6; R35, 3.9; E39, 1.4;
2E30	3	I522, 5.5; H523, 1.0; E535, 1.2;
2E9X	3	L175, 2.3; F186, 3.3; W189, 4.0;
2E9X	4	L139, 1.1; F142, 1.4; F146, 3.4; M150, 2.1;
2EHO	3	W71, 1.5; L72, 3.2; L76, 1.5;
2EY4	4	R45, 2.8; K49, 2.2; R50, 1.4; L53, 1.4;
2F66	6	L356, 2.7; F359, 1.0; R368, 1.1; F371, 3.0; W375, 2.3; H376, 3.0;
2FUG	2	M107, 5.1; L113, 1.7;
2G38	2	Y153, 3.0; L161, 1.9;
2GGM	4	W848, 5.4; L851, 2.1; L855, 2.9; L856, 1.8;
2GL7	3	V44, 1.1; L48, 3.6; V49, 1.6;
2HUE	5	L100, 2.0; V101, 1.5; F104, 1.9; L92, 2.8; Y99, 2.1;
2HUE	7	I50, 2.7; L58, 1.3; K59, 1.0; F61, 2.8; E63, 4.9; I66, 3.3; V70, 1.2;
2IBF	6	I566, 2.4; Y567, 10.2; K571, 1.2; L577, 3.2; S578, 1.1; L581, 1.7;
2IOS	4	L100, 1.9; F104, 3.0; L92, 1.5; Y99, 1.4;
2J9U	2	H178, 1.7; R190, 2.2;
2NLA	4	L78, 2.8; I81, 1.6; D83, 2.8; V85, 1.4;
2NUP	4	D116, 6.6; Q120, 1.2; K121, 1.2; K124, 1.1;

TABLE S2

Bullock, et. al

A. PDB CODE	L. HOTSPOT RESIDUE HELIX POSITIONS	M. HOTSPOT RESIDUE END TO END LENGTH	N. HELIX LENGTH	O. HELIX START RESIDUE #	P. HELIX END RESIDUE #
1R8U	i; i+3; i+6;	12	12	225	236
1RF8	i; i+5; i+7;	11	12	280	291
1RIW	i; i+1; i+4; i+5;	9	10	277	286
1RK8	i; i+3; i+7; i+8;	8	26	117	142
1RM1	i; i+1; i+9; i+12;	6	16	14	29
1RM1	i; i+3; i+4; i+11; i+16;	8	22	34	55
1RP3	i; i+2; i+3; i+4; i+7; i+8; i+10; i+11;	9	13	76	88
1SA0	i; i+1; i+5;	9	8	405	412
1SB0	i; i+4; i+10;	21	21	89	109
1SYQ	i; i+1; i+5; i+7; i+14; i+15; i+16;	17	20	608	627
1TCO	i; i+1; i+5; i+7; i+11; i+15; i+20;	14	22	349	370
1TN6	i; i+3; i+6;	12	15	353	367
1TQY	i; i+5;	11	12	145	156
1TQY	i; i+4; i+5;	18	12	111	122
1TUE	i; i+4; i+5;	7	22	5	26
1UKL	i; i+5;	15	21	371	391
1VCB	i; i+3; i+8; i+11;	9	13	158	170
1VYT	i; i+4; i+7; i+10; i+11;	9	22	424	445
1WA8	i; i+11;	6	34	610	643
1XB2	i; i+7;	11	15	57	71
1XLS	i; i+1; i+5;	9	9	743	751
1Y74	i; i+3; i+14;	12	19	19	37
1YFN	i; i+5;	12	6	6	11
1YOV	i; i+3; i+6;	13	11	476	486
1Z8U	i; i+4; i+5; i+8;	21	21	34	54
1ZDT	i; i+1; i+4; i+5;	12	9	743	751
1ZUN	i; i+4; i+13;	8	20	7	26
1ZW3	i; i+7; 15; 16;	16	19	1631	1649
2A6Q	i; i+3; i+4; i+11;	13	16	67	82
2A6Q	i; i+2; i+5;	16	12	7	18
2AST	i; i+1; i+2; i+4; i+5;	13	8	3040	3047
2B87	i; i+3; i+6;	8	15	4	18
2B9S	i; i+1; i+2; i+5;	9	10	225	234
2BZW	i; i+4; i+9; i+11; i+12;	8	20	100	119
2C2V	i; i+3; i+6;	8	14	40	53
2D1P	i; i+1; i+3; i+4; i+5; i+8;	8	11	79	89
2DOQ	i; i+3; i+8;	9	26	224	249
2DOQ	i; i+6; i+10; i+13;	9	41	252	292
2DYM	i; i+1; i+3; i+4; i+7; i+11;	9	18	24	41
2E30	i; i+1; i+13;	14	21	518	538
2E9X	i; i+11; i+14;	12	23	170	192
2E9X	i; i+3; i+7; i+11;	6	24	131	154
2EHO	i; i+1; i+5;	9	8	70	77
2EY4	i; i+4; i+5; i+8;	7	13	42	54
2F66	i; i+3; i+12; i+15; i+19; i+20;	8	26	356	381
2FUG	i; i+6;	11	17	98	114
2G38	i; i+8;	12	36	129	164
2GGM	i; i+3; i+7; i+8;	7	16	848	863
2GL7	i; i+4; i+5;	12	9	42	50
2HUE	i; i+7; i+8; i+9; i+12;	7	29	86	114
2HUE	i; i+8; i+9; i+11; i+13; i+16; i+20;	19	27	50	76
2IBF	i; i+1; i+5; i+11; i+12; i+15;	20	18	565	582
2IOS	i; i+7; i+8; i+12;	8	29	86	114
2J9U	i; i+12;	7	19	174	192
2NLA	i; i+3; i+5; i+7;	8	15	77	91
2NUP	i; i+4; i+5; i+8;	8	10	116	125

TABLE S2

Bullock, et. al

A. PDB CODE	Q. HELIX SEQUENCE	R. RESOLUTION
1R8U	EEVLMQLVIEMG	NOT APP
1RF8	PTFLLQFKDKLN	NOT APP
1RIW	KKWIQKVIDQ	2.04
1RK8	PEGLRCFYYLVQDLKCLVFSLIGLHF	1.90
1RM1	TIGNSLVDALDTLISD	2.50
1RM1	ASLAMRVLETFDKVVAETLKDN	2.50
1RP3	DEKVVKGTLIEFFT	2.30
1SA0	VHWYVGEG	3.58
1SB0	EKRIKELELLLMSTENELKGQ	NOT APP
1SYQ	LLQAQKLAGAVSELLRSAQ	2.42
1TCO	VFTWSLPFVGKVTEmLVNVLN	2.50
1TN6	KEYWRYIGRSLQSKH	1.80
1TQY	PSVMPAEVAVAV	2.00
1TQY	ATSLEREYLLS	2.00
1TUE	KETLSERLSALQDKIIDHYEND	2.10
1UKL	RKAIDYIKYLQQVNHKLRQEN	3.00
1VCB	LKERCLQVVRSLV	2.70
1VYT	LREKQQLEEDLKGYLDWITQAE	2.60
1WA8	GIEAAASAIQGNVTSIHSLLDEGKQSLTKLAAAW	NOT APP
1XB2	ASSKELLMKLRRKTG	2.20
1XLS	ALLRYLLDK	2.96
1Y74	LERDVSRAVELLERLQRSG	NOT APP
1YFN	PHQWQK	1.80
1YOV	DDYVHEFCRYG	2.60
1Z8U	EEDMVTVVEDWMNFYINYYRQ	2.40
1ZDT	ALLRYLLDK	2.10
1ZUN	HLKQLEAESIHIIREVAAEF	2.70
1ZW3	SVLAGHSRTVSDSIKKLIT	3.30
2A6Q	PANARRLMDSIDSLKS	2.05
2A6Q	EESWDDYLYWQE	2.05
2AST	ESEWRNLG	2.30
2B87	KFNKELGWATWEIFN	NOT APP
2B9S	PRIICSWAKA	2.27
2BZW	WAAQRYGRELRRMSDEFEGS	2.30
2C2V	RNFRLLEELEEGQK	2.90
2D1P	YTDFVRLTVKH	2.15
2DOQ	FANQAKLRVQEAVFYIWSDKTLKYSQ	3.00
2DOQ	NDEAESFRNTWLLFRSFQQWITLTQTFKEQSRLADQAFLNK	3.00
2DYM	MDDLLIRRLLDRNDKEAH	2.20
2E30	INEEHTQFLDHLLTGIEDIC	NOT APP
2E9X	EMERGLFQTGQKGLNDFQCWEKG	2.30
2E9X	NADISQSLLQTFIGRFRRIMDSSQ	2.30
2EHO	LWLAKGLF	3.00
2EY4	GEYRRRWKREVLG	2.11
2F66	LDTFVKQGRELARQQFLVRWHIQRIT	2.80
2FUG	DVVREAQAGMVEFTLLN	3.30
2G38	TAQIADLDQEYDDFWDEDGEVEMRDYRLRVSDLASKL	2.20
2GGM	WKLLAKGLLIRERLKR	2.35
2GL7	ADVKSSLVN	2.60
2HUE	SSAVMALQEASEAYLVALFEDTNLCAIHA	1.70
2HUE	IYEETRGVLKVLENVIRDAVTYTEHA	1.70
2IBF	AIYEKAKEVSSALSKVLS	3.20
2IOS	SSAVMALQEASEAYLVGLFEDTNLCAIHA	2.70
2J9U	KDQLHPLLAELLISINRT	2.00
2NLA	QLRRIGDKVNLRQKL	2.80
2NUP	DTFIQKTKKL	2.80

TABLE S2

Bullock, et. al

A. PDB CODE	B. INTERFACE CHAINS	C. CHAIN	D. TITLE
2O8F	A B	B	HUMAN MUTSALPHA (MSH2/MSH6) BOUND TO DNA WITH A SINGLE BASE T INSERT
2OBH	A C	C	CENTRIN-XPC PEPTIDE
2ODE	A B	A	CRYSTAL STRUCTURE OF THE HETEROGLIMERIC COMPLEX OF HUMAN RGS8 AND ACTIVATED G <sub>i</sub> /G <sub>o</sub>
2ONL	B D	B	CRYSTAL STRUCTURE OF THE P38A-MAPKAP KINASE 2 HETEROGLIMERIC COMPLEX
2OZA	A B	B	STRUCTURE OF P38ALPHA COMPLEX
2P1L	A B	B	STRUCTURE OF THE BCL-XL:BECLIN 1 COMPLEX
2PIN	D E	D	MECHANISM OF AUXIN PERCEPTION BY THE TIR1 UBIQUITIN LIGASE
2P22	A C	A	STRUCTURE OF THE YEAST ESCRT-I HETEROCTETRAMER CORE
2P22	A C	C	STRUCTURE OF THE YEAST ESCRT-I HETEROCTETRAMER CORE
2PB1	A B	A	THE MULTIFUNCTIONAL NATURE OF GBETA5/RGS9 REVEALED FROM ITS CRYSTAL STRUCTURE
2PB1	A B	A	THE MULTIFUNCTIONAL NATURE OF GBETA5/RGS9 REVEALED FROM ITS CRYSTAL STRUCTURE
2PRG	A C	C	LIGAND-BINDING DOMAIN OF THE HUMAN PEROXISOME PROLIFERATOR ACTIVATED RECEPTOR
2PSM	B C	B	CRYSTAL STRUCTURE OF INTERLEUKIN 15 IN COMPLEX WITH INTERLEUKIN 15 RECEPTOR ALPH
2PV2	D F	F	CRYSTALLOGRAPHIC STRUCTURE OF SURA FIRST PEPTIDYL-PROLYL ISOMERASE DOMAIN COMPI
2Q00	A C	C	CRYSTAL STRUCTURE OF AN ANTI-ACTIVATION COMPLEX IN BACTERIAL QUORUM SENSING
2QB0	A D	A	STRUCTURE OF THE 2TEL CRYSTALLIZATION MODULE FUSED TO T4 LYSOZYME WITH AN ALA-GI
2QL2	A B	B	CRYSTAL STRUCTURE OF THE BASIC-HELIX-LOOP-HELIX DOMAINS OF THE HETEROGLIMERIC E47/N
2QXV	A B	B	STRUCTURAL BASIS OF EZH2 RECOGNITION BY EED
2RGN	D E	E	CRYSTAL STRUCTURE OF P63RHOGEF COMPLEX WITH GALPHA-Q AND RHOA
2ROC	A B	B	SOLUTION STRUCTURE OF MCL-1 COMPLEXED WITH PUMA
2ROD	A B	B	SOLUTION STRUCTURE OF MCL-1 COMPLEXED WITH NOXAA
2SIV	C D	D	SIV GP41 CORE STRUCTURE
2UXN	A B	A	STRUCTURAL BASIS OF HISTONE DEMETHYLATION BY LSD1 REVEALED BY SUICIDE INACTIVATI
2V6X	A B	A	STRUCTURAL INSIGHT INTO THE INTERACTION BETWEEN ESCRT-III AND VPS4
2VE7	A C	C	CRYSTAL STRUCTURE OF A BONSAI VERSION OF THE HUMAN NDC80 COMPLEX
2VOF	C D	D	STRUCTURE OF MOUSE A1 BOUND TO THE PUMA BH3-DOMAIN
2VOI	A B	B	STRUCTURE OF MOUSE A1 BOUND TO THE BID BH3-DOMAIN
2W85	A B	B	STRUCTURE OF PEX14 IN COMPEX WITH PEX19
2Z2S	A B	A	CRYSTAL STRUCTURE OF RHODOBACTER SPHAEROIDES SIGE IN COMPLEX WITH THE ANTI-SIGNAL
2Z2T	B E	B	CRYSTAL STRUCTURE OF THE COMPLEX BETWEEN GP41 FRAGMENT N36 AND FUSION INHIBITOR
2Z2T	C F	C	CRYSTAL STRUCTURE OF THE COMPLEX BETWEEN GP41 FRAGMENT N36 AND FUSION INHIBITOR
3B9F	L H	L	1.6 Å STRUCTURE OF THE PCI-THROMBIN-HEPARIN COMPLEX
3BC1	A B	B	CRYSTAL STRUCTURE OF THE COMPLEX RAB27A-SLP2A
3BL2	A C	C	CRYSTAL STRUCTURE OF M11, THE BCL-2 HOMOLOG OF MURINE GAMMA- HERPESVIRUS 68, COM
3BOW	B C	C	STRUCTURE OF M-CALPAIN IN COMPLEX WITH CALPASTATIN
3BPL	A B	A	CRYSTAL STRUCTURE OF THE IL4-IL4R-COMMON GAMMA TERNARY COMPLEX
3BPQ	A B	A	CRYSTAL STRUCTURE OF RELB-RELE ANTITOXIN-TOXIN COMPLEX FROM METHANOCOCCUS JAR
3BXK	A B	B	CRYSTAL STRUCTURE OF THE P/Q-TYPE CALCIUM CHANNEL (CAV2.1) IQ DOMAIN AND CA2+CAL
3C4M	A C	C	STRUCTURE OF HUMAN PARATHYROID HORMONE IN COMPLEX WITH THE EXTRACELLULAR DO
3DI2	A B	A	CRYSTAL STRUCTURE OF THE COMPLEX OF HUMAN INTERLEUKIN-7 WITH UNGLYCOSYLATED H
3DVU	B D	D	CRYSTAL STRUCTURE OF THE COMPLEX OF MURINE GAMMA- HERPESVIRUS 68 BCL-2 HOMOLOC
3E95	B C	C	CRYSTAL STRUCTURE OF THE PLASMODIUM FALCIPARUM UBIQUITIN CONJUGATING ENZYME C
3EX7	A C	C	THE CRYSTAL STRUCTURE OF EJC IN ITS TRANSITION STATE
3FAL	C D	D	HUMANRXR ALPHA & MOUSE LXR ALPHA COMPLEXED WITH RETENOIC ACID AND GSK2186
3GJX	E D	D	CRYSTAL STRUCTURE OF THE NUCLEAR EXPORT COMPLEX CRM1- SNURPORTIN1-RANGTP
3HHR	A C	A	HUMAN GROWTH HORMONE AND EXTRACELLULAR DOMAIN OF ITS RECEPTOR: CRYSTAL STRU
3HJW	A B	B	STRUCTURE OF A FUNCTIONAL RIBONUCLEOPROTEIN PSEUDOURIDINE SYNTHASE BOUND TO A

TABLE S2

Bullock, et. al

A. PDB CODE	E. FUNCTION	F. $\Delta\Delta G_{AVG,HELIX}$ (KCAL/MOL)	G. $\Delta\Delta G_{SUM, HELIX}$ (KCAL/MOL)	H. $\Delta\Delta G_{SUM, CHAIN}$ (KCAL/MOL)	I. HELIX CONTRIBUTION
2O8F	DNA BINDING PROTEIN/DNA	2.1	4.2	25.5	16%
2OBH	CELL CYCLE	3.6	14.4	14.4	100%
2ODE	SIGNALING PROTEIN	2.1	6.3	8.6	73%
2ONL	TRANSFERASE	2.6	10.5	14.1	74%
2OZA	SIGNALING PROTEIN/TRANSFERASE	2.2	6.6	27.8	24%
2P1L	APOPTOSIS	2.0	10.2	10.2	100%
2PIN	SIGNALING PROTEIN	2.1	4.1	12.4	33%
2P22	TRANSPORT PROTEIN	3.2	12.8	27.7	46%
2P22	TRANSPORT PROTEIN	2.0	8.0	19.9	40%
2PBI	SIGNALING PROTEIN	2.1	8.2	45.7	18%
2PBI	SIGNALING PROTEIN	2.7	10.7	45.7	23%
2PRG	COMPLEX (THIAZOLIDINEDIONE/RECEPTOR)	2.0	8.1	8.1	100%
2PSM	CYTOKINE	2.7	13.5	19.5	69%
2PV2	ISOMERASE	2.1	10.4	11.5	90%
2Q0O	TRANSCRIPTION	2.4	9.4	14.2	66%
2QB0	HYDROLASE REGULATOR	3.0	9.0	11.5	78%
2QL2	TRANSCRIPTION/DNA	2.0	12.0	13.8	87%
2QXV	GENE REGULATION	2.4	14.2	14.2	100%
2RGN	SIGNALING PROTEIN COMPLEX	2.1	6.3	13.8	46%
2ROC	APOPTOSIS	2.4	12.1	12.1	100%
2ROD	APOPTOSIS	2.5	12.4	12.4	100%
2SIV	ENVELOPE GLYCOPROTEIN	2.0	3.9	9.6	41%
2UXN	OXIDOREDUCTASE/TRANSCRIPTION REGULATOR	2.4	9.7	26.6	36%
2V6X	PROTEIN TRANSPORT	2.3	6.8	11.5	59%
2VE7	CELL CYCLE	2.7	13.4	28.9	46%
2VOF	APOPTOSIS	2.5	17.3	19.4	89%
2VOI	APOPTOSIS	2.1	8.2	8.2	100%
2W85	PROTEIN TRANSPORT	2.0	4.0	4.0	100%
2Z2S	TRANSCRIPTION	2.4	7.1	27.8	26%
2Z2T	VIRAL PROTEIN/INHIBITOR	2.0	7.8	7.8	100%
2Z2T	VIRAL PROTEIN/INHIBITOR	2.2	6.6	9.0	73%
3B9F	HYDROLASE/HYDROLASE INHIBITOR	2.3	9.0	17.6	51%
3BC1	SIGNALING PROTEIN/TRANSPORT PROTEIN	2.1	10.6	15.3	69%
3BL2	VIRAL PROTEIN/APOPTOSIS	2.4	12.1	12.1	100%
3BOW	HYDROLASE/HYDROLASE INHIBITOR	2.2	6.5	8.8	74%
3BPL	CYTOKINE/CYTOKINE RECEPTOR	2.0	8.1	12.6	64%
3BPQ	TOXIN	2.2	11.1	13.1	85%
3BXK	MEMBRANE PROTEIN, SIGNALING PROTEIN	2.1	12.3	12.3	100%
3C4M	MEMBRANE PROTEIN	2.8	11.3	12.4	91%
3DI2	CYTOKINE/CYTOKINE RECEPTOR	2.4	9.7	13.5	72%
3DVU	VIRAL PROTEIN/APOPTOSIS	2.0	7.9	9.1	87%
3E95	LIGASE	2.2	11.2	11.2	100%
3EX7	HYDROLASE/RNA BINDING PROTEIN/RNA	2.7	10.6	10.6	100%
3FAL	SIGNALING PROTEIN	2.0	3.9	6.2	63%
3GJX	PROTEIN TRANSPORT	2.0	3.9	9.7	40%
3HHR	HORMONE/RECEPTOR	2.1	8.3	8.3	100%
3HJW	ISOMERASE/RNA	2.1	8.3	18.7	44%

**TABLE S2**

Bullock, et. al

A. PDB CODE	J. # HOTSPOT RESIDUES	K. HOTSPOT RESIDUES, RESIDUE # ΔΔG (KCAL/MOL)
2O8F	2	F1222, 2.8; I1227, 1.4;
2OBH	4	W848, 7.7; L851, 1.7; L855, 3.1; L856, 1.9;
2ODE	3	E207, 2.7; K210, 2.4; H213, 1.2;
2ONL	4	H126, 2.6; F129, 4.4; L130, 2.5; R136, 1.0;
2OZA	3	H126, 2.6; F129, 1.9; Y132, 2.1;
2P1L	5	L112, 1.6; L116, 2.2; K117, 1.3; D121, 2.0; F123, 3.1;
2PIN	2	V151, 3.0; W157, 1.1;
2P22	4	Y329, 9.2; D340, 1.4; L345, 1.0; R347, 1.2;
2P22	4	L150, 2.6; K153, 2.4; L154, 1.0; E169, 2.0;
2PB1	4	L244, 2.5; I247, 1.4; V248, 1.6; Y250, 2.7;
2PB1	4	I226, 1.8; Y228, 3.2; Y229, 2.7; L233, 3.0;
2PRG	4	K632, 1.1; L633, 2.3; L636, 1.5; L637, 3.2;
2PSM	5	E46, 4.6; Q48, 1.1; V49, 2.4; H52, 2.0; E53, 3.4;
2PV2	5	F10, 1.1; T3, 1.2; L4, 1.6; W7, 5.2; D8, 1.3;
2QOO	4	R40, 1.8; Y50, 2.6; W53, 3.8; L54, 1.2;
2QB0	3	E68, 1.3; Y72, 3.4; R73, 4.3;
2QL2	6	K139, 1.1; L143, 3.0; K147, 2.1; Y149, 1.9; I150, 1.9; L153, 2.0;
2QXV	6	F42, 4.3; R46, 1.5; I49, 2.2; R52, 2.4; L56, 1.7; W60, 2.1;
2RGN	3	E215, 1.4; W216, 1.3; Y220, 3.6;
2ROC	5	L141, 3.9; I144, 2.1; D146, 1.1; L148, 1.8; Y152, 3.2;
2ROD	5	F23, 3.6; L27, 2.4; I30, 2.7; D32, 1.1; W38, 2.6;
2SIV	2	W631, 2.6; I642, 1.3;
2UXN	4	I474, 2.4; F478, 3.7; D486, 1.5; Y494, 2.1;
2V6X	3	F60, 2.1; L64, 1.5; R66, 3.2;
2VE7	5	F127, 1.1; F130, 4.2; R131, 1.2; Y138, 5.7; F141, 1.2;
2VOF	7	W133, 3.2; I137, 2.2; L141, 2.1; R142, 2.7; I144, 1.1; D146, 3.9; L148, 2.1;
2VOI	4	I82, 1.5; I86, 2.3; L90, 2.0; D95, 2.4;
2W85	2	F105, 1.3; F110, 2.7;
2Z2S	3	F30, 3.6; H32, 1.1; K38, 2.4;
2Z2T	4	H2564, 1.0; L2565, 2.1; L2568, 2.2; W2571, 2.5;
2Z2T	3	Q3551, 1.6; L3568, 2.3; W3571, 2.7;
3B9F	4	E14, 1.4; E14, 2.9; L14, 2.1; Y14, 2.6;
3BC1	5	I15, 1.3; V18, 1.7; R21, 2.6; L25, 2.0; R32, 3.0;
3BL2	5	L110, 2.9; L114, 2.5; K115, 1.3; D119, 1.3; F121, 4.1;
3BOW	3	I653, 2.7; L656, 2.7; D659, 1.1;
3BPL	4	R81, 2.1; R85, 1.0; R88, 3.4; W91, 1.6;
3BPQ	5	E21, 3.0; I23, 1.0; L24, 2.4; L28, 2.6; M32, 2.1;
3BXK	6	I1961, 1.9; Y1962, 1.6; M1965, 1.0; I1967, 3.1; Y1971, 2.7; R1972, 2.0;
3C4M	4	R20, 5.9; W23, 1.8; L24, 2.6; L28, 1.0;
3DI2	4	K10, 3.2; V15, 1.8; L16, 3.3; V18, 1.4;
3DVU	4	L112, 1.9; L116, 1.6; D121, 1.2; F123, 3.2;
3E95	5	F28, 5.1; L31, 1.3; D32, 1.6; L34, 2.2; Q38, 1.0;
3EX7	4	R387, 2.0; R390, 4.5; D391, 2.2; Q394, 1.9;
3FAL	2	L400, 1.4; R413, 2.5;
3GJX	2	V518, 1.2; L525, 2.7;
3HHR	4	D11, 2.1; N12, 2.0; R16, 1.9; R8, 2.3;
3HJW	4	R45, 2.8; R46, 2.3; K49, 1.7; R50, 1.5;

TABLE S2

Bullock, et. al

A. PDB CODE	L. HOTSPOT RESIDUE HELIX POSITIONS	M. HOTSPOT RESIDUE END TO END LENGTH	N. HELIX LENGTH	O. HELIX START RESIDUE #	P. HELIX END RESIDUE #
2O8F	i; i+5;	19	20	1221	1240
2OBH	i; i+3; i+7; i+8;	9	15	848	862
2ODE	i; i+3; i+6;	12	10	205	214
2ONL	i; i+3; i+4; i+10;	6	21	124	144
2OZA	i; i+3; i+6;	8	21	124	144
2P1L	i; i+4; i+5; i+9; i+11;	8	21	106	126
2PIN	i; i+6;	15	14	146	159
2P22	i; i+11; i+16; i+18;	8	30	323	352
2P22	i; i+3; i+4; i+19;	6	25	147	171
2PB1	i; i+3; i+4; i+6;	9	15	240	254
2PB1	i; i+2; i+3; i+7;	15	17	219	235
2PRG	i; i+1; i+4; i+5;	8	8	631	638
2PSM	i; i+2; i+3; i+6; i+7;	19	19	36	54
2PV2	i; i+1; i+4; i+5; i+7;	8	9	3	11
2Q0O	i; i+10; i+13; i+14;	6	33	25	57
2QB0	i; i+4; i+5;	12	8	67	74
2QL2	i; i+4; i+8; i+10; i+11; i+14;	16	19	139	157
2QXV	i; i+4; i+7; i+10; i+14; i+18;	19	23	41	63
2RGN	i; i+1; i+5;	12	21	210	230
2ROC	i; i+3; i+5; i+7; i+11;	21	25	131	155
2ROD	i; i+4; i+7; i+9; i+15;	9	19	22	40
2SIV	i; i+11;	13	32	629	660
2UXN	i; i+4; i+12; i+20;	7	40	474	513
2V6X	i; i+4; i+6;	15	31	50	80
2VE7	i; i+3; i+4; i+11; i+14;	8	29	114	142
2VOF	i; i+4; i+8; i+9; i+11; i+13; i+15;	17	20	133	152
2VOI	i; i+4; i+8; i+13;	15	21	79	99
2W85	i; i+5;	9	11	102	112
2Z2S	i; i+2; i+8;	16	19	23	41
2Z2T	i; i+1; i+4; i+7;	14	34	2547	2580
2Z2T	i; 18; 21;	6	35	3547	3581
3B9F	i; i+2; i+3; i+7;	8	9	14	14
3BC1	i; i+3; i+6; i+10; i+17;	9	29	7	35
3BL2	i; i+4; i+5; i+9; i+11;	8	17	107	123
3BOW	i; i+3; i+6;	9	9	652	660
3BPL	i; i+4; i+7; i+10;	21	26	70	95
3BPQ	i; i+2; i+3; i+7; i+11;	8	22	14	35
3BXK	i; i+1; i+4; i+6; 11; 12;	21	16	1961	1976
3C4M	i; i+3; i+4; i+8;	8	19	16	34
3DI2	i; i+5; i+6; i+8;	9	18	9	26
3DVU	i; i+4; i+9; i+11;	8	18	108	125
3E95	i; i+3; i+4; i+6; i+10;	18	15	26	40
3EX7	i; i+3; i+4; i+7;	8	12	385	396
3FAL	i; i+13;	12	30	399	428
3GJX	i; i+7;	8	22	510	531
3HHR	i; i+3; i+4; i+8;	7	28	6	33
3HJW	i; i+1; i+4; i+5;	11	12	42	53

TABLE S2

Bullock, et. al

A. PDB CODE	Q. HELIX SEQUENCE	R. RESOLUTION
2O8F	TFDGTAIANAVVKELAETK	3.25
2OBH	WKLLAKGLLIRERLK	1.80
2ODE	RSERKKWIHC	1.90
2ONL	DDHVQFLIYQILRGLKYIHSA	4.00
2OZA	DDHVQFLIYQILRGLKYIHSA	2.70
2P1L	SGTMENLSRRLKVTGDLFDIM	2.50
2PIN	EEEEEVRENQWAF	2.50
2P22	DGLNQLYNLVAQDYALTDIECLSRMLHRG	2.70
2P22	DIALKKKLEQNTKKLDEESSQLETT	2.70
2PBI	SSVSLGGIVKYSEQF	1.95
2PBI	VTAVRKEIMYYQQALMR	1.95
2PRG	HKLVQLLT	2.30
2PSM	KVTAMNCFLLELQVILHEY	2.19
2PV2	TLKFWDIFR	1.30
2Q0O	KSELEALAVSAIREHRRLLWADQAVYEEWLRA	2.00
2QB0	KEDFRYRS	2.56
2QL2	KIETLRLAKNYIWALSEIL	2.50
2QXV	MFSSNRQKILERETLNQEWKQR	1.82
2RGN	IQQIYEWRDYLQELQRCLK	3.50
2ROC	EEWAREIGAQLRRIADDLNAQYERR	NOT APP
2ROD	EFAAQLRKIGDKVYCTWSA	NOT APP
2SIV	QEWERKVDFLEENITALLEEAQIQQEKNMYEL	2.20
2UXN	ITAEFLVSKHRDLTALCKEYDELAETQGKLEEKLQLEEA	2.72
2V6X	PKSKDLIRAKTEYLNRAEQLKKHLESEEAN	1.98
2VE7	AKRTSRFLSGIINFIHFREACRETYMEFL	2.88
2VOF	WAREIGAQLRRIADDLNAQY	1.80
2VOI	QEEIIHNIARHLAQIGDEMHD	2.10
2W85	QEKKFQELFDS	NOT APP
2Z2S	EAAFAELFQHFAPKVKKGFL	2.70
2Z2T	DIVQQQNLLRAIEAQHQHLLQLTVWGIKQLQARI	2.10
2Z2T	DIVQQQNLLRAIEAQHQHLLQLTVWGIKQLQARI	2.10
3B9F	ERELLESYI	1.60
3BC1	PEFEEQEAIMVKLQRDAALKRAEEERVH	1.80
3BL2	MENLSRRLKVTGDLFDI	2.30
3BOW	PIDALSEDL	2.40
3BPL	AQQFHRHKQLIRFLKRLDRNLWGLAG	2.93
3BPQ	RKEYEKIEEILDIGLAKAMEET	2.20
3BXK	IYAAMMIMEYYRQSKA	2.55
3C4M	NSMERVEWLRKKLQDVHNF	1.95
3DI2	GKQYESVLMVSIDQLLDS	2.70
3DVU	TMENLSRRLKVTGDLFDI	2.50
3E95	RSFRLLDALERGQKG	2.50
3EX7	DIRILRDIEQYY	2.30
3FAL	PLMFPRMLMKLVLSSLRTLSSVHSEQVFALRL	2.36
3GJX	EEDEKRFLVTVIKDLLGLCEQK	2.50
3HHR	LSRLFDNAMLRAHRLHQLAFDTYQEFE	2.80
3HJW	GEYRRRWKREVL	2.35

**Table S3.** Dataset of HIPP interactions with hotspots on three helical faces

## Description of Entries:

- A. PDB code of predicted target.
- B. Chains in the complex featuring a helix at the interface.
- C. Candidate helix to be mimicked is part of the indicated chain.
- D. Title of PDB entry.
- E. Function of protein complex.
- F.  $\Delta\Delta G_{\text{avg}}$ /helix is derived from Rosetta computational alanine mutagenesis studies and indicates the average free energy penalty for mutating two or more key residues in the helix at the interface to alanine.
- G.  $\Delta\Delta G_{\text{sum}}$ /helix is derived from Rosetta computational alanine mutagenesis studies and indicates the average free energy penalty for mutating two or more key residues at the interface to alanine.
- H.  $\Delta\Delta G_{\text{sum}}$ /chain is derived from Rosetta computational alanine mutagenesis studies and indicates the sum free energy penalty for mutating two or more key residues in the helix at the interface to alanine.
- I. Helix contribution refers to the proportion of key contact residues positioned on the candidate helix as compared to the chain (see text for a detailed explanation).
- J. Number of hot spot residues in helix.
- K. Relative positioning of the hot spot residues on a helix.
- L. Hot spot residues derived from Rosetta computational alanine scanning mutagenesis.
- M. Number of residues separating end hot spot residues (see Methods for more details).
- N. Length of candidate helix to be mimicked.
- O. First residue of the candidate helix segment.
- P. Last residue of the candidate helix segment.
- Q. Sequence of candidate helix to be mimicked.
- R. Resolution of PDB structure (NOT APP indicates NMR structure).

TABLE S3

Bullock, et. al

A. PDB CODE	B. INTERFACE CHAINS	C. CHAIN	D. TITLE
1FQV	A B	A	INSIGHTS INTO SCF UBIQUITIN LIGASES FROM THE STRUCTURE OF THE SKP1-SKP2 COMPLEX
2ZFD	A B	B	THE CRYSTAL STRUCTURE OF PLANT SPECIFIC CALCIUM BINDING PROTEIN ATCBL2 IN COMPLEX
1CDL	A E	E	TARGET ENZYME RECOGNITION BY CALMODULIN: 2.4 ANGSTROMS STRUCTURE OF A CALMODULIN
1E3A	A B	A	A SLOW PROCESSING PRECURSOR PENICILLIN ACYLASE FROM ESCHERICHIA COLI
1E3A	A B	A	A SLOW PROCESSING PRECURSOR PENICILLIN ACYLASE FROM ESCHERICHIA COLI
1IHF	A B	B	INTEGRATION HOST FACTOR/DNA COMPLEX
1JFI	B C	B	CRYSTAL STRUCTURE OF THE NC2-TBP-DNA TERNARY COMPLEX
1MXE	A E	E	STRUCTURE OF THE COMPLEX OF CALMODULIN WITH THE TARGET SEQUENCE OF CAMKII
1N1J	A B	B	CRYSTAL STRUCTURE OF THE NF-YB/NF-YC HISTONE PAIR
1N2D	A C	C	TERNARY COMPLEX OF MLC1P BOUND TO IQ2 AND IQ3 OF MYO2P, A CLASS V MYOSIN
1OR7	A C	C	CRYSTAL STRUCTURE OF ESCHERICHIA COLI SIGMAE WITH THE CYTOPLASMIC DOMAIN OF ITS
1PQ1	A B	B	CRYSTAL STRUCTURE OF BCL-XL/BIM
1RP3	E F	E	COCRYSTAL STRUCTURE OF THE FLAGELLAR SIGMA/ANTI-SIGMA COMPLEX, SIGMA-28/FLGM
1ZUZ	A B	B	CALMODULIN IN COMPLEX WITH A MUTANT PEPTIDE FROM HUMAN DRP- 1 KINASE
2BCX	A B	B	CRYSTAL STRUCTURE OF CALMODULIN IN COMPLEX WITH A RYANODINE RECEPTOR PEPTIDE
2BE6	B E	E	2.0 Å CRYSTAL STRUCTURE OF THE CAV1.2 IQ DOMAIN-CA/CAM COMPLEX
2F66	A C	A	STRUCTURE OF THE ESCRT-I ENDOSOMAL TRAFFICKING COMPLEX
2F66	A C	C	STRUCTURE OF THE ESCRT-I ENDOSOMAL TRAFFICKING COMPLEX
2FOT	A C	C	CRYSTAL STRUCTURE OF THE COMPLEX BETWEEN CALMODULIN AND ALPHAI1I-SPECTRIN
2JF9	B Q	Q	ESTROGEN RECEPTOR ALPHA LBD IN COMPLEX WITH A TAMOXIFEN- SPECIFIC PEPTIDE ANTAGONIST
2O60	A B	B	CALMODULIN BOUND TO PEPTIDE FROM NEURONAL NITRIC OXIDE SYNTHASE
2PKQ	A B	B	X-RAY CRYSTAL STRUCTURE OF HUMAN MCL-1 IN COMPLEX WITH BIM BH3
2QAC	A T	T	THE CLOSED MTIP-MYOSINA-TAIL COMPLEX FROM THE MALARIA PARASITE INVASION MACHINERY
2V6Q	A B	B	CRYSTAL STRUCTURE OF A BHRF-1 : BIM BH3 COMPLEX
3BS5	A B	B	CRYSTAL STRUCTURE OF HCNK2-SAM/DHYP-SAM COMPLEX
3D7V	A B	B	CRYSTAL STRUCTURE OF MCL-1 IN COMPLEX WITH AN MCL-1 SELECTIVE BH3 LIGAND
3DA7	G H	H	A CONFORMATIONALLY STRAINED, CIRCULAR PERMUTANT OF BARNASE
3DD7	C D	D	STRUCTURE OF DOCH66Y IN COMPLEX WITH THE C-TERMINAL DOMAIN OF PHD
3DI2	C D	C	CRYSTAL STRUCTURE OF THE COMPLEX OF HUMAN INTERLEUKIN-7 WITH UNGLYCOSYLATED H
3DVE	A B	B	CRYSTAL STRUCTURE OF CA2+/CAM-CAV2.2 IQ DOMAIN COMPLEX
3EAB	D J	J	CRYSTAL STRUCTURE OF SPASTIN MIT IN COMPLEX WITH ESCRT III
3FWB	A B	B	SAC3:SUS1:CDC31 COMPLEX

TABLE S3

Bullock, et. al

A. PDB CODE	E. FUNCTION	F. $\Delta\Delta G_{AVG,HELIX}$ (KCAL/MOL)	G. $\Delta\Delta G_{SUM,HELIX}$ (KCAL/MOL)	H. $\Delta\Delta G_{SUM,CHAIN}$ (KCAL/MOL)	I. HELIX CONTRIBUTION
1FQV	LIGASE	2.0	8.1	11.7	69%
2ZFD	SIGNALING PROTEIN/TRANSFERASE	2.8	11.1	23.2	48%
1CDL	CALCIUM-BINDING PROTEIN	2.4	21.8	23.3	94%
1E3A	ANTIBIOTIC RESISTANCE	2.4	11.9	110.8	11%
1E3A	ANTIBIOTIC RESISTANCE	2.8	19.7	110.8	18%
1IHF	TRANSCRIPTION/DNA	2.4	11.9	32.3	37%
1JFI	TRANSCRIPTION/DNA	2.7	8.1	8.1	100%
1MXE	METAL BINDING PROTEIN	2.4	23.8	27.5	87%
1N1J	DNA BINDING PROTEIN	2.5	17.2	43.7	39%
1N2D	CELL CYCLE	2.0	15.7	15.7	100%
1OR7	TRANSCRIPTION	2.2	11.1	33.3	33%
1PQ1	APOPTOSIS	2.3	20.4	20.4	100%
1RP3	TRANSCRIPTION	2.0	10.0	25.0	40%
1ZUZ	METAL BINDING PROTEIN/TRANSFERASE	2.6	21.1	22.7	93%
2BCX	CALCIUM BINDING PROTEIN	2.2	15.1	15.1	100%
2BE6	MEMBRANE PROTEIN	2.1	14.9	14.9	100%
2F66	TRANSPORT PROTEIN	3.4	10.2	11.3	90%
2F66	TRANSPORT PROTEIN	2.6	20.5	21.5	95%
2FOT	METAL BINDING, STRUCTURAL PROTEIN	2.9	20.3	20.3	100%
2JF9	TRANSCRIPTION	2.2	10.9	10.9	100%
2O60	METAL BINDING PROTEIN	2.5	25.1	25.1	100%
2PKQ	APOPTOSIS	2.2	20.0	21.1	95%
2QAC	MEMBRANE PROTEIN	2.3	18.0	18.0	100%
2V6Q	APOPTOSIS	2.1	12.7	12.7	100%
3BS5	SIGNALING PROTEIN/MEMBRANE PROTEIN	2.3	11.5	11.5	100%
3D7V	APOPTOSIS	2.4	17.1	17.1	100%
3DA7	PROTEIN BINDING	2.7	13.7	18.3	75%
3DD7	RIBOSOME INHIBITOR	4.9	24.4	26.6	92%
3DI2	CYTOKINE/CYTOKINE RECEPTOR	2.1	6.4	9.2	70%
3DVE	MEMBRANE PROTEIN	2.6	18.1	20.0	91%
3EAB	CELL CYCLE	2.1	10.6	12.1	88%
3FWB	CELL CYCLE, TRANSCRIPTION	3.3	19.9	19.9	100%

**TABLE S3**

Bullock, et. al

A. PDB CODE	J. # HOTSPOT RESIDUES	K. HOTSPOT RESIDUES, RESIDUE # $\Delta\Delta G$ (kcal/mol)
1FQV	4	K137, 1.9; R138, 1.2; W139, 2.5; Y140, 2.5;
2ZFD	4	F313, 5.1; D314, 1.0; I315, 2.1; I316, 2.9;
1CDL	9	R798, 2.1; K799, 2.2; W800, 7.1; H805, 2.3; V807, 2.1; R808, 2.1; I810, 1.2; R812, 1.3; L813, 1.4;
1E3A	5	E152, 3.2; I153, 2.1; D154, 1.7; N155, 2.6; L158, 2.3;
1E3A	7	W25, 3.5; L27, 3.0; F28, 1.9; Y29, 1.2; Y31, 6.1; Y33, 2.3; D38, 1.7;
1IHF	5	E28, 4.2; M29, 1.9; L30, 2.3; H32, 2.3; M33, 1.2;
1JFI	3	L219, 1.1; Q222, 1.2; L225, 5.8;
1MXE	10	F298, 2.8; K302, 1.6; W303, 6.9; K304, 1.1; F307, 2.6; V312, 1.4; V313, 1.6; R314, 2.1; H315, 1.8; M316, 1.9;
1N1J	7	V67, 1.1; L68, 2.7; F69, 4.7; K71, 1.5; I75, 1.3; I77, 3.0; W85, 2.9;
1N2D	8	K812, 1.4; L814, 2.5; Q815, 2.8; I818, 1.7; F821, 2.4; I822, 1.4; I823, 1.1; R824, 2.4;
1OR7	5	W33, 2.8; H37, 2.4; L38, 1.2; I39, 2.4; M43, 2.3;
1PQ1	9	F101, 4.3; Y105, 2.8; E87, 1.7; I90, 1.5; E93, 1.0; L94, 1.9; R95, 1.6; I97, 2.0; D99, 3.6;
1RP3	5	K190, 1.8; Q194, 2.1; L195, 1.2; F197, 2.4; Y198, 2.5;
1ZUZ	8	R304, 1.9; W305, 6.6; L307, 1.6; F309, 3.2; V312, 2.2; L314, 1.6; H317, 2.3; L318, 1.7;
2BCX	7	L3623, 2.3; K3626, 1.0; R3628, 2.7; R3629, 1.6; V3632, 1.5; V3633, 1.8; F3636, 4.2;
2BE6	7	T1614, 1.3; K1617, 1.5; F1618, 4.5; Y1619, 1.6; F1622, 2.6; L1623, 1.0; I1624, 2.4;
2F66	3	V332, 2.4; D340, 6.5; M348, 1.3;
2F66	8	F184, 1.0; I185, 1.7; Y188, 4.9; L189, 1.7; R192, 4.1; H196, 2.4; L197, 2.4; E200, 2.3;
2FOT	7	W1192, 4.5; R1196, 2.1; L1197, 2.8; V1199, 2.3; T1204, 1.2; F1205, 4.4; K1209, 3.0;
2JF9	5	L12, 2.1; R5, 1.0; W7, 2.8; F8, 4.0; K9, 1.0;
2O60	10	L10, 4.5; E12, 1.0; V14, 2.1; K15, 1.0; F16, 3.9; K19, 1.0; L20, 2.0; F7, 5.0; K8, 1.4; K9, 3.2;
2PKQ	9	L10, 2.2; R11, 3.2; I13, 2.2; D15, 2.7; F17, 2.7; Y21, 2.2; E3, 1.8; W5, 1.0; I6, 2.0;
2QAC	8	R806, 4.3; V807, 1.7; Q808, 2.2; H810, 3.4; I811, 2.3; R812, 1.1; K813, 2.0; V816, 1.0;
2V6Q	6	W57, 2.2; I58, 1.8; E61, 3.1; L62, 2.3; R63, 1.4; F69, 1.9;
3BS5	5	I165, 1.7; H167, 2.9; Q168, 1.6; L170, 3.2; E173, 2.1;
3D7V	7	E55, 2.7; W57, 1.0; I58, 3.3; R63, 2.7; I65, 2.4; D67, 2.9; Y73, 2.1;
3DA7	5	L35, 1.6; D36, 1.5; D40, 6.7; C41, 1.0; W45, 2.9;
3DD7	5	E55, 1.6; F56, 2.6; L59, 2.0; F60, 17.0; D61, 1.2;
3DI2	3	D74, 1.0; L77, 1.4; L80, 4.0;
3DVE	7	M1854, 1.5; K1856, 1.6; I1863, 3.1; F1864, 1.9; F1866, 3.9; Y1867, 4.3; K1868, 1.8;
3EAB	5	E184, 2.9; Q185, 3.7; D186, 1.1; L188, 1.9; R191, 1.0;
3FWB	6	K789, 1.7; L794, 1.0; K795, 3.5; F798, 1.3; F799, 4.1; W802, 8.3;

**TABLE S3**

Bullock, et. al

A. PDB CODE	B. HOTSPOT RESIDUE HELIX POSITIONS	C. HOTSPOT RESIDUE END TO END LENGTH	D. HELIX LENGTH	E. HELIX START RESIDUE #
1FQV	i; i+1; i+2; i+3;	5	8	137
2ZFD	i; i+1; i+2; i+3;	2	7	312
1CDL	i; i+1; i+2; i+7; i+9; i+10; i+12; i+14; i+15;	12	17	798
1E3A	i; i+1; i+2; i+3; i+6;	19	15	152
1E3A	i; i+2; i+3; i+4; i+6; i+8; i+13;	18	16	24
1IHF	i; i+1; i+2; i+4; i+5;	9	21	19
1JFI	i; i+3; i+6;	12	28	215
1MXE	i; i+4; i+5; i+6; i+9; i+14; i+15; i+16; i+17; i+18;	9	21	298
1N1J	i; i+1; i+2; i+4; i+8; i+10; i+18;	8	29	63
1N2D	i; i+2; i+3; i+6; i+9; i+10; i+11; i+12;	19	46	808
1OR7	i; i+4; i+5; i+6; i+10;	11	18	27
1PQ1	i; i+3; i+6; i+7; i+8; i+10; i+12; i+14; i+18;	8	27	86
1RP3	i; i+4; i+5; i+7; i+8;	7	13	187
1ZUZ	i; i+1; i+3; i+5; i+8; i+10; i+13; i+14;	9	16	304
2BCX	i; i+3; i+5; i+6; 10; 11; 14;	7	23	3617
2BE6	i; i+3; i+4; i+5; i+8; 10; 11;	15	13	1613
2F66	i; i+8; i+16;	12	29	323
2F66	i; i+1; i+4; i+5; i+8; i+12; i+13; i+16;	11	26	178
2FOT	i; i+4; i+5; i+7; 13; 14; 18;	8	21	1191
2JF9	i; i+2; i+3; i+4; i+7;	8	9	5
2O60	i; i+1; i+2; i+3; i+5; i+7; i+8; i+9; i+12; i+13;	17	15	7
2PKQ	i; i+2; i+3; i+7; i+8; i+10; i+12; i+14; i+18;	8	22	1
2QAC	i; i+1; i+2; i+4; i+5; i+6; i+7; i+10;	15	13	805
2V6Q	i; i+1; i+4; i+5; i+6; i+12;	14	19	53
3BS5	i; i+2; i+3; i+5; i+8;	14	19	165
3D7V	i; i+2; i+3; i+8; i+10; i+12; i+18;	8	22	54
3DA7	i; i+1; i+5; i+10;	8	12	35
3DD7	i; i+1; i+4; i+5; i+6;	8	11	53
3DI2	i; i+3; i+6;	8	18	74
3DVE	i; i+2; i+9; i+10; i+12; i+13; i+14;	12	17	1854
3EAB	i; i+1; i+2; i+4; i+7;	9	19	174
3FWB	i; i+5; i+6; i+9; i+10; i+13;	6	52	753

TABLE S3

Bullock, et. al

A. PDB CODE	P. HELIX END RESIDUE #	Q. HELIX SEQUENCE	R. RESOLUTION
1FQV	144	KRWYRLAS	2.80
2ZFD	318	AFDIISG	1.20
1CDL	814	RKWQKTGHAVRAIGRLS	2.00
1E3A	166	EIDNLALLTALKDKY	1.80
1E3A	39	TWHLFYGYGYVVAQDR	1.80
1IHF	39	AKTVEDAVKEMLEHMASTLAQ	2.20
1JFI	242	EEELLRQQQELFAKARQQQAELAQEWL	2.62
1MXE	318	FAKSWKWQAFNATAVVVRHMRK	1.70
1N1J	91	AEAPVLFAKAAQIFITELTLLRAWIHTEDN	1.67
1N2D	853	SQAIKYLNQNNIKGFIIRQRVNDEMVKNCATLLQAAYRGHSIRANVF	2.00
1OR7	44	PEMQKTWESYHLIRDMSR	2.00
1PQ1	112	PEIRIAQELRRIGDEFNETYTRRVFAN	1.65
1RP3	199	EREKLVIQLIFYE	2.30
1ZUZ	319	RWKLDFSIVSLCNHLT	1.91
2BCX	3639	KAVWHKLLSKQRRRAVVACFRMT	2.00
2BE6	1625	VTVGKFYATFLIQ	2.00
2F66	351	DGLNQLYNLVAQDYALTDIEALSRMLHR	2.80
2F66	203	ADDLDQFIKNYLDIRTQYHLRREKLA	2.80
2FOT	1211	PWKSARLMVHTVATFNSIKER	2.45
2JF9	13	REWFKDMLS	2.10
2O60	21	FKKLAEVKFSAKLM	1.55
2PKK	22	RPEIWIAQELRRIGDEFNAYYA	2.00
2QAC	817	MRVQAHIRKRMA	1.70
2V6Q	71	RPEIWIAQELRRIGDEFNA	2.70
3BS5	183	IGHQELILEAVDLLCALNY	2.00
3D7V	75	PEIWIAQEARRIGDEANAYYAR	2.03
3DA7	46	LDALWDCLTGWV	2.25
3DD7	63	DAEFASLFDTL	1.70
3DI2	123	DFDLHLLKVSEGTTILLK	2.70
3DVE	1870	MGKVYALMIFDFYKQN	2.35
3EAB	192	GSGVGTTSVASAEQDELSQRL	2.50
3FWB	804	EANYRKDFIDTMRELYDAFLHERLYLIYMDSRAELKRNSTLKKFFEKWQA	2.50